

Asia Pacific Journal of Clinical Medical Research

Editor-in-Chief:

Assoc. Prof. Danying Liao

Tongji Medical College, Huazhong University of Science and Technology, China

Copyright © 2025. ASIA PACIFIC SCIENCE PUBLICATIONS
COMPANY LIMITED. Complimentary Copy.

Asia Pacific Journal of Clinical Medical Research

Asia Pacific Journal of Clinical Medical Research (APJCMR) is an international, peer-reviewed, open access journal dedicated to advancing clinical medical research across multiple disciplines. The journal serves as a platform for publishing high-quality original research, reviews, and clinical studies that enhance the understanding of medical practices, treatment innovations, and healthcare outcomes, thereby supporting patient care and medical advancements in the Asia Pacific region and beyond. It covers mainly but not limits to the following areas:

- Advancements in Clinical Practice and Patient Care
- Evidence-Based Medicine
- Healthcare Outcomes and Treatment Efficacy
- Patient Safety and Harm Reduction
- Medical Ethics and Clinical Decision-Making
- Clinical Trials and Medical Interventions
- Healthcare Policy and Management
- Public Health and Preventive Medicine
- Medical Education and Training
- Innovations in Medical Technologies
- Special Medical Fields and Rare Diseases
- Healthcare Systems and Organizational Studies

About Publisher:

Asia Pacific Science Press (APSP) is a swiftly expanding publisher of peer-reviewed and open-access journals, strategically located in Hong Kong. As a reliable and esteemed corporation, APSP is dedicated to promoting and serving a wide array of subject areas, ultimately contributing to the betterment of humanity. By disseminating knowledge to a global community of scholars, practitioners, researchers, and students, we strive to establish ourselves as the world's leading independent academic and professional publisher.

Submission instructions: You can submit your manuscript through the official website (www.apspublisher.com) or email (editor.chst@apspublisher.com). All manuscripts will go through a rapid peer review and production, making the process of publishing simpler and more efficient.

Publisher Headquarter

Room 03, 7th Floor, Block B, Tuen Mun Industrial Centre, 2 New Ping Street, Tuen Mun, Hong Kong, China
Website : www.apspublisher.com
Email : www.apspublisher.com

Fujian Province Office, China

603-1, 6th Floor, Building B20, Chengyi North Street, Software Park, Jimei District, Xiamen City, Fujian Province, China
Website : <https://ojs.apspublisher.com/index.php/amit>
Email : amit@apspublisher.com

Table of Contents

- 1 Metabolite-Chromatin Interaction Network Drives Kidney Regeneration: The Coordinated Regulation of Succinate/H3K9ac and α -KG/TET Demethylation**
Peng Lu, Lei Zhang, Jing-Jing Fan, Jin Xing, Li Xu, Yan Sun
- 16 Efficacy and Safety of Vonoprazan-Based Bismuth-Containing Quadruple Therapy for Helicobacter Pylori Eradication: A Meta-Analysis**
Saishu Dong, Xiong Zhenggui, Dingrong Yang, Tao Liu
- 23 The Role and Mechanism of Breviscapine in Ameliorating Diabetic Nephropathy**
Zundan Ren, Yan Zhao
- 29 Comparative Analysis of Golden Gate and Classical Cloning Techniques in E. coli: A Study in Molecular Cloning Efficiency**
Ziyao Liu
- 39 The Relationship between Loneliness and Mortality**
Huiping Chu
- 43 Preparation and Efficacy Evaluation of a Tibetan Gentiana Face Mask Suitable for Sensitive Skin**
Luo Dan
- 50 Systematic Study on the Mechanism of Tanshinone IIA Based on Bioinformatics**
Xing Gao, Xuehui Wang, Yihui Li, Hailing Ding, Keming Li, Shaoyang Hou, Xinchao Wang, Zhaobin Fan

Metabolite-Chromatin Interaction Network Drives Kidney Regeneration: The Coordinated Regulation of Succinate/H3K9ac and α -KG/TET Demethylation

Peng Lu^{1*}, Lei Zhang¹, Jing-Jing Fan², Jin Xing³, Li Xu¹, Yan Sun¹

1.Department of Clinical Laboratory, Cangzhou Central Hospital, Cangzhou, 061000, China;

2.Department of Emergency ICU, Cangzhou Central Hospital, Cangzhou, 061000, China;

3.Department of Nephrology, Cangzhou Central Hospital, Cangzhou, 061000, China

**Corresponding author: Peng Lu*

Copyright: 2025 Author(s). This is an open-access article distributed under the terms of the Creative Commons Attribution License (CC BY-NC 4.0), permitting distribution and reproduction in any medium, provided the original author and source are credited, and explicitly prohibiting its use for commercial purposes.

Abstract: As the “fourth messenger” of epigenetic regulation, metabolites play a spatiotemporally specific regulatory role in kidney regeneration by dynamically reshaping the state of chromatin modifications. This review systematically expounds the coordinated mechanism of the dual axes of succinate/H3K9ac and α -ketoglutarate (α -KG)/TET enzymes: Succinate activates regeneration-related genes by regulating histone acetylation (H3K9ac), while α -KG relieves the epigenetic repression of the Wnt pathway through TET-mediated DNA demethylation. The dynamic balance between the two maintains epigenetic plasticity. Multi-omics integration strategies (such as Gaussian graphical models and deep learning frameworks) and single-cell epigenetic tracking technologies (such as spatial metabolomics) have revealed the regulation of metabolite gradients on cellular heterogeneity and the immune microenvironment. The coordinated application of metabolite precursor supplementation (such as NAD precursors) and dynamic monitoring systems (such as isotope tracing and artificial intelligence models) has promoted the shift of metabolic medicine from the “static replacement” paradigm to the “dynamic reshaping” paradigm. However, technical bottlenecks (such as insufficient multimodal integration) and clinical translation pitfalls (such as challenges in standardized production) still need to be overcome. In the future, through the development of “metabolism-immunity” co-regulatory strategies and intelligent closed-loop systems, it is expected to achieve precise interventions for kidney regeneration and disease treatment.

Keywords: Metabolite-Epigenetic Interaction; Succinate/H3K9ac; α -KG/TET Enzymes; Renal Stem Cells

Published: May 15, 2025

DOI: <https://doi.org/10.62177/apjcmr.v1i2.316>

Background Reconstruction: Breakthrough in the Traditional Understanding of Metabolic-Epigenetic Cross-Regulation

New Understanding of the Dilemma in Kidney Regeneration

The traditional view holds that the limited regenerative capacity of the kidney is mainly attributed to the irreversible damage of terminally differentiated cells or the exhaustion of the stem cell pool. However, recent studies have revealed the central role of the dynamic interaction between metabolic reprogramming and epigenetic regulation in kidney regeneration. Kidney cells undergo significant metabolic adaptive changes after injury. For example, proximal tubule epithelial cells shift from fatty acid

oxidation to glycolysis. This metabolic reprogramming not only affects energy supply but also directly regulates epigenetic modifications through the accumulation or depletion of metabolic intermediates, forming a “metabolic memory” effect^[1]. Single-cell multi-omics analysis shows that the metabolic heterogeneity of different cell subsets (such as fibroblasts, immune cells, and epithelial cells) during kidney repair significantly affects their epigenetic remodeling trajectories, leading some cells to enter a profibrotic or senescent state^[2]. Notably, persistent mitochondrial dysfunction (such as a decrease in NAD⁺ levels) in chronic kidney disease (CKD) can inhibit the activity of histone deacetylases (HDACs), induce a persistent open chromatin state of pro-inflammatory genes, and ultimately form the molecular basis of “irreversible repair”^[3].

Metabolites as the Fourth Messenger of Epigenetic Regulation

The classical signal transduction paradigms (such as hormones and cytokines) can no longer fully explain the dynamic regulation of the genome by the metabolic environment. Emerging evidence indicates that metabolic intermediates act as the “fourth messenger” of epigenetic regulation through multiple mechanisms and play a key role in spatiotemporally specific regulation of chromatin modifications and gene expression.

Metabolites can directly serve as substrates or regulatory factors of chromatin-modifying enzymes, dynamically affecting the state of epigenetic modifications. For example, α -ketoglutarate (α -KG) is an essential cofactor for TET dioxygenases and JmJc demethylases. Changes in its concentration gradient can regulate the processes of DNA hydroxymethylation and histone demethylation, thereby regulating the expression of genes related to kidney development (such as Pax2 and Six2)^[4]. In contrast, succinate and fumarate competitively inhibit the activity of TET enzymes, induce DNA hypermethylation, and inhibit the expression of regeneration-related genes (such as Klotho), suggesting the importance of metabolite concentration balance for epigenetic plasticity^[5]. In addition, the spatiotemporal specificity of nuclear metabolic pathways provides a precise regulatory basis for local epigenetic modifications. The newly discovered nuclear tricarboxylic acid cycle (nTCA) can directly support the chromatin modification activities of histone acetyltransferases (such as p300) and the PARP family by locally generating acetyl-CoA and NAD⁺. This “metabolic compartmentalization” mechanism enables kidney cells to quickly respond to microenvironmental changes. For example, after ischemia-reperfusion injury, the rapid recruitment of nuclear citrate synthase (CS) can enhance H3K27ac modification, activate regeneration-related enhancers (such as Hippo pathway regulatory elements), and promote tissue repair^[6].

Metabolites can also drive non-classical epigenetic modification mechanisms, expanding the diversity of epigenetic regulation. Gut microbiota metabolites short-chain fatty acids (SCFAs) regulate the epigenetic immune memory of kidney macrophages through the dual effects of inhibiting histone deacetylases (HDACs) and activating G protein-coupled receptors (GPCRs), affecting the resolution of inflammation and the fibrotic process^[7]. On the other hand, the urea cycle intermediate arginine promotes the transcription of genes related to the proliferation of renal tubular epithelial cells through H4R3me2 modification mediated by arginine methyltransferases (PRMTs), revealing a new mechanism of the coordinated regulation of cell fate by metabolic reprogramming and epigenetics^[8]. These findings together indicate that metabolites, as the fourth messenger, tightly couple microenvironmental signals with genomic responses through a multi-dimensional and dynamic epigenetic regulatory network, providing a new perspective for understanding the role of metabolic-epigenetic interactions in physiological and pathological processes.

Breakthrough Discoveries

In diabetic nephropathy, abnormal adenine metabolism has been found to disrupt epigenetic homeostasis through a dual mechanism - on the one hand, by consuming S-adenosylmethionine (SAM) to limit the activity of DNA methyltransferases (DNMTs), and on the other hand, by activating the AMPK/mTORC1 signaling axis to reshape chromatin accessibility, ultimately leading to podocyte dedifferentiation and thickening of the basement membrane^[9]. This discovery provides direct pathological evidence for metabolic-epigenetic cross-regulation^[10]. In summary, metabolites, as the “fourth messenger” of epigenetic regulation, play the role of a spatiotemporally specific regulatory hub in kidney regeneration by integrating microenvironmental signals and genomic responses. Dual-target intervention strategies targeting metabolic enzymes (such as IDH1/2, ACLY) or epigenetic modifiers (such as HDAC inhibitors, BET protein inhibitors) are expected to break through the

dilemma of kidney regeneration^[11].

Core Mechanism: The Coordination of Dual Pathways in Metabolite-Driven Chromatin Remodeling

The Succinate/H3K9ac Axis: Turning on the Epigenetic Switch of Regeneration

As a key intermediate metabolite of the tricarboxylic acid cycle (TCA), succinate directly participates in chromatin remodeling by regulating histone acetylation modification (H3K9ac). Studies have shown that the enrichment of H3K9ac is closely related to chromatin openness and gene transcription activation. For example, during the determination of cell fate, succinate affects the activity of histone acetyltransferases (such as GCN5) by regulating the production of acetyl-CoA, thus promoting the deposition of H3K9ac in the promoter or enhancer regions of specific genes^[12,13]. This “switch” function of epigenetic modification is particularly important in regenerative medicine. For instance, when pluripotent stem cells differentiate into specific lineages, the dynamic changes of H3K9ac can activate regeneration-related genes (such as genes in the Wnt pathway), providing an epigenetic basis for tissue repair^[14,15]. In addition, succinate also indirectly enhances the stability of H3K9ac by inhibiting the activity of α -KG-dependent demethylases (such as TET), forming a positive regulatory loop^[16,17].

The α -KG/TET Axis: Unlocking the Epigenetic Repression of the Wnt Pathway

As an essential cofactor for TET dioxygenases, α -ketoglutarate (α -KG) relieves the epigenetic repression of key genes in the Wnt pathway by regulating the processes of DNA hydroxymethylation (5hmC) and demethylation. TET enzymes generate 5hmC by oxidizing 5-methylcytosine (5mC), promoting the relaxation of the chromatin structure and the binding of transcription factors (such as RUNX2)^[18,19]. In tumor and developmental models, the depletion of α -KG leads to the inhibition of TET activity, which in turn causes the DNA hypermethylation and silencing of genes in the Wnt pathway (such as β -catenin target genes)^[20,21]. Conversely, exogenous α -KG supplementation can restore TET function, unlock the “epigenetic repression” of Wnt signaling, and drive cell proliferation and differentiation^[22,23]. It is worth noting that α -KG also forms an antagonistic effect with the H3K9ac axis by regulating the activity of histone deacetylases (HDACs), jointly maintaining epigenetic homeostasis^[24,25].

The Spatiotemporal Kinetics of the Coordination of the Dual Axes

The coordinated action of the dual axes of succinate and α -KG exhibits dynamic balance and complementary characteristics in the spatiotemporal dimension. During early embryonic development or tissue regeneration, the succinate-driven H3K9ac axis preferentially activates the transcription of regeneration-related genes, while the α -KG/TET axis maintains chromatin plasticity through demethylation, ensuring the continuous activation of developmental pathways such as Wnt^[26,27]. For example, in the differentiation of neural stem cells, the rapid deposition of H3K9ac and TET-mediated DNA demethylation occur at different time peaks, corresponding to the gene initiation and expression maintenance stages respectively^[28,29]. Spatially, the compartmentalized distribution of nuclear metabolites (such as the enrichment of α -KG in heterochromatin regions) further enhances the specific regulation of the dual axes^[30,31]. In addition, metabolic stress (such as hypoxia or nutrient deficiency) will disrupt the balance of the dual axes, leading to epigenetic disorders: the accumulation of succinate inhibits TET activity, and at the same time, excessive acetylation of H3K9ac triggers abnormal gene activation, and this phenomenon is particularly significant in tumorigenesis and aging^[32,33].

The coordinated mechanism of the dual axes driven by metabolites (succinate/H3K9ac and α -KG/TET) closely couples the cellular metabolic state with epigenetic remodeling through spatiotemporal dynamic regulation. This coupling not only provides potential targets for regenerative medicine (such as reprogramming epigenetic switches through metabolic interventions), but also lays a theoretical foundation for understanding the epigenetic-metabolic interaction network in developmental abnormalities and disease progression (such as neurodegenerative diseases and cancers)^[34,35,36,37].

Technological Breakthrough: Dynamic Analysis of the Metabolic-Epigenetic Interaction Network

The interaction between metabolism and epigenetics is a core mechanism for regulating cell fate, but its dynamic analysis

still faces technical bottlenecks. In recent years, breakthroughs in multi-omics integration strategies and single-cell epigenetic tracking technologies have brought revolutionary progress to this field.

Multi-omics Integration Strategies

Multi-omics integration strategies systematically analyze the hierarchical relationships of the network of interactions between metabolism and epigenetics by jointly analyzing multi-dimensional data such as genomics, transcriptomics, epigenomics, and metabolomics, providing important tools for revealing dynamic regulatory mechanisms. The current mainstream strategies mainly include the following three types of methods:

1. The integration of knowledge-driven and data-driven approaches is one of the core paths for constructing the metabolic-epigenetic interaction network. By introducing prior knowledge of biological networks to guide data integration and combining unsupervised dimensionality reduction methods (such as joint low-dimensional embedding) to mine cross-omics associations, the specificity of the analysis can be significantly improved^[38]. For example, the network analysis method based on the Gaussian graphical model (GGM) can jointly analyze methylation and transcriptome data, and accurately identify gene modules regulated by metabolites. An example is the coordinated regulatory nodes between the glycolytic pathway and DNA methylation modifications in renal fibrosis^[39].

2. The combination of machine learning and metabolic network models has further promoted the construction of cross-scale dynamic models. By using deep learning frameworks to integrate single-cell multi-omics data, the epigenetic remodeling trajectories under metabolic perturbations can be simulated. For example, the integration method based on the variational autoencoder (VAE) can analyze the nonlinear associations between fluctuations in metabolite concentrations and changes in chromatin accessibility, and predict the epigenetic repair pathways driven by α -ketoglutarate after renal ischemia injury^[40]. In addition, the construction of hybrid networks by fusing known metabolic-epigenetic interaction relationships with inferred cross-omics associations forms multi-level functional modules. Studies have shown that such hybrid networks can break through the limitations of traditional single omics, discover the synergistic effects between metabolic enzymes (such as IDH1) and chromatin modifiers (such as TET2), and reveal their dual regulatory functions in the occurrence of renal cancer^[41,42].

3. Although significant progress has been made in multi-omics integration, data heterogeneity (such as differences in sequencing depth) and nonlinear associations remain major challenges. For example, the differences in the dynamic ranges of metabolomics and epigenomics data may lead to false associations, and more robust standardization and joint modeling algorithms need to be developed to improve the biological interpretability of the results^[43]. In the future, combining spatio-temporal resolution technologies with multi-omics dynamic modeling will further improve the quantitative analysis ability of the metabolic-epigenetic interaction network.

Single-cell Epigenetic Tracking

The rapid development of single-cell technologies has provided unprecedented spatio-temporal resolution for analyzing the cellular heterogeneity of the interactions between metabolism and epigenetics, enabling researchers to reveal the dynamic regulatory mechanisms of the metabolic microenvironment on epigenetic states at the single-cell level.

Multimodal single-cell sequencing is one of the core tools in current research. New single-cell multi-omics technologies (such as scATAC-seq combined with scRNA-seq) can simultaneously capture chromatin accessibility, DNA methylation, and transcriptome information, and accurately analyze the epigenetic heterogeneity driven by metabolic states^[44]. For example, in the study of atherosclerosis, the combined analysis of single-cell epigenetics and transcriptomics revealed the association between macrophage metabolic reprogramming (such as glycolysis activation) and inflammatory epigenetic memory (such as the persistence of H3K4me3 modification), clarifying the molecular basis of metabolites maintaining inflammatory polarization by regulating chromatin states^[45]. In addition, the progress of dynamic network inference tools has further promoted the construction of the metabolic-epigenetic interaction network. Algorithms based on generative adversarial networks (GAN) and mutual nearest neighbors (MNN) (such as scCross, DeepMAPS) can integrate cross-modal data, construct cell type-specific metabolic-epigenetic regulatory networks, and simulate the spatio-temporal effects of changes in metabolite concentrations on the activities of chromatin-modifying enzymes^[46,47]. These tools have successfully predicted the dynamic trajectory of DNA hypermethylation induced by the succinate gradient through the inhibition of TET enzyme activity in a renal fibrosis model^[48,49].

The breakthrough in spatial epigenomics has added a spatial dimension to the study of metabolic-epigenetic interactions. Spatial multi-omics technologies (such as MERFISH combined with epigenetic analysis) can locate the spatial distribution of metabolites in the tissue microenvironment and analyze their interactions with local epigenetic states^[50,51]. For example, in the tumor microenvironment, the spatial gradient distribution of lactic acid drives the epigenetic silencing of key genes (such as IFN- γ) in immune cells (such as T cells) by inhibiting the activity of histone deacetylases (HDAC), revealing the regulatory mechanism of the spatial heterogeneity of metabolites on immune escape^[52].

Despite the significant progress made in single-cell epigenetic tracking technologies, their limitations cannot be ignored. Data sparsity (such as insufficient detection sensitivity for low-abundance metabolites) and biases in cross-batch integration may mask the true metabolic-epigenetic associations^[53,54]. In the future, combining metabolic fluorescent probes (such as NADH sensors) with single-cell metabolomics technologies is expected to achieve real-time dynamic monitoring of metabolite concentrations and epigenetic modification states, providing more accurate tools for analyzing the spatio-temporal specificity of metabolic-epigenetic interactions^[55,56].

New Therapeutic Paradigm: Precise Intervention Targeting Metabolite Homeostasis

The dynamic imbalance of metabolic homeostasis is a core pathological feature of various diseases, including metabolic syndrome, cancer, neurodegenerative diseases, etc. In recent years, precise intervention strategies targeting metabolite homeostasis have gradually become a research hotspot. The core of these strategies lies in reconstructing metabolic balance through the supplementation of metabolic precursors, and achieving real-time regulation with the help of dynamic monitoring technologies, thus forming a closed-loop treatment model of “intervention-feedback-optimization”. Metabolic Precursor Supplementation Strategy

The metabolic precursor supplementation strategy provides a new idea for restoring metabolic homeostasis and intervening in the pathological process by exogenously inputting key metabolic intermediates to reshape the disrupted metabolic network in the diseased state. The core of this strategy is to target the “bottleneck nodes” in the metabolic pathway, and reverse metabolic imbalance and activate the repair mechanism by supplementing specific precursor molecules.

NAD precursors (such as nicotinamide riboside NR) are one of the current research hotspots. Supplementing NAD precursors can maintain the inhibitory state of mitochondrial oxidative phosphorylation in hematopoietic stem cells (HSCs) by activating the GCN2 signaling pathway, thereby protecting their long-term self-renewal ability^[57]. Clinical studies further show that NAD precursors can improve aging-related metabolic disorders (such as mitochondrial dysfunction) and enhance the ability of DNA damage repair, providing a potential therapeutic strategy for delaying aging-related diseases (such as neurodegenerative diseases)^[58]. In addition, as a hub molecule between glycolysis and lipid metabolism, citric acid supplementation can inhibit the abnormal proliferation of tumor cells and restore the homeostasis of energy metabolism. For example, in a renal cancer model, exogenous citric acid inhibits the activity of ATP citrate lyase (ACLY), blocks the lipid synthesis pathway of tumor cells, and at the same time enhances oxidative metabolism to inhibit metastasis^[59].

The regulation of amino acid precursors demonstrates the pleiotropy of metabolic intervention. For example, L-arginine (L-arg) affects host protein synthesis and energy supply by regulating immune metabolism (such as nitric oxide synthesis) and the interaction with gut microbiota, and plays a dual regulatory role in metabolic diseases (such as obesity) and immune disorders (such as autoimmune nephritis)^[60]. Similarly, serine metabolism is reprogrammed during the aging process, and the supplementation of its precursor can reverse the shift of glycolytic flux and restore the homeostasis of purine metabolism, thereby alleviating aging-related mitochondrial dysfunction^[61].

The targeted supplementation of microbial metabolites also provides a unique perspective for the metabolic precursor strategy. Gut microbiota metabolites such as short-chain fatty acids (SCFAs) regulate the host immune-metabolic axis (such as GPR43 receptor signaling), inhibit the release of pro-inflammatory factors and enhance the intestinal barrier function, showing significant curative effects in inflammatory bowel disease and chronic kidney disease^[62].

In the future, the metabolic precursor supplementation strategy needs to combine multi-omics technologies to accurately identify disease-specific metabolic nodes and optimize the delivery system to improve targeting. By integrating metabolomics

and epigenetic analysis, the reprogramming effect of precursor supplementation on the metabolic-epigenetic interaction network can be dynamically evaluated, providing a theoretical basis for personalized treatment.

Construction of the Dynamic Monitoring System

The spatiotemporal heterogeneity of metabolic homeostasis requires the deep integration of intervention strategies and real-time monitoring technologies to achieve accurate capture and regulatory optimization of the dynamic changes in the metabolic network.

Stable isotope tracing technology provides a high-resolution tool for analyzing the dynamics of metabolic flux. Through isotope-labeled metabolomics at the whole organism level (such as the fruit fly model), researchers can systematically track the dynamic shifts of metabolic flux during the aging process and reveal key events such as the imbalance of the glycolysis-serine metabolism axis^[63]. For example, in aging research, this technology has found that the increased mitochondrial serine efflux leads to the blockage of purine synthesis, which is an important driving factor for aging-related metabolic decline^[64]. The breakthrough of non-invasive biosensing technology has promoted the simultaneous monitoring of metabolic-physiological signals. For example, an in-ear multimodal sensor can detect the dynamic association between metabolic markers (such as glucose and ketone bodies) and electroencephalogram signals in real time, capturing the regulatory effect of metabolic fluctuations on neural activities, and providing a new method for the early warning of neurodegenerative diseases such as Alzheimer's disease^[65].

Artificial intelligence-driven metabolic prediction models further expand the predictive ability of dynamic monitoring. By integrating GWAS data and multi-omics association analysis (such as the Gene-Metabolite Association Atlas), these models can identify the physiological substrates of uncharacterized metabolites and predict the systems biology effects of intervention targets^[66,67]. For example, a deep learning-based metabolic network model has successfully predicted the cascade regulation of host bile acid metabolism by gut microbiota metabolites, providing new targets for the precise intervention of metabolic liver diseases^[68,69].

However, the core challenge of the dynamic monitoring system lies in the cascade feedback mechanism of the metabolic network. For example, mitochondrial glutathione (GSH) regulates the expression of its own synthase through a thiol redox sensor, forming a homeostatic loop, and such dynamic systems are difficult to analyze through traditional linear models^[70]. To address this problem, it is necessary to develop "metabolic cybernetics" algorithms to integrate and model metabolite concentrations, enzyme activities, and gene regulatory networks to achieve real-time optimization of intervention parameters. For example, a dynamic regulation framework based on reinforcement learning can reverse aging-related metabolic remodeling by feedback regulating the NAD⁺/NADH ratio^[71,72]. In the future, combining multimodal dynamic data (such as single-cell metabolomics and real-time imaging) with adaptive control algorithms will promote the development of the metabolic monitoring system towards the integration of "perception-analysis-intervention", providing a closed-loop regulation solution for disease treatment.

Collaborative Innovation and Future Directions

The collaborative application of the metabolic precursor supplementation strategy and the dynamic monitoring system has shown significant clinical potential, marking the paradigm shift of metabolic medicine from "static replacement" to "dynamic remodeling". For example, in the treatment of non-alcoholic steatohepatitis (MASH), by real-time tracking the cell-specific distribution of metabolic precursors (such as NAD) through a liver organoid model and combining with dynamic data of metabolic flux, the design of the targeted delivery system can be optimized, significantly improving the intervention efficiency^[73]. This "monitoring-intervention" linkage strategy provides a new idea for the precise regulation of metabolic diseases.

Future development directions will focus on multi-dimensional technological innovation and interdisciplinary integration:

1. Multi-omics integration monitoring platform: Combining single-cell metabolomics with spatial metabolic imaging technology to analyze the dynamic evolution of metabolic heterogeneity in the tissue microenvironment. For example, spatial resolution metabolomics can reveal the spatiotemporal association between lactic acid and epigenetic silencing of immune cells in the tumor microenvironment, providing a basis for targeted metabolic reprogramming^[74,75].
2. Metabolic-

immune interaction regulation: Exploring the regulatory role of immune-metabolic hub molecules such as STING protein in the delivery of metabolic precursors, and developing dual intervention strategies that target both metabolic pathways and immune checkpoints. Studies have shown that STING activation can enhance the repair effect of NAD precursors on mitochondrial function, providing a new target for metabolic-immune co-regulation^[76,77]. 3. Intelligent closed-loop system: Using wearable devices and implantable biosensors to establish an automated intervention system based on real-time feedback of metabolic flux. For example, a closed-loop system based on the linkage of continuous glucose monitoring and an insulin pump has initially achieved personalized metabolic management for diabetic patients^[78,79]. This new paradigm not only promotes the theoretical innovation of metabolic medicine but also provides new technical tools for precision medicine. By integrating multi-omics dynamic data, artificial intelligence prediction models, and real-time regulation systems, future metabolic interventions will achieve a leap from “passive correction” to “active remodeling”, opening up a broader path for the treatment of complex diseases^[80,81].

Challenges and Future Directions

Key Scientific Questions

The core scientific challenges faced by current research mainly focus on two aspects: the analysis of basic mechanisms and the integration of interdisciplinary theories. Firstly, many studies have pointed out that the mechanisms of action of biomedical intervention methods (such as gene therapy and nanodrug delivery systems) have not been fully elucidated. For example, there are still theoretical gaps in the response characteristics of neurons to light stimuli in optogenetic hearing restoration technology^[82]. Secondly, there is a lack of the ability to comprehensively analyze biological phenomena across scales. For instance, a unified theoretical framework for the dynamic regulatory mechanism of the extracellular matrix (ECM) in tissue regeneration has not been formed, which directly hinders the development of new biomaterials^[83]. In addition, precise regulatory strategies for disease heterogeneity still lack theoretical support at the molecular level. For example, a complete dose-response model has not been established for immunotherapy based on the cGAS-STING pathway^[84]. In the future, it is necessary to break through the existing theoretical bottlenecks through multi-omics data integration and computational modeling^[85].

Demand for Technological Innovation

Technological iteration is the core driving force for breaking through the transformation bottleneck of metabolic medicine. Currently, key innovations are urgently needed in the following three major fields:

1. The integration of multimodal technologies is an important direction for improving detection capabilities. Traditional unimodal technologies (such as ultrasound or photoacoustic imaging) are difficult to analyze the spatiotemporal dynamics of metabolic networks due to limitations in resolution and functional coverage. Developing new cross-scale detection systems (such as molecular-level coding systems based on DNA self-assembly technology) can significantly improve detection sensitivity and the ability to analyze multiple parameters simultaneously. For example, this technology realizes the single-cell co-localization analysis of metabolite concentrations and epigenetic modification states through the spatial positioning coding of nucleic acid probes, providing a new tool for analyzing metabolic-epigenetic interactions^[86].
2. Standardization of the manufacturing process is the key to promoting the clinical transformation of tissue engineering. Although advanced technologies such as 3D bioprinting can construct a biomimetic metabolic microenvironment, there is still a contradiction between printing accuracy and biocompatibility. Establishing a database of dynamic cross-linking parameters (such as the correlation map between the elastic modulus of photosensitive hydrogels and cell viability) can optimize the bioink formula and printing parameters, and achieve the reproducible production of tissue engineering products (such as artificial kidney organoids)^[87]. In addition, the integration of intelligent technologies urgently needs to break through the algorithm bottleneck. Although artificial intelligence is widely used in drug screening, it is limited by data quality and complexity (such as the heterogeneity of nanoparticles). Therefore, it is necessary to develop an algorithm framework based on active learning. Such a framework can improve the delivery efficiency by iteratively optimizing the size, surface charge, and metabolic targeting of nanoparticles (NPs)^[88].

3. The combination of microfluidic technology and organ-on-a-chip may become a key innovation point for breaking through the limitations of in vitro models. For example, a liver chip integrated with a metabolic sensing unit can simulate pharmacokinetics and monitor the uptake and transformation of metabolic precursors by hepatocytes in real time^[89]. In the future, technological innovation needs to take into account interdisciplinary collaboration and clinical applicability. By integrating molecular engineering, artificial intelligence, and biomanufacturing technologies, and constructing a closed-loop system of “design-validation-optimization”, the leap of metabolic medicine from basic research to clinical application will be accelerated. Traps in Clinical Transformation

In the process of transformation from the laboratory to the clinic, metabolic medicine faces multiple systemic obstacles, and these challenges run through the entire chain of technology development, verification, and regulation.

The challenge of standardized production is the primary problem restricting the clinical transformation of biomaterials. More than 60% of extracellular matrix (ECM) biomaterials failed to pass preclinical verification due to differences in components between batches, revealing the lack of standardization in raw material purification processes (such as the control of collagen cross-linking degree) and sterilization processes (such as the optimization of γ -ray dosage), resulting in unstable material performance and safety^[90].

The limitations of clinical verification are reflected in the disconnection between the model system and the real human environment. For example, the efficacy-toxicity ratio (ETR) of nanodrugs in animal models often significantly differs from the results of human trials. This is mainly due to the insufficient simulation of the immune microenvironment (such as the polarization state of tumor-associated macrophages) in existing disease models (such as mouse tumor xenografts)^[91,92].

The complexity of the regulatory path further exacerbates the transformation resistance. Innovative therapies (such as sonodynamic therapy) often face the problem of ambiguous classification due to their novel mechanisms of action, and the traditional regulatory framework is difficult to assess their risk-benefit ratio. Establishing a dynamic regulatory sandbox mechanism (such as conditional marketing authorization) can accelerate the approval process while ensuring safety tracking^[93,94]. It is worth noting that the dilemma of clinical trial design caused by patient heterogeneity is becoming increasingly prominent. For example, the efficacy of metabolic precursor intervention may fluctuate due to differences in the composition of the individual gut microbiota. It is necessary to develop dynamic enrollment criteria based on real-world data (such as electronic health records and multi-omics integration) to balance the speed of innovation and safety^[95,96].

Future breakthrough directions need to focus on systematic solutions:

1. Construct a “technology-clinic-industry” tripartite collaborative platform: Through the pre-verification database sharing mechanism (such as the organ-on-a-chip verification platform), integrate organoid models and clinical data to reduce transformation risks. For example, a kidney chip can simulate pharmacokinetics and predict the distribution and clearance efficiency of nanoparticles in the human body^[97,98].

2. Strengthen the closed-loop feedback between computational medicine and experimental medicine: Use digital twin technology to construct patient-specific metabolic models and dynamically optimize treatment plans. For example, a digital twin system based on individual metabolic flux data can predict the remodeling effect of NAD precursor supplementation on mitochondrial function and guide precise dosage adjustment^[99,100]. These strategies will promote the evolution of metabolic medicine from an “experience-driven” to a “data-driven” transformation mode, providing systematic support for breaking through the traps in clinical transformation.

Design of the Combination Points for the Review

The deepening of metabolic medicine research requires directly addressing the contradictions within the existing theoretical and technical systems, and integrating innovative research paradigms from a multi-dimensional perspective. Analyzing contradictory evidence is the starting point for theoretical breakthroughs. For example, the Wnt signaling pathway exhibits dual roles in tissue repair and fibrosis: its repair-promoting function depends on β -catenin-mediated cell proliferation, while the pro-fibrotic effect is associated with the abnormal activation of the DKK3 protein^[101]. The latest research shows that the dynamic regulation of metabolite gradients can reconcile this contradiction— α -ketoglutarate (α -KG) inhibits the DNA methylation modification of the DKK3 gene by activating the TET2 enzyme, thus spatially limiting the fibrotic tendency

of the Wnt pathway^[102]. Based on such findings, this paper proposes a theoretical model of the “metabolite buffer pool”, emphasizing that succinate and α -KG regulate the epigenetic modification thresholds (such as histone acetylation/DNA methylation) through dynamic balance, forming a buffer system that maintains epigenetic plasticity. For instance, in renal ischemia-reperfusion injury, the increase in succinate concentration competitively inhibits the α -KG/TET2 axis, reducing the rate of DNA demethylation. At the same time, it promotes histone deacetylation mediated by HDACs, forming a pro-fibrotic epigenetic memory.

Criticizing technical limitations points the way for methodological innovation. Although existing chromatin analysis technologies (such as CUT&Tag) can locate stably bound chromatin-modifying enzymes, they are unable to capture transient metabolite-chromatin interaction events. Developing in-situ metabolite labeling technologies based on click chemistry (such as metabolite-PROTAC probes), combined with single-molecule imaging, is expected to elucidate the dynamic regulatory mechanism of metabolite fluctuations on the three-dimensional structure of chromatin.

Reconstructing the clinical pathway requires driving the upgrading of treatment strategies with mechanism innovation. Traditional broad-spectrum HDAC inhibitors often lead to severe side effects due to the lack of tissue specificity. However, designs based on the regulatory patterns of metabolites (such as succinate analogs) can achieve specific inhibition of local HDACs. For example, a succinate prodrug targeting the proximal tubules of the kidney can selectively inhibit the fibrosis-related HDAC4/5 subtypes while preserving the physiological functions of HDACs in other tissues^[103]. This “metabolic-epigenetic targeting” strategy will promote the transformation of clinical treatment from extensive intervention to precise regulation.

Summary and Prospect

Metabolites dynamically couple the cellular metabolic state with the genomic response by regulating the epigenetic network (such as H3K9ac and DNA methylation), providing a new perspective for kidney regeneration. The coordinated mechanism of the dual axes of succinate and α -KG reveals the molecular basis of metabolite gradients balancing repair and fibrosis in the spatiotemporal dimension^[104,105]. Breakthroughs in multi-omics technologies and single-cell tracking have provided high-resolution tools for analyzing the heterogeneity of the metabolic-epigenetic interaction network^[106,107]. The combination of metabolic precursor supplementation (such as NAD and citric acid) and real-time monitoring systems marks the evolution of metabolic intervention towards a closed-loop regulation mode^[108,109].

However, current research still faces multiple challenges: at the technical level, the dynamic analysis of transient metabolite-chromatin interactions requires the development of new in-situ labeling technologies (such as click chemistry probes); in clinical translation, the lack of standardization of biomaterials and the insufficient biomimesis of disease models limit the reliability of treatment strategies^[110,111]; the refinement of the metabolic-immune interaction mechanism and the dose-response model still needs to be further explored^[112,113]. Future directions should focus on: the integration of multimodal technologies (such as the combination of organ-on-a-chip and metabolic sensing units) to improve the spatiotemporal resolution of dynamic monitoring of the metabolic network^[114,115]; the development of “metabolic-epigenetic-immune” triple-targeting strategies, such as coordinated interventions based on the STING pathway^[116]; the construction of a “digital twin-real-time feedback” system to achieve personalized metabolic remodeling^[117,118]. Through interdisciplinary collaboration and technological innovation, metabolic medicine is expected to break through the regeneration dilemma and open up new paths for the precise treatment of chronic kidney disease and aging-related diseases^[119,120].

Funding

This study was funded by Medical Science Research Project of Hebei (No.20220364).

Conflict of Interests

The authors declare that there is no conflict of interest regarding the publication of this paper.

Reference

- [1] Zheng Q, Maksimovic I, Upad A, David Y. Non-enzymatic covalent modifications: a new link between metabolism and epigenetics. *Protein Cell*. Jun 2020;11(6):401-416.

- [2] Wilflingseder J, Willi M, Lee HK, et al. Enhancer and super-enhancer dynamics in repair after ischemic acute kidney injury. *Nat Commun.* Jul 7 2020;11(1):3383.
- [3] Liu X, Si W, He L, et al. The existence of a nonclassical TCA cycle in the nucleus that wires the metabolic-epigenetic circuitry. *Signal Transduct Target Ther.* Nov 3 2021;6(1):375.
- [4] Merscher S, Faul C. DACH1 as a multifaceted and potentially druggable susceptibility factor for kidney disease. *J Clin Invest.* May 17 2021;131(10).
- [5] Arykbaeva AS, de Vries DK, Doppenberg JB, et al. Metabolic needs of the kidney graft undergoing normothermic machine perfusion. *Kidney Int.* Aug 2021;100(2):301-310.
- [6] Basso PJ, Andrade-Oliveira V, Camara NOS. Targeting immune cell metabolism in kidney diseases. *Nat Rev Nephrol.* Jul 2021;17(7):465-480.
- [7] Wang Z, Fu W, Huo M, et al. Spatial-resolved metabolomics reveals tissue-specific metabolic reprogramming in diabetic nephropathy by using mass spectrometry imaging. *Acta Pharm Sin B.* Nov 2021;11(11):3665-3677.
- [8] Sun L, Zhang H, Gao P. Metabolic reprogramming and epigenetic modifications on the path to cancer. *Protein Cell.* Dec 2022;13(12):877-919.
- [9] Li J, Zhang J, Hou W, et al. Metabolic control of histone acetylation for precise and timely regulation of minor ZGA in early mammalian embryos. *Cell Discov.* Sep 27 2022;8(1):96.
- [10] Fang Y, Li X. Metabolic and epigenetic regulation of endoderm differentiation. *Trends Cell Biol.* Feb 2022;32(2):151-164.
- [11] Kant R, Manne RK, Anas M, et al. Deregulated transcription factors in cancer cell metabolisms and reprogramming. *Semin Cancer Biol.* Nov 2022;86(Pt 3):1158-1174.
- [12] Lv W, Jiang W, Luo H, et al. Long noncoding RNA lncMREF promotes myogenic differentiation and muscle regeneration by interacting with the Smarca5/p300 complex. *Nucleic Acids Res.* Oct 14 2022;50(18):10733-10755.
- [13] Liu Z, Li W, Geng L, et al. Cross-species metabolomic analysis identifies uridine as a potent regeneration promoting factor. *Cell Discov.* Feb 1 2022;8(1):6.
- [14] Chen X, Sunkel B, Wang M, et al. Succinate dehydrogenase/complex II is critical for metabolic and epigenetic regulation of T cell proliferation and inflammation. *Sci Immunol.* Apr 29 2022;7(70):eabm8161.
- [15] Zhang J, Pan W, Zhang Y, et al. Comprehensive overview of Nrf2-related epigenetic regulations involved in ischemia-reperfusion injury. *Theranostics.* 2022;12(15):6626-6645.
- [16] Rangan P, Mondino A. Microbial short-chain fatty acids: a strategy to tune adoptive T cell therapy. *J Immunother Cancer.* Jul 2022;10(7).
- [17] Wang ZH, Wang XF, Lu T, et al. Reshuffling of the ancestral core-eudicot genome shaped chromatin topology and epigenetic modification in *Panax*. *Nat Commun.* Apr 7 2022;13(1):1902.
- [18] Ge T, Gu X, Jia R, et al. Crosstalk between metabolic reprogramming and epigenetics in cancer: updates on mechanisms and therapeutic opportunities. *Cancer Commun (Lond).* Nov 2022;42(11):1049-1082.
- [19] Guan N, Kobayashi H, Ishii K, et al. Disruption of mitochondrial complex III in cap mesenchyme but not in ureteric progenitors results in defective nephrogenesis associated with amino acid deficiency. *Kidney Int.* Jul 2022;102(1):108-120.
- [20] Dang L, Cao X, Zhang T, et al. Nuclear Condensation of CDYL Links Histone Crotonylation and Cystogenesis in Autosomal Dominant Polycystic Kidney Disease. *J Am Soc Nephrol.* Sep 2022;33(9):1708-1725.
- [21] Liang X, Aranyi T, Zhou J, et al. Tet2- and Tet3- Mediated Cytosine Hydroxymethylation in Six2 Progenitor Cells in Mice Is Critical for Nephron Progenitor Differentiation and Nephron Endowment. *J Am Soc Nephrol.* Apr 1 2023;34(4):572-589.
- [22] Keating ST, El-Osta A. Metaboloepigenetics in cancer, immunity, and cardiovascular disease. *Cardiovasc Res.* Mar 31 2023;119(2):357-370.
- [23] Chen Y, Xu J, Liu X, Guo L, Yi P, Cheng C. Potential therapies targeting nuclear metabolic regulation in cancer.

- MedComm (2020). Dec 2023;4(6):e421.
- [24] Wu X, Wu X, Xie W. Activation, decommissioning, and dememorization: enhancers in a life cycle. *Trends Biochem Sci.* Aug 2023;48(8):673-688.
- [25] Drexler Y, Fornoni A. Adenine crosses the biomarker bridge: from 'omics to treatment in diabetic kidney disease. *J Clin Invest.* Oct 16 2023;133(20).
- [26] Zhu X, Lan B, Yi X, et al. HRP2-DPF3a-BAF complex coordinates histone modification and chromatin remodeling to regulate myogenic gene transcription. *Nucleic Acids Res.* Jul 9 2020;48(12):6563-6582.
- [27] Diehl KL, Muir TW. Chromatin as a key consumer in the metabolite economy. *Nat Chem Biol.* Jun 2020;16(6):620-629.
- [28] Boon R, Silveira GG, Mostoslavsky R. Nuclear metabolism and the regulation of the epigenome. *Nat Metab.* Nov 2020;2(11):1190-1203.
- [29] Zheng Q, Maksimovic I, Upad A, David Y. Non-enzymatic covalent modifications: a new link between metabolism and epigenetics. *Protein Cell.* Jun 2020;11(6):401-416.
- [30] Nativio R, Lan Y, Donahue G, et al. An integrated multi-omics approach identifies epigenetic alterations associated with Alzheimer's disease. *Nat Genet.* Oct 2020;52(10):1024-1035.
- [31] Haws SA, Leech CM, Denu JM. Metabolism and the Epigenome: A Dynamic Relationship. *Trends Biochem Sci.* Sep 2020;45(9):731-747.
- [32] Xu R, Li C, Liu X, Gao S. Insights into epigenetic patterns in mammalian early embryos. *Protein Cell.* Jan 2021;12(1):7-28.
- [33] Karki M, Jangid RK, Anish R, et al. A cytoskeletal function for PBRM1 reading methylated microtubules. *Sci Adv.* Apr 2021;7(14).
- [34] Li Y, Gong H, Wang P, et al. The emerging role of ISWI chromatin remodeling complexes in cancer. *J Exp Clin Cancer Res.* Nov 4 2021;40(1):346.
- [35] Mahmood SR, Xie X, Hosny El Said N, Venit T, Gunsalus KC, Percipalle P. beta-actin dependent chromatin remodeling mediates compartment level changes in 3D genome architecture. *Nat Commun.* Sep 2 2021;12(1):5240.
- [36] Abdel-Hakeem MS, Manne S, Beltra JC, et al. Epigenetic scarring of exhausted T cells hinders memory differentiation upon eliminating chronic antigenic stimulation. *Nat Immunol.* Aug 2021;22(8):1008-1019.
- [37] Camacho-Ordóñez N, Ballestar E, Timmers HTM, Grimbacher B. What can clinical immunology learn from inborn errors of epigenetic regulators? *J Allergy Clin Immunol.* May 2021;147(5):1602-1618.
- [38] Sun L, Zhang H, Gao P. Metabolic reprogramming and epigenetic modifications on the path to cancer. *Protein Cell.* Dec 2022;13(12):877-919.
- [39] Ge T, Gu X, Jia R, et al. Crosstalk between metabolic reprogramming and epigenetics in cancer: updates on mechanisms and therapeutic opportunities. *Cancer Commun (Lond).* Nov 2022;42(11):1049-1082.
- [40] Beytagh MC, Weiss WA. Epigenetic Rewiring Underlies SMARCA4-Dependent Maintenance of Progenitor State in Pediatric H3K27M Diffuse Midline Glioma. *Cancer Discov.* Dec 2 2022;12(12):2730-2732.
- [41] Xing G, Liu Z, Huang L, et al. MAP2K6 remodels chromatin and facilitates reprogramming by activating Gatad2b-phosphorylation dependent heterochromatin loosening. *Cell Death Differ.* May 2022;29(5):1042-1054.
- [42] Wang L, You X, Ruan D, et al. TET enzymes regulate skeletal development through increasing chromatin accessibility of RUNX2 target genes. *Nat Commun.* Aug 11 2022;13(1):4709.
- [43] Wang K, Liu H, Hu Q, et al. Epigenetic regulation of aging: implications for interventions of aging and diseases. *Signal Transduct Target Ther.* Nov 7 2022;7(1):374.
- [44] Ramakrishnan M, Papolu PK, Satish L, et al. Redox status of the plant cell determines epigenetic modifications under abiotic stress conditions and during developmental processes. *J Adv Res.* Dec 2022;42:99-116.
- [45] McClellan BL, Haase S, Nunez FJ, et al. Impact of epigenetic reprogramming on antitumor immune responses in glioma. *J Clin Invest.* Jan 17 2023;133(2).
- [46] Church MC, Price A, Li H, Workman JL. The Swi-Snf chromatin remodeling complex mediates gene repression through

- metabolic control. *Nucleic Acids Res.* Oct 27 2023;51(19):10278-10291.
- [47] Ji R, Chen J, Xie Y, et al. Multi-omics profiling of cholangiocytes reveals sex-specific chromatin state dynamics during hepatic cystogenesis in polycystic liver disease. *J Hepatol.* Apr 2023;78(4):754-769.
- [48] Baxter AE, Huang H, Giles JR, et al. The SWI/SNF chromatin remodeling complexes BAF and PBAF differentially regulate epigenetic transitions in exhausted CD8(+) T cells. *Immunity.* Jun 13 2023;56(6):1320-1340.e1310.
- [49] Gonzalez-Rodriguez P, Fullgrabe J, Joseph B. The hunger strikes back: an epigenetic memory for autophagy. *Cell Death Differ.* Jun 2023;30(6):1404-1415.
- [50] Wang B, Zhao T, Chen XX, et al. Gestational 1-nitropyrene exposure causes anxiety-like behavior partially by altering hippocampal epigenetic reprogramming of synaptic plasticity in male adult offspring. *J Hazard Mater.* Jul 5 2023;453:131427.
- [51] Chen CCL, Andrade AF, Jabado N. SMARCA4 vulnerability in H3K27M midline glioma: A silver bullet for a lethal disease. *Mol Cell.* Jan 19 2023;83(2):163-164.
- [52] Pascual-Carreras E, Marin-Barba M, Castillo-Lara S, et al. Wnt/beta-catenin signalling is required for pole-specific chromatin remodeling during planarian regeneration. *Nat Commun.* Jan 18 2023;14(1):298.
- [53] Penagos-Puig A, Claudio-Galeana S, Stephenson-Gussinye A, et al. RNA polymerase II pausing regulates chromatin organization in erythrocytes. *Nat Struct Mol Biol.* Aug 2023;30(8):1092-1104.
- [54] Ranasinghe A, Holohan M, Borger KM, et al. Altered Smooth Muscle Cell Histone Acetylome by the SPHK2/S1P Axis Promotes Pulmonary Hypertension. *Circ Res.* Sep 29 2023;133(8):704-719.
- [55] Yu PC, Hou D, Chang B, et al. SMARCA5 reprograms AKR1B1-mediated fructose metabolism to control leukemogenesis. *Dev Cell.* Aug 5 2024;59(15):1954-1971.e1957.
- [56] Yu X, Li S. Specific regulation of epigenome landscape by metabolic enzymes and metabolites. *Biol Rev Camb Philos Soc.* Jun 2024;99(3):878-900.
- [57] Chang CH, Liu F, Militi S, et al. The pRb/RBL2-E2F1/4-GCN5 axis regulates cancer stem cell formation and G0 phase entry/exit by paracrine mechanisms. *Nat Commun.* Apr 27 2024;15(1):3580.
- [58] Lopez-Moyado IF, Ko M, Hogan PG, Rao A. TET Enzymes in the Immune System: From DNA Demethylation to Immunotherapy, Inflammation, and Cancer. *Annu Rev Immunol.* Jun 2024;42(1):455-488.
- [59] Zhang M, Wu K, Zhang W, et al. The therapeutic potential of targeting the CHD protein family in cancer. *Pharmacol Ther.* Apr 2024;256:108610.
- [60] Wang Y, Liu H, Zhang M, et al. Epigenetic reprogramming in gastrointestinal cancer: biology and translational perspectives. *MedComm* (2020). Sep 2024;5(9):e670.
- [61] Pane R, Laib L, Formoso K, et al. Macromolecular Complex Including MLL3, Carabin and Calcineurin Regulates Cardiac Remodeling. *Circ Res.* Jan 5 2024;134(1):100-113.
- [62] Wilfahrt D, Delgoffe GM. Metabolic waypoints during T cell differentiation. *Nat Immunol.* Feb 2024;25(2):206-217.
- [63] Li Q, Duncan S, Li Y, Huang S, Luo M. Decoding plant specialized metabolism: new mechanistic insights. *Trends Plant Sci.* May 2024;29(5):535-545.
- [64] Saito Y, Harada A, Ushijima M, et al. Plasma cell differentiation is regulated by the expression of histone variant H3.3. *Nat Commun.* Jun 20 2024;15(1):5004.
- [65] Zhao T, Huang CQ, Zhang YH, et al. Prenatal 1-Nitropyrene Exposure Causes Autism-Like Behavior Partially by Altering DNA Hydroxymethylation in Developing Brain. *Adv Sci (Weinh).* Jul 2024;11(28):e2306294.
- [66] Merkuri F, Rothstein M, Simoes-Costa M. Histone lactylation couples cellular metabolism with developmental gene regulatory networks. *Nat Commun.* Jan 2 2024;15(1):90.
- [67] Liu Y, Xu X, He C, et al. Chromatin loops gather targets of upstream regulators together for efficient gene transcription regulation during vernalization in wheat. *Genome Biol.* Dec 3 2024;25(1):306.
- [68] Sahu V, Lu C. Metabolism-driven chromatin dynamics: Molecular principles and technological advances. *Mol Cell.* Jan 16 2025;85(2):262-275.

- [69] Schroder CM, Zissel L, Mersiowsky SL, et al. EOMES establishes mesoderm and endoderm differentiation potential through SWI/SNF-mediated global enhancer remodeling. *Dev Cell*. Mar 10 2025;60(5):735-748.e735.
- [70] van der Knaap JA, Verrijzer CP. Moonlighting Enzymes at the Interface Between Metabolism and Epigenetics. *Annu Rev Biochem*. Mar 17 2025.
- [71] Ying Z, Xin Y, Liu Z, et al. The mitochondrial unfolded protein response inhibits pluripotency acquisition and mesenchymal-to-epithelial transition in somatic cell reprogramming. *Nat Metab*. Apr 9 2025.
- [72] Shutta KH, Weighill D, Burkholz R, et al. DRAGON: Determining Regulatory Associations using Graphical models on multi-Omic Networks. *Nucleic Acids Res*. Feb 22 2023;51(3):e15.
- [73] Jin MZ, Jin WL. Spatial epigenome-transcriptome comapping technology. *Trends Cell Biol*. Jun 2023;33(6):449-450.
- [74] Zhang Z, Sun H, Mariappan R, et al. scMoMaT jointly performs single cell mosaic integration and multi-modal bio-marker detection. *Nat Commun*. Jan 24 2023;14(1):384.
- [75] Keating ST, El-Osta A. Metaboloepigenetics in cancer, immunity, and cardiovascular disease. *Cardiovasc Res*. Mar 31 2023;119(2):357-370.
- [76] Li Y, Zhang D, Yang M, et al. scBridge embraces cell heterogeneity in single-cell RNA-seq and ATAC-seq data integration. *Nat Commun*. Sep 28 2023;14(1):6045.
- [77] Bi X, Cheng Y, Lv X, et al. A Multi-Omics, Machine Learning-Aware, Genome-Wide Metabolic Model of *Bacillus Subtilis* Refines the Gene Expression and Cell Growth Prediction. *Adv Sci (Weinh)*. Nov 2024;11(42):e2408705.
- [78] Ewald JD, Zhou G, Lu Y, et al. Web-based multi-omics integration using the Analyst software suite. *Nat Protoc*. May 2024;19(5):1467-1497.
- [79] Charidemou E, Kirmizis A. A two-way relationship between histone acetylation and metabolism. *Trends Biochem Sci*. Dec 2024;49(12):1046-1062.
- [80] Yang B, Meng T, Wang X, et al. CAT Bridge: an efficient toolkit for gene-metabolite association mining from multiomics data. *Gigascience*. Jan 2 2024;13.
- [81] Yang X, Mann KK, Wu H, Ding J. scCross: a deep generative model for unifying single-cell multi-omics with seamless integration, cross-modal generation, and in silico exploration. *Genome Biol*. Jul 29 2024;25(1):198.
- [82] Zhao G, Wang Y, Wang S, Li N. Comprehensive multi-omics analysis provides biological insights and therapeutic strategies for small-cell lung cancer. *MedComm (2020)*. Jun 2024;5(6):e569.
- [83] Liu J, Ma J, Wen J, Zhou X. A Cell Cycle-Aware Network for Data Integration and Label Transferring of Single-Cell RNA-Seq and ATAC-Seq. *Adv Sci (Weinh)*. Aug 2024;11(31):e2401815.
- [84] Schafer PSL, Dimitrov D, Villablanca EJ, Saez-Rodriguez J. Integrating single-cell multi-omics and prior biological knowledge for a functional characterization of the immune system. *Nat Immunol*. Mar 2024;25(3):405-417.
- [85] Hu Y, Wan S, Luo Y, et al. Benchmarking algorithms for single-cell multi-omics prediction and integration. *Nat Methods*. Nov 2024;21(11):2182-2194.
- [86] An J, Wang J, Kong S, et al. GametesOmics: A Comprehensive Multi-omics Database for Exploring the Gametogenesis in Humans and Mice. *Genomics Proteomics Bioinformatics*. May 9 2024;22(1).
- [87] Bernard MJ, Goldstein AS. A Metabolic-Epigenetic Mechanism Directs Cell Fate and Therapeutic Sensitivity in Breast Cancer. *Cancer Res*. May 2 2024;84(9):1382-1383.
- [88] Dou J, Tan Y, Kock KH, et al. Single-nucleotide variant calling in single-cell sequencing data with Monopogen. *Nat Biotechnol*. May 2024;42(5):803-812.
- [89] Liu M, Xu Y, Song Y, et al. Hierarchical Regulatory Networks Reveal Conserved Drivers of Plant Drought Response at the Cell-Type Level. *Adv Sci (Weinh)*. Mar 16 2025:e2415106.
- [90] Tost J, Ak-Aksoy S, Campa D, et al. Leveraging epigenetic alterations in pancreatic ductal adenocarcinoma for clinical applications. *Semin Cancer Biol*. Feb 2025;109:101-124.
- [91] Guo P, Mao L, Chen Y, et al. Multiplexed spatial mapping of chromatin features, transcriptome and proteins in tissues. *Nat Methods*. Mar 2025;22(3):520-529.

- [92] Sahu V, Lu C. Metabolism-driven chromatin dynamics: Molecular principles and technological advances. *Mol Cell*. Jan 16 2025;85(2):262-275.
- [93] Li J, Pan J, Wang L, Ji G, Dang Y. Colorectal Cancer: Pathogenesis and Targeted Therapy. *MedComm* (2020). Mar 2025;6(3):e70127.
- [94] Makhani K, Yang X, Dierick F, et al. Single-Cell Multi-Omics Profiling of Immune Cells Isolated from Atherosclerotic Plaques in Male ApoE Knockout Mice Exposed to Arsenic. *Environ Health Perspect*. Jan 2025;133(1):17007.
- [95] Mao X, Xia D, Xu M, et al. Single-Cell Simultaneous Metabolome and Transcriptome Profiling Revealing Metabolite-Gene Correlation Network. *Adv Sci (Weinh)*. Jan 2025;12(4):e2411276.
- [96] Xie X, Liu W, Yuan Z, Chen H, Mao W. Bridging epigenomics and tumor immunometabolism: molecular mechanisms and therapeutic implications. *Mol Cancer*. Mar 8 2025;24(1):71.
- [97] Xu Y, De la Paz E, Paul A, et al. In-ear integrated sensor array for the continuous monitoring of brain activity and of lactate in sweat. *Nat Biomed Eng*. Oct 2023;7(10):1307-1320.
- [98] Lu J, Shang X, Yao B, et al. The role of CYP1A1/2 in cholesterol ester accumulation provides a new perspective for the treatment of hypercholesterolemia. *Acta Pharm Sin B*. Feb 2023;13(2):648-661.
- [99] Liu Y, Liu S, Tomar A, et al. Autoregulatory control of mitochondrial glutathione homeostasis. *Science*. Nov 17 2023;382(6672):820-828.
- [100] Hicks KG, Cluntun AA, Schubert HL, et al. Protein-metabolite interactomics of carbohydrate metabolism reveal regulation of lactate dehydrogenase. *Science*. Mar 10 2023;379(6636):996-1003.
- [101] Nuse B, Holland T, Rauh M, Gerlach RG, Mattner J. L-arginine metabolism as pivotal interface of mutual host-microbe interactions in the gut. *Gut Microbes*. Jan-Dec 2023;15(1):2222961.
- [102] He L, Ding Y, Zhou X, Li T, Yin Y. Serine signaling governs metabolic homeostasis and health. *Trends Endocrinol Metab*. Jun 2023;34(6):361-372.
- [103] Brennan L, de Roos B. Role of metabolomics in the delivery of precision nutrition. *Redox Biol*. Sep 2023;65:102808.
- [104] Xu W, Wu Y, Xu Y, Cai X, Gu W, Zhu C. Metal-Organic Framework-Based Artificial Organelle Corrects Microenvironment Interference for Accurate Intratumoral Glucose Analysis. *Angew Chem Int Ed Engl*. Nov 20 2023;62(47):e202308827.
- [105] Moldakozhayev A, Gladyshev VN. Metabolism, homeostasis, and aging. *Trends Endocrinol Metab*. Mar 2023;34(3):158-169.
- [106] Alexandrov K, Vickers CE. In vivo protein-based biosensors: seeing metabolism in real time. *Trends Biotechnol*. Jan 2023;41(1):19-26.
- [107] Wilson N, Kataura T, Korsgen ME, Sun C, Sarkar S, Korolchuk VI. The autophagy-NAD axis in longevity and disease. *Trends Cell Biol*. Sep 2023;33(9):788-802.
- [108] Williams LM, Cao S. Harnessing and delivering microbial metabolites as therapeutics via advanced pharmaceutical approaches. *Pharmacol Ther*. Apr 2024;256:108605.
- [109] Nogueira M, Enfissi EMA, Price EJ, et al. Ketocarotenoid production in tomato triggers metabolic reprogramming and cellular adaptation: The quest for homeostasis. *Plant Biotechnol J*. Feb 2024;22(2):427-444.
- [110] Reghupaty SC, Dall NR, Svensson KJ. Hallmarks of the metabolic secretome. *Trends Endocrinol Metab*. Jan 2024;35(1):49-61.
- [111] Khan A, Unlu G, Lin P, et al. Metabolic gene function discovery platform GeneMAP identifies SLC25A48 as necessary for mitochondrial choline import. *Nat Genet*. Aug 2024;56(8):1614-1623.
- [112] Wang W, Wang Y, Su L, et al. Endothelial Cells Mediated by STING Regulate Oligodendrogenesis and Myelination During Brain Development. *Adv Sci (Weinh)*. Oct 2024;11(38):e2308508.
- [113] Nichols AR, Chavarro JE, Oken E. Reproductive risk factors across the female lifecourse and later metabolic health. *Cell Metab*. Feb 6 2024;36(2):240-262.
- [114] Axelrod CL, Hari A, Dantas WS, Kashyap SR, Schauer PR, Kirwan JP. Metabolomic Fingerprints of Medical Therapy

Versus Bariatric Surgery in Patients With Obesity and Type 2 Diabetes: The STAMPEDE Trial. *Diabetes Care*. Nov 1 2024;47(11):2024-2032.

- [115] Su T, He Y, Wang M, et al. Macrophage-Hepatocyte Circuits Mediated by Grancalcin Aggravate the Progression of Metabolic Dysfunction Associated Steatohepatitis. *Adv Sci (Weinh)*. Nov 2024;11(42):e2406500.
- [116] Kokkorakis M, Muzurovic E, Volcansek S, et al. Steatotic Liver Disease: Pathophysiology and Emerging Pharmacotherapies. *Pharmacol Rev*. May 2 2024;76(3):454-499.
- [117] Yan R, Zhang P, Shen S, et al. Carnosine regulation of intracellular pH homeostasis promotes lysosome-dependent tumor immunoevasion. *Nat Immunol*. Mar 2024;25(3):483-495.
- [118] Meijnikman AS, Nieuwdorp M, Schnabl B. Endogenous ethanol production in health and disease. *Nat Rev Gastroenterol Hepatol*. Aug 2024;21(8):556-571.
- [119] Yesian AR, Chalom MM, Knudsen NH, et al. Preadipocyte IL-13/IL-13Ralpha1 signaling regulates beige adipogenesis through modulation of PPARgamma activity. *J Clin Invest*. Apr 8 2025.
- [120] Sun P, Wang M, Chai X, et al. Disruption of tryptophan metabolism by high-fat diet-triggered maternal immune activation promotes social behavioral deficits in male mice. *Nat Commun*. Mar 2 2025;16(1):2105.

Efficacy and Safety of Vonoprazan-Based Bismuth-Containing Quadruple Therapy for Helicobacter Pylori Eradication: A Meta-Analysis

Saishu Dong¹, Xiong Zhenggui², Dingrong Yang², Tao Liu^{2*}

1.Tengchong Houqiao Health-center, Tengchong Yunnan, 679100, China

2.Tengchong People's Hospital, Tengchong, Yunnan, 679100, China

*Corresponding author: Tao Liu, 365354782@qq.com

Copyright: 2025 Author(s). This is an open-access article distributed under the terms of the Creative Commons Attribution License (CC BY-NC 4.0), permitting distribution and reproduction in any medium, provided the original author and source are credited, and explicitly prohibiting its use for commercial purposes.

Abstract: Aims: To compare the efficacy and safety of vonoprazan-based bismuth-containing quadruple therapy (VBCQ) versus proton pump inhibitor (PPI)-based bismuth-containing quadruple Therapy (PBCQ) for Helicobacter pylori eradication. **Methods:** We performed a systematic search in PubMed, Embase, Web of Science, Cochrane Library, CNKI, Wanfang databases for relevant randomized controlled trials up to March 2024. Meta-analysis by RevMan 5.4 software. **Results:** Ten randomized controlled trials were evaluated in this meta-analysis. In intention-to-treat (ITT) analysis and per-protocol (PP) analysis, the eradication rate of VBCQ was significantly higher than PBCQ [ITT overall eradication rate: 86.7% vs 82.8%, RR: 1.05, 95% CI (1.05, 1.09), $P < 0.05$; PP overall eradication rate: 92.0% vs 88.0%; RR = 1.05, 95% CI (1.05, 1.08), $P < 0.05$]. The incidence of adverse events in VBCQ was higher than PBCQ (36.7% vs 36.5%), there was no significant difference ($P > 0.05$). **Conclusions:** VBCQ has a higher eradication rate and comparable safety.

Keywords: Vonoprazan; Helicobacter Pylori; Proton Pump Inhibitor; Quadruple Therapy; Efficacy; Safety

Published: May 15, 2025

DOI: <https://doi.org/10.62177/apjcmr.v1i2.325>

Helicobacter pylori (H. pylori, Hp) infection has a global prevalence of approximately 50%, varying across regions and populations. In mainland China, over 500 million individuals are infected with Hp^[1]. Digestive diseases such as gastritis, peptic ulcer disease, and gastric cancer are closely associated with Hp infection. The "National Sixth Consensus" recommends eradication therapy for confirmed Hp infections in the absence of contraindications^[2]. Vonoprazan (VPZ), a potassium-competitive acid blocker (P-CAB), was introduced in China in December 2019. Compared to proton pump inhibitors (PPIs), VPZ offers more potent and prolonged acid suppression. The 2022 Chinese guidelines recommend a VPZ-based bismuth quadruple therapy for Hp eradication^[3]. However, the efficacy and safety differences between VPZ-based and PPI-based quadruple regimens remain unclear. Comparative studies between VPZ-based bismuth quadruple therapy (VBCQ) and PPI-based bismuth quadruple therapy (PBCQ) are limited, and the superiority of VPZ-based therapy in improving eradication rates remains uncertain. This study systematically analyzes randomized controlled trials (RCTs) comparing VPZ- and PPI-based bismuth quadruple therapies to provide evidence-based recommendations for clinical application.

1. Materials and Methods

1.1 Search Strategy

This study was registered in the International Prospective Register of Systematic Reviews (ID: CRD42024501043). Literature search was conducted up to March 2024 in both Chinese and English databases, including PubMed, Embase, Web of Science, Cochrane Library, China National Knowledge Infrastructure (CNKI), and Wanfang Database. Keywords used in the search included "Helicobacter pylori," "H. pylori," "Hp," "Vonoprazan," "TAK-438," "Potassium-competitive acid blocker," and "Quadruple".

1.2 Inclusion and Exclusion Criteria

Inclusion criteria:(1) Patients of any age or gender with confirmed Hp infection via the urea breath test (UBT), stool antigen test, or histopathological examination;(2) Treatment group receiving VBCQ for 14 days;(3) Control group receiving PBCQ for 14 days;(4) Primary outcome: Hp eradication rate; Secondary outcome: adverse event (AE) incidence;(5) RCTs.

Exclusion criteria:(1) Non-RCT studies;(2) Incomplete data or unavailable full text.

1.3 Literature Screening and Data Extraction

Two independent reviewers screened studies and extracted relevant data, including study author, location, sample size, treatment regimen, and eradication confirmation method. Discrepancies were resolved through discussion. The primary outcome was Hp eradication rate, analyzed via intention-to-treat (ITT) and per-protocol (PP) methods. The secondary outcome was AE incidence.

1.4 Quality Assessment

The methodological quality of RCTs was evaluated based on:(1) Randomization method;(2) Allocation concealment;(3) Blinding of participants and investigators;(4) Blinding of outcome assessors;(5) Completeness of outcome data;(6) Selective reporting;(7) Other potential biases.

1.5 Statistical Analysis

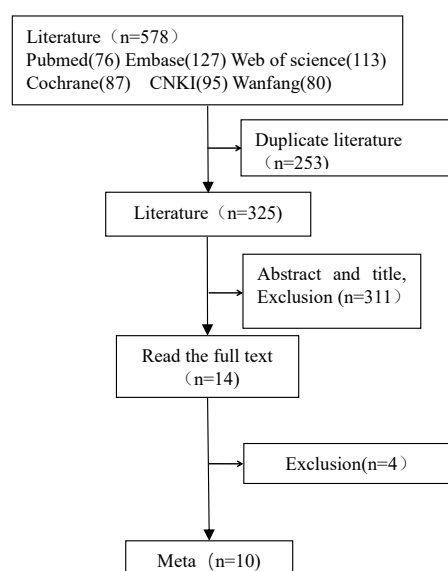
Risk ratio (RR) with a 95% confidence interval (CI) was used to assess eradication rates and safety. Heterogeneity was evaluated using I^2 statistics: $I^2 \leq 50\%$ indicated a fixed-effects model, while $I^2 > 50\%$ necessitated a random-effects model. A significance level of $P < 0.05$ was set. Funnel plots assessed publication bias. Sensitivity analysis was conducted by changing effect models. Data analysis was performed using RevMan 5.4 software.

2.Results

2.1 Literature Search Results

A total of 578 articles were obtained from the search, which were introduced into EndNote 20.6 and NoteExpress 3.7 literature manager. 253 duplicate articles were removed by software and manual removal. 311 articles were excluded from reviews, comments, letters, case reports and research contents, 4 articles were excluded, and 10 studies were finally included. Figure 1.

Figure 1. The literature search process



2.2 Characteristics of Included Studies

Ten studies (6 in English, 4 in Chinese) published between 2022 and 2024 were included^[4-13], involving 8 studies from China, 1 from South Korea, and 1 multinational East Asian study. Most studies confirmed Hp eradication using the ¹³C-UBT test. Table 1

Table 1 Basic characteristics of literature

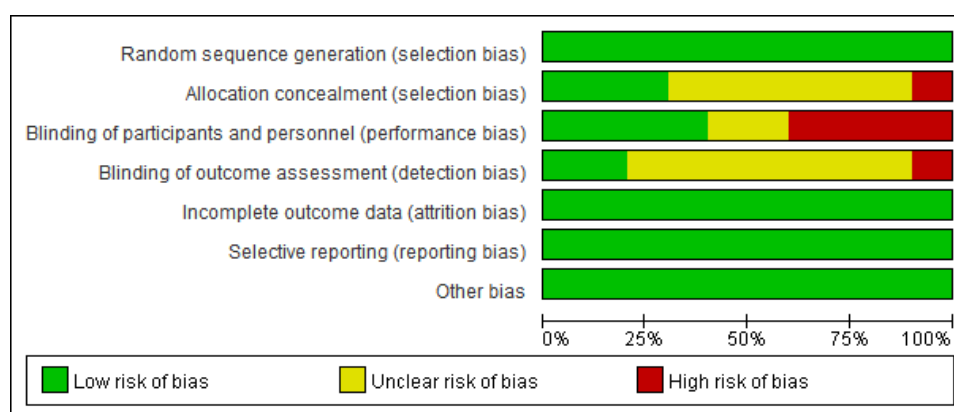
	Age	Country / region	Sample	experimental / control	VPZ	PPI	Confirmation of eradication
Chen et al[4]	18-75	China	90	45/45	V 20mg bid,14d	I 5mg bid,14d	¹³ C-UBT
Deng et al[5]	19-78	China	222	113/109	V 20mg qd,14d	R 20mg bid,14d	¹³ C-UBT
Hou et al[6]	≥18	East Asia	415	211/204	V 20mg bid,14d	L 30mg bid,14d	¹³ C-UBT
Huh et al[7]	18-60	Korea	30	15/15	V 20mg bid,14d	L 30mg bid,14d	¹³ C-UBT
Lian et al[8]	19-70	China	214	107/107	V 20mg bid,14d	E 20mg bid 14d	¹³ C-UBT
Li ea al[9]	60-75	China	60	30/30	V 20mg bid,14d	L 30mg bid,14d	¹³ C/ ¹⁴ C-UBT HpSAT
Lu et al[10]	18-65	China	156	78/78	V 20mg bid,14d	E 20mg bid,14d	¹³ C/ ¹⁴ C-UBT
Miao et al[11]	18-60	China	44	22/22	V 20mg bid,14d	E 20mg bid,14d	¹³ C-UBT
Ran et al[12]	20-70	China	160	80/80	V 20mg bid,14d	O 20mg bid,14d	¹³ C-UBT
Song et al[13]	≥18	China	510	256/254	V 20mg bid,14d	E 20mg bid,14d	¹³ C-UBT

Note: V: vororacin; E: esomeprazole; L: lansoprazole; O: omeprazole; R: rabeprazole; I: eprazole;; qd: 1 per day; bid: 2 per day; UBT urea breath test; HpSAT: antigen test for H. pylori stool.

2.3 Risk of Bias Assessment

All 10 studies implemented randomization. The risk of incomplete outcomes, selective reporting, and other biases was low, indicating high study quality. Figure 2.

Figure 2. Literature quality evaluation

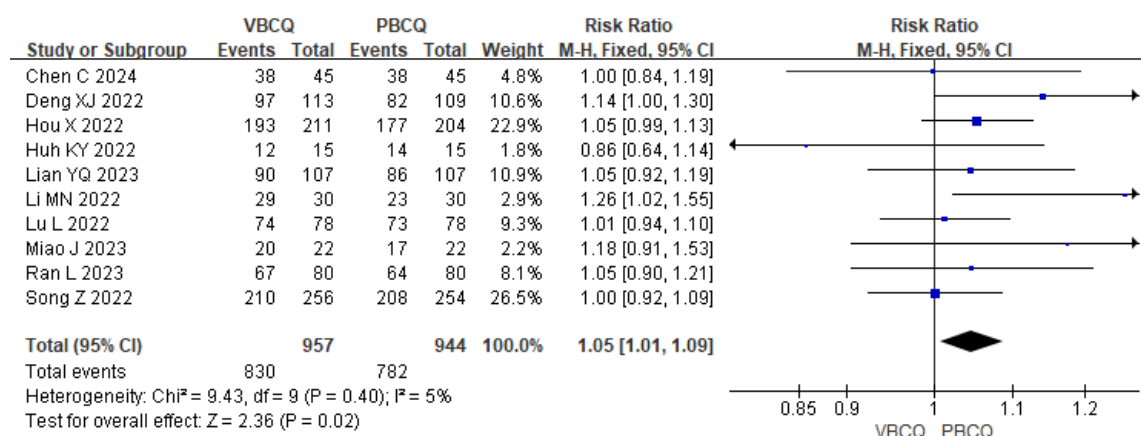


2.4 Meta-Analysis Results

2.4.1 Eradication Rate (ITT Analysis)

10 studies were included in the intention-to-treat (ITT) analysis. The eradication rates for VBCQ and PBCQ were 86.7% (830/957) and 82.8% (782/944), respectively. Heterogeneity testing indicated no significant variability among the studies ($I^2 = 5\%$, $P = 0.40$). The results from the fixed-effect model meta-analysis demonstrated that VBCQ had a significantly higher eradication rate compared to PBCQ (overall eradication rate: 86.7% vs. 82.8%, $RR = 1.05$, 95% CI: 1.01–1.09, $P < 0.05$), as shown in Figure 3.

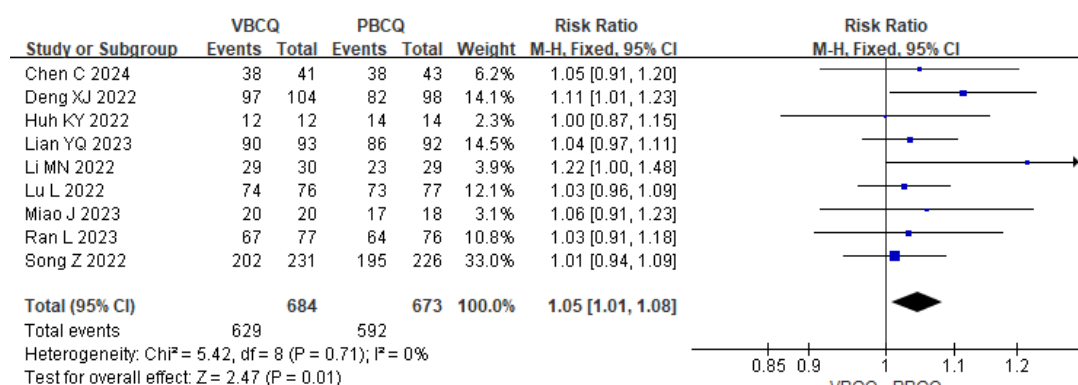
Figure 3. Forest plot of ITT analysis comparing eradication rates between VBCQ and PBCQ



2.4.2 Eradication Rate (PP Analysis)

9 studies were included in the per-protocol (PP) analysis. The eradication rates for VBCQ and PBCQ were 92.0% (629/684) and 88.0% (592/673), respectively. Heterogeneity testing indicated no significant differences among the studies ($I^2 = 0\%$, $P = 0.71$). The fixed-effect model meta-analysis showed that VBCQ had a higher eradication rate compared to PBCQ (overall eradication rate: 92.0% vs. 88.0%; $RR = 1.05$, 95% CI: 1.01–1.08, $P < 0.05$), Figure 4.

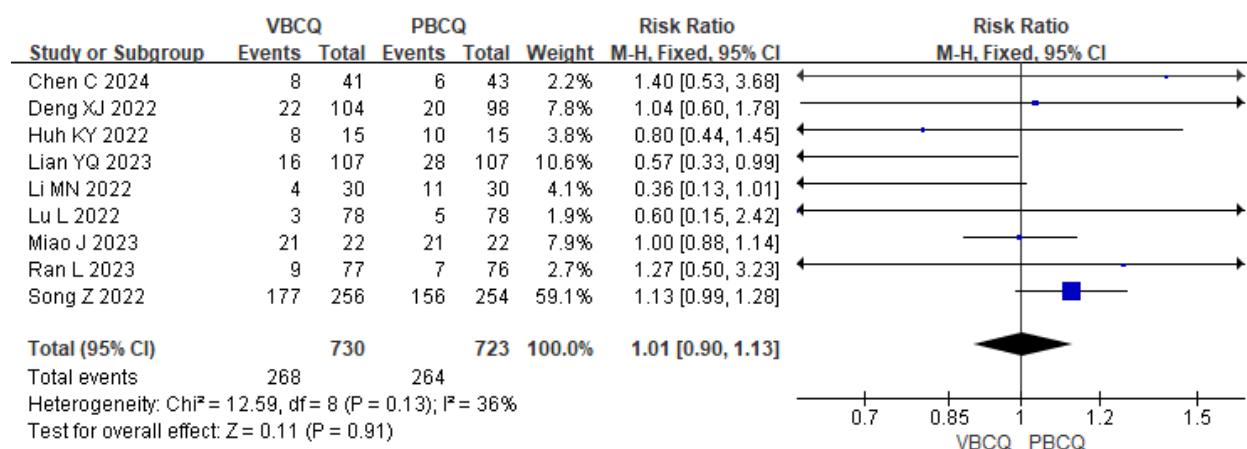
Figure 4. Forest plot of PP analysis comparing eradication rates between VBCQ and PBCQ



2.4.3 Safety Analysis

9 studies were included in the safety analysis. The incidence of adverse events for VBCQ and PBCQ was 36.7% (268/730) and 36.5% (264/723), respectively. Heterogeneity testing showed no significant differences among the studies ($I^2 = 36\%$, $P = 0.13$). The fixed-effect model meta-analysis indicated no significant difference in the incidence of adverse events between VBCQ and PBCQ (overall incidence: 36.7% vs. 36.5%; $RR = 1.01$, 95% CI: 0.90–1.13, $P > 0.05$), Figure 5.

Figure 5. Forest plot of safety analysis between VBCQ and PBCQ



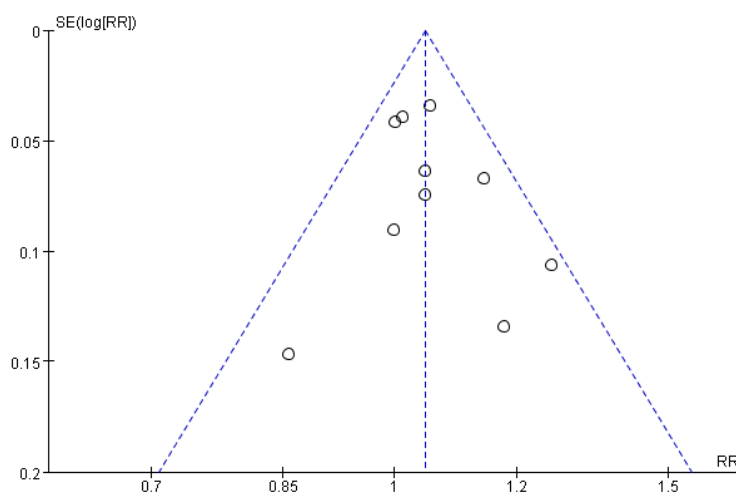
2.5 Sensitivity Analysis

Sensitivity analysis was conducted using model selection methods. In the ITT analysis, switching to a random-effects model in the meta-analysis still showed that the eradication rate of VBCQ was significantly higher than that of PBCQ ($P < 0.05$), consistent with the results from the fixed-effect model. In the PP analysis, the meta-analysis results remained consistent after switching to the random-effects model ($P < 0.05$). For the safety analysis, the results from the random-effects model also showed no significant difference, indicating that the findings are relatively stable.

2.6 Publication Bias

A funnel plot for studies comparing the eradication of *H. pylori* by VBCQ and PBCQ was generated using RevMan 5.4 software. The funnel plot indicated minimal publication bias, as the included studies were relatively symmetrically distributed on both sides of the plot (Figure 6).

Figure 6. Funnel plot of the efficacy of VBCQ versus PBCQ for *H. pylori* eradication (ITT analysis)



3. Discussion

The intragastric acid environment is a key factor influencing the eradication of *Helicobacter pylori* (Hp). Increasing gastric pH can enhance the bacterium's susceptibility to antibiotics^[14]. Compared with proton pump inhibitors (PPIs), vonoprazan (VPZ) exhibits a faster and more potent acid-suppressing effect. VPZ is primarily metabolized by cytochrome P450 enzyme CYP3A4^[15], and is thus less affected by CYP2C19 gene polymorphisms, which commonly influence the efficacy of PPIs. Studies have shown that VPZ suppresses gastric acidity more rapidly and effectively than lansoprazole^[16]. In recent years, the issue of antibiotic resistance in *H. pylori* has become increasingly severe, with resistance rates for metronidazole, clarithromycin, and levofloxacin rising significantly^[17–18], potentially reducing the effectiveness of eradication therapies. The introduction of potassium-competitive acid blockers (P-CABs) like VPZ may bring a paradigm shift in *H. pylori* eradication regimens. International consensus guidelines have also recommended the use of P-CABs for *H. pylori* eradication^[19–20]. Currently, the PPI-based bismuth-containing quadruple therapy (PBCQ) is the most widely used *H. pylori* eradication regimen in China. Compared with PBCQ, the widespread use of P-CAB-based therapies may improve eradication rates. As a representative P-CAB, VPZ has been the focus of a growing body of research, both domestically and internationally. In China, VPZ-based eradication regimens primarily include dual and quadruple therapies. Our research team has previously conducted a meta-analysis comparing a VPZ-amoxicillin dual therapy with the traditional PPI-based bismuth quadruple regimen, showing that the dual therapy was not inferior^[21]. However, whether VPZ-based bismuth quadruple therapy (VBCQ) can further improve eradication rates remains a subject of debate.

This meta-analysis included 10 randomized controlled trials, with low heterogeneity and minimal bias among the studies, indicating relatively stable results. Both ITT and PP analyses demonstrated that the eradication rate of VBCQ was higher than that of PBCQ. In terms of safety, there was no significant difference in adverse event rates between the two regimens. Compared with PBCQ, VBCQ increased eradication rates by 3.9% in ITT analysis and 4.0% in PP analysis. These findings support that VBCQ offers a higher eradication rate with acceptable tolerability.

Limitations: This study included only publications in Chinese and English, and the number of included studies was limited, with some having small sample sizes, potentially introducing bias. The safety analysis only assessed the overall incidence of adverse events and did not examine specific adverse reactions. Additionally, other types of P-CAB-based bismuth quadruple therapies were not included. Since all study populations were East Asian, the generalizability of the findings to other regions remains to be confirmed.

In conclusion, the results of this study suggest that VBCQ provides a higher eradication rate than PPI-based bismuth quadruple therapy, with comparable tolerability. VBCQ is recommended for the treatment of *H. pylori* infection. Further in-depth research is warranted to confirm these findings, and the potential of other P-CAB-based bismuth quadruple therapies in *H. pylori* eradication should also be explored.

Funding

no

Conflict of Interests

The authors declare that there is no conflict of interest regarding the publication of this paper.

Reference

- [1] Ren, S., Cai, P., Liu, Y., et al. (2021). Prevalence of *Helicobacter pylori* infection in China: A systematic review and meta-analysis. *Journal of Gastroenterology and Hepatology*, 37(3), 464–470.
- [2] *Helicobacter pylori* Study Group, Chinese Society of Gastroenterology, Chinese Medical Association. (2022). Sixth Chinese national consensus report on the management of *Helicobacter pylori* infection (treatment excluded). *Chinese Journal of Digestion*, 42(5), 289–303.
- [3] *Helicobacter pylori* Study Group, Chinese Society of Gastroenterology, Chinese Medical Association. (2022). 2022 Chinese national clinical practice guideline on *Helicobacter pylori* eradication treatment. *Chinese Journal of Digestion*, 42(11), 745–756.
- [4] Chen, C., Zhang, D., Huang, S., et al. (2024). Comparison of vonoprazan dual therapy, quadruple therapy and standard quadruple therapy for *Helicobacter pylori* infection in Hainan: A single-center, open-label, non-inferiority, randomized controlled trial. *BMC Gastroenterology*, 24(1), 131.
- [5] Deng, X. J., Wang, Z., Cheng, Z. Y., et al. (2022). Observation of efficacy of a novel potassium-competitive acid blocker vonoprazan in the treatment of *H. pylori* infection. *Chinese Journal of Integrated Traditional and Western Medicine on Digestion*, 30(11), 789–793.
- [6] Hou, X., Meng, F., Wang, J., et al. (2022). Vonoprazan non-inferior to lansoprazole in treating duodenal ulcer and eradicating *Helicobacter pylori* in Asian patients. *Journal of Gastroenterology and Hepatology*, 37(7), 1275–1283.
- [7] Huh, K. Y., Chung, H., Kim, Y. K., et al. (2022). Evaluation of safety and pharmacokinetics of bismuth-containing quadruple therapy with either vonoprazan or lansoprazole for *Helicobacter pylori* eradication. *British Journal of Clinical Pharmacology*, 88(1), 138–144.
- [8] Lian, Y. Q. (2023). *Clinical study of fourfold therapy with vonoprazan fumarate in the treatment of *Helicobacter pylori* [Master's thesis, Yichun University].
- [9] Li, M. N. (2022). Efficacy and safety of vonoprazan against *Helicobacter pylori* in the elderly [Master's thesis, Xi'an Medical University].
- [10] Lu, L., Wang, Y., Ye, J., et al. (2023). Quadruple therapy with vonoprazan 20 mg daily as a first-line treatment for *Helicobacter pylori* infection: A single-center, open-label, noninferiority, randomized controlled trial. *Helicobacter*, 28(1), e12940.
- [11] Miao, J., Hu, C., Tang, J., et al. (2023). Pharmacokinetics, safety, and tolerability of vonoprazan- or esomeprazole-based bismuth-containing quadruple therapy: A Phase 1, double-blind, parallel-group study in adults with *Helicobacter pylori* infection in China. *Clinical Pharmacology in Drug Development*, 12(10), 1036–1044.
- [12] Ran, L., Liu, L. L., Wang, Y., et al. (2023). Study on the efficacy of vonoprazan in the treatment of *Helicobacter pylori*.

- Journal of Modern Medicine and Health, 39(20), 3437–3441, 3448.
- [13] Song, Z., Du, Q., Zhang, G., et al. (2022). A randomized, double-blind, phase 3 study to evaluate the efficacy and safety of vonoprazan-based versus esomeprazole-based bismuth-containing quadruple therapy for the eradication of *Helicobacter pylori* infection in China. *United European Gastroenterology Journal*, 10, 42.
- [14] Han, Y. Y., Guan, J. L., Tian, D. A., et al. (2022). The role and research progress of acid suppressants in *Helicobacter pylori* infection eradication. *Chinese Journal of Digestion*, 42(6), 426–429.
- [15] Miftahussurur, M., Pratama, P. B., & Yamaoka, Y. (2020). The potential benefits of vonoprazan as *Helicobacter pylori* infection therapy. *Pharmaceuticals (Basel)*, 13(10), 276.
- [16] Laine, L., Sharma, P., Mulford, D. J., et al. (2022). Pharmacodynamics and pharmacokinetics of the potassium-competitive acid blocker vonoprazan and the proton pump inhibitor lansoprazole in US subjects. *American Journal of Gastroenterology*, 117(7), 1158–1161.
- [17] Wang, Y., Du, J., Zhang, D., et al. (2023). Primary antibiotic resistance in *Helicobacter pylori* in China: A systematic review and meta-analysis. *Journal of Global Antimicrobial Resistance*, 34, 30–38.
- [18] Hong, T. C., El-Omar, E. M., Kuo, Y. T., et al. (2024). Primary antibiotic resistance of *Helicobacter pylori* in the Asia-Pacific region between 1990 and 2022: An updated systematic review and meta-analysis. *Lancet Gastroenterology & Hepatology*, 9(1), 56–67.
- [19] Malfertheiner, P., Megraud, F., Rokkas, T., et al. (2022). Management of *Helicobacter pylori* infection: The Maastricht VI/Florence consensus report. *Gut*, 71, 1724–1762.
- [20] Chey, W. D., Howden, C. W., Moss, S. F., et al. (2024). ACG clinical guideline: Treatment of *Helicobacter pylori* infection. *American Journal of Gastroenterology*, 119(9), 1730–1753.
- [21] Liu, T., Zheng, S., Yang, J., et al. (2024). Efficacy and safety of vonoprazan-amoxicillin dual therapy for *Helicobacter pylori* eradication: A meta-analysis. *Journal of Hainan Medical University*, 30(16), 1259–1265.

The Role and Mechanism of Breviscapine in Ameliorating Diabetic Nephropathy

Zundan Ren¹, Yan Zhao^{2*}

1.Department of Endocrinology, The First Affiliated Hospital of Kunming Medical University, Kunming, 650000, China

2.Endocrinology Department of the First Affiliated Hospital of Dali University, Dali, 671000, China

**Corresponding author: Yan Zhao*

Copyright: 2025 Author(s). This is an open-access article distributed under the terms of the Creative Commons Attribution License (CC BY-NC 4.0), permitting distribution and reproduction in any medium, provided the original author and source are credited, and explicitly prohibiting its use for commercial purposes.

Abstracts: Diabetic nephropathy (DN) is one of the most serious complications of diabetes and a major cause of end-stage renal disease. However, due to the complexity of its pathogenesis, no new therapeutic drugs have been developed in the past 20 years, except for angiotensin-converting enzyme inhibitors (ACEIs) and angiotensin receptor blockers (ARBs). Breviscapine is a flavonoid active component isolated from *Erigeron breviscapus*, a member of the Asteraceae family. Pharmacological studies have confirmed that this compound has antioxidant stress, anti-inflammatory regulation, anti-fibrosis and neuroprotective effects. Currently, it is mainly used in clinical practice as an adjuvant treatment for ischemic stroke and non-alcoholic fatty liver disease. Notably, although its antioxidant and anti-fibrotic properties have been verified in organs such as the liver and lungs, the mechanism of action in the field of DN has not been fully elucidated, especially the regulatory effect on the interstitial transformation of renal tubular epithelial cells remains to be revealed. Our research group has for the first time systematically explored the molecular mechanism by which breviscapine improves high glucose-induced renal tubular fibrosis, providing a new theoretical basis for expanding its clinical application.

Keywords: Diabetic Nephropathy; Natural Products; Breviscapine; Fibrosis

Published: May 13, 2025

DOI: <https://doi.org/10.62177/apjcmr.v1i2.356>

1.Introduction

Diabetic nephropathy is the leading cause of chronic kidney disease, and in recent years, the high morbidity and mortality of patients with DN has attracted widespread attention. According to statistics, 30% of diabetic patients are affected by diabetic nephropathy, thus creating a huge burden on public health^[1]. Diabetic nephropathy is one of the most common microvascular complications of diabetes mellitus, defined as hyperglycemia-induced decline in renal function characterized by progressive decrease in glomerular filtration rate and persistent proteinuria^[2]. The lesions mainly accumulate the glomerular basement membrane, the tunica and tubular interstitial matrix, and the podocytes, leading to a decline in renal function^[3]. To date, diabetic nephropathy treatment and management strategies have primarily involved weight reduction, glycemic and blood pressure control, and the use of ACEIs or ARBs as first-line therapies, but they are single-targeted and insufficient to slow progression of diabetic nephropathy to end-stage renal disease^[4]. Therefore, the exploration of novel drugs for the treatment of diabetic nephropathy is a top priority for modern medical research. Natural products, mainly derived from herbal medicines, have long been used as a source of drugs for the treatment of various major diseases. To date, many experimental

studies have been made to support and validate the potential impact of natural products for clinical applications. Recently, a large number of natural products have been reported in preclinical studies to alleviate DN-induced renal diseases by modulating various biological signaling pathways^[5]. Several natural products have further shown beneficial efficacy in clinical trials for the treatment of diabetic nephropathy, which validates promising therapeutic strategies. Brevi-scapine (Bre) is a flavonoid component extracted and refined from marigold flowers with the chemical name of 4', 5, 6-trihydroxyflavone-7-glucuronide, which has been shown to have a wide range of pharmacological effects such as antioxidant, vascular endothelial cell protection, antithrombotic, and protection of brain tissues, and is clinically used in cerebral infarction, Cerebral hemorrhage, stroke, coronary heart disease and other ischemic cardiovascular and cerebrovascular diseases and the treatment of diabetes mellitus. Previous studies have initially shown that calendulin can regulate the disorders of glucose and lipid metabolism, enhance insulin sensitivity, and have a certain therapeutic effect on insulin resistance, but its deep-rooted pharmacological material basis and its mechanism of action can not yet be fully elucidated^[6]. It has been found to have various pharmacological effects such as anti-inflammatory, antioxidant and anti-tumor effects, and can be used in the treatment of disorders of glucose and lipid metabolism such as diabetes mellitus, hyperlipidemia, and non-alcoholic fatty liver disease^[7]. The combination of calendulin and valsartan has been shown to have a protective effect on DN. Other studies have shown that calendulin combined with the angiotensin-converting enzyme inhibitor natripril ameliorates streptozotocin-induced DN. These studies suggest that calendulin is beneficial for patients with tangzhi metabolic disorders. However, whether it is effective in diabetic nephropathy is not known and our study was designed to explore this question.

2. Materials and methods

HK2 cells were purchased from ATCC and were cultured in low glucose DMEM/F12 medium (GIBCO, cat# A5670701) containing 10% FBS (GIBCO, cat# 11320033), 100 U/mL penicillin, 0.1 mg/mL streptomycin at 37°C in a 5% CO₂ incubator (Thermo Electron Corporation).

2.1 Cell Image Capture

HK2 cells were cultured with high glucose for 48 hours, and cell morphology was observed using photographs taken with a Nikon inverted microscope and Nikon digital camera system.

2.2 Cell viability assay

Cell viability was detected using the CCK8 kit (UElandy, cat# C6005S), HK2 cells were inoculated in 96-well culture plates at a suitable density per well, and after the cells grew adherently to the wall to about 80% confluence, 200 µL of treatment solution containing 1% DMSO (solvent control) and 10, 20, 40, 80 µM concentration gradients of Bre (dissolved in the medium) were added, respectively. that intervened for 24 hours; the Con group (blank control group) was not treated with drugs only maintained in basal medium culture. At the end of the intervention, the drug-containing medium was discarded, and 100 µL of freshly prepared CCK8 assay mixture (basal medium mixed with CCK8 reagent at a ratio of 9:1 by volume) was added to each well, which was incubated for 1 h at 37°C under 5% CO₂ and protected from light. After the incubation was completed, 70 µL of reaction solution per well was aspirated and transferred to a new 96-well plate, and the absorbance of each well was measured at 492 nm using an enzyme labeling instrument, and the relative cell survival rate of each treatment group was calculated using the Con group as the reference (100% survival rate).

2.3 Western blot

Cell samples were analyzed by western blot to determine the expression levels of fibronectin Col1α1 and FN1. Cells were washed with PBS and homogenized in RIPA lysis buffer containing protease inhibitors. Protein concentration was determined by BCA assay (Biyuntian, China). Equal amounts of proteins were loaded and electrophoresed on sodium dodecyl sulfate-polyadenosine-amide gel electrophoresis (SDS-PAGE). Proteins were transferred to PVDF membranes and incubated overnight at 4 °C with anti-Col1α (1:1000, HUABIO, Cat# ET1609-68), anti-FN1 (1:1000, HUABIO, Cat# HA211024), and Tublin (1:2000, HUABIO, Cat# ET1602-4). The membranes were then incubated with horseradish peroxidase (HRP)-coupled secondary antibodies for 2 hours at room temperature. The intensity of the bands was analyzed semi-quantitatively by ImageJ software, and values were normalized using β-actin bands as a loading control.

2.4 Statistical analysis

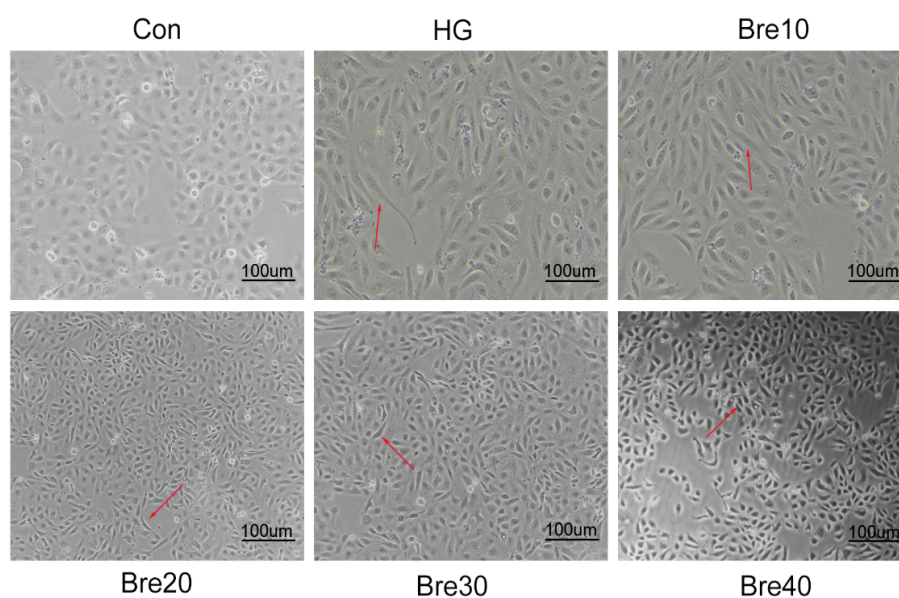
All data are expressed as mean \pm standard deviation (SD). Between-group differences between the two groups were assessed by t-test for unpaired students using Prism 6.0 software. P values less than 0.05 were considered statistically significant.

3.Results

3.1 Bre reverses cell morphology in high glucose

Under low-glycemic culture conditions, HK2 cells maintained a typical paving-stone-like phenotype, displaying a tight mosaic structure with polar arrangement and forming a continuous monolayer growth pattern with clear boundaries. In contrast, high glucose stimulation triggered significant pathological remodeling: the cells underwent transdifferentiation (L/D ratio > low glucose group), with approximately 60% of the cells assuming a spindle-shaped morphology, and the more 30% of the cells assuming an irregular polygonal conformation with blurred boundaries. Notably, after Bre (10-40 μ M, dose-dependent) intervention, the proportion of spindle-shaped cells in the high-glucose group was significantly reduced to, and the percentage of paving-stone-like cells was increased, and the cell area and L/D ratio of Bre (40 μ M) were not statistically different from those of the low-glucose control group, suggesting that the Bre intervention was effective in reversing the high-glucose-induced morphological abnormalities.

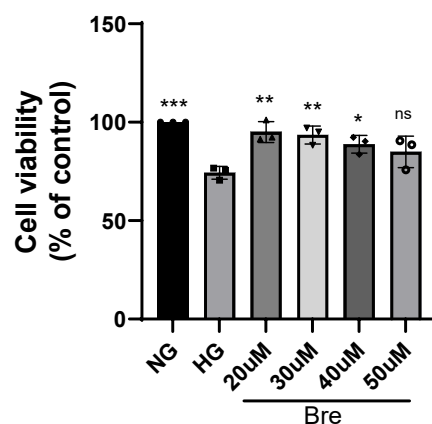
Fig.1 HG constructed a DN model and intervened with a series of concentrations of Bre to observe the changes in cell morphology. Con: control group; HG: model group and drug Bre group.



3.2 Bre improves HK2 cell viability due to high glucose

To assess the regulatory effect of Bre on HK2 cell activity, cell proliferation was systematically assayed using the CCK-8 assay. The experimental data showed that the cell viability was significantly lower than that of the control group after 48 h of treatment with high sugar environment (25 mM glucose). When Bre intervention was given in a dose-dependent manner (20-40 μ M), the cell viability showed a concentration-dependent increase, which was significantly higher than that of the high glucose group. Notably, when the Bre concentration was elevated to 50 μ M, the cell viability did not show a significant improvement effect, and the CC50 of Bre was 48.5 μ M (95% CI:45.3-51.7) obtained from the dose-effect curve, which may be related to the mitochondrial toxicity induced by the high Bre concentration (e.g., 1.8-fold elevation of the ROS level), which is consistent with the similar polyphenols cytotoxicity thresholds reported by the previous studies. This phenomenon may be related to the mitochondrial toxicity triggered by high concentration of Bre (e.g. 1.8-fold increase in ROS level), which is consistent with the cytotoxicity threshold of similar polyphenols reported in previous studies, and the mechanism will be investigated in subsequent studies by using gradient concentration (10-45 μ M). false

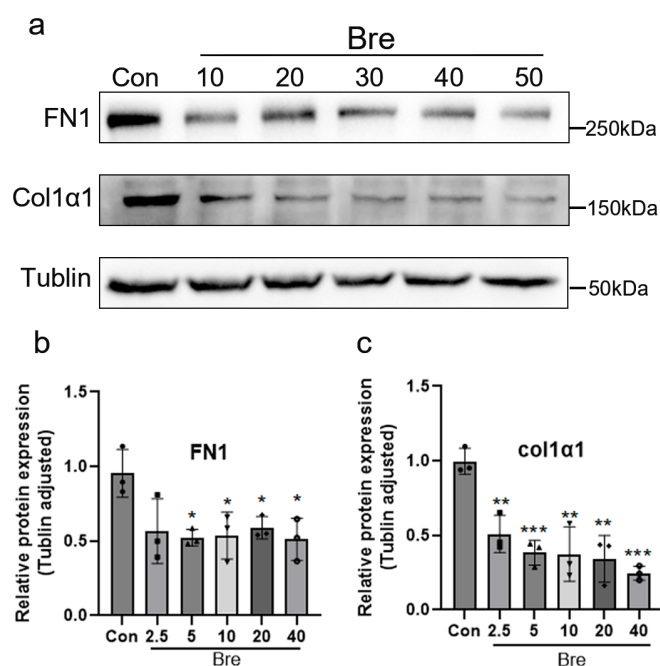
Fig.2 CCK8 Assay Kit detects the normalized value of HK2 cell viability after intervention with a series of Bre concentrations.



3.3 Bre improves inhibition of HK2 cell fibrosis

In the pathological process of diabetic nephropathy, progressive fibrosis driven by abnormal extracellular matrix deposition is a central pathological feature. To elucidate whether Bre has an antifibrotic effect, we assessed the expression of fibrotic markers in HK2 cells stimulated by Bre (10-50 μ M, 48 h) by Western blot system. Quantitative analysis showed that compared with the normal control group, the expression of FN1 and Col1 α 1 in the Bre group showed a significant dose-dependent inhibition after 48 h of intervention with gradient concentration of Bre (10-50 μ M), suggesting that Bre may inhibit extracellular matrix remodeling by regulating the EMT process.

Fig.3 Western blot detection of relative expression of HK2 fibrotic protein FN1 and Col1 α 1 with Tublin as an internal reference.



4. Discussion

Diabetic nephropathy is one of the most important microvascular complications of diabetes mellitus. Long-term chronic hyperglycemia leads to impaired renal function and structure, which in turn leads to a series of injuries such as thickening of the glomerular basement membrane, small arteriolar hyaluronidosis, dilatation of the tethered stroma, nodular glomerulosclerosis, fusion and loss of pedicle cell pedicle synapses, and structural damage to the glomerular filtration barrier^[8]. The pathogenesis of DN has not yet been clarified, and the known pathogenesis mainly focuses on the inflammatory

response, abnormalities in the RASS system, autophagy, oxidative stress, and the interaction between genetic factors and the environment^[9]. Glomerulosclerosis, tubulointerstitial fibrosis and podocyte injury are common final pathways leading to various progressive kidney injuries including DN^[10].

In the study of the pathogenesis of diabetic nephropathy, electron microscopic ultrastructural analysis revealed that the high glucose microenvironment (30 mM glucose, 72 h) induced characteristic phenotypic transformations in HK2 cells: (1) morphology showed a significant tendency of transdifferentiation, with an increase in the ratio of L/D and the formation of a typical fibroblast-like spindle-like conformation; (2) at the level of ultrastructural features, there was an increase in the proportion of the area of rough endoplasmic reticulum, a decrease in mitochondrial density and actin microfilament bundle remodeling; (3) at the pathological level, cytoskeletal remodeling was accompanied by enhanced expression of waveform protein and down-regulation of E-cadherin. This epithelial-mesenchymal transition (EMT) process is closely related to the activation of the TGF- β 1/Smad3 pathway, which forms a pro-fibrotic microenvironment through the secretion of extracellular matrix components, such as FN1 and Coll α 1, corroborating the central driving role of metabolic stress-induced transdifferentiation of renal tubular epithelial cells in diabetic renal fibrosis, and therefore, the change in HK2 cell morphology is closely related to fibrotic injury are closely related to^[11]. In this study, we found that after high glucose treatment, HK2 cells were transformed from paving-stone-like to long shuttle shape, and after Bre intervention, the cell morphology changes induced by high glucose could be improved, and most of the cells were still arranged in a cobblestone paving-like pattern, and the cell morphology changes were significantly reduced compared with that in the high glucose group; the cell morphology results showed that Bre could inhibit the high glucose-induced transdifferentiation of HK-2 cells, which suggested that Bre could improve the morphology changes of HK2 and thus improve the development of renal fibrosis and kidney injury. This suggests that Bre can improve the development of renal fibrosis and kidney injury by improving the morphology of HK2.

In this study, we investigated the mechanism of injury to renal tubular epithelial cells by chronic hyperglycemia and the intervention effect of Bre. The results showed that persistent high glucose exposure induced necrotic death of HK2 cells (a human renal tubular epithelial cell line) and significantly promoted the fibrotic process. The cell viability assessed by CCK-8 assay revealed that the cell survival rate in the high glucose-treated group was decreased compared with that in the control group, while the survival rate was restored to the level of the control group after Bre intervention. Notably, when the Bre concentration was increased to 50 μ M, its protective effect instead disappeared, suggesting that the compound may produce cytotoxic effects at high concentrations.

Renal fibrosis is a core pathologic mechanism in the course of diabetic nephropathy - abnormal deposition of extracellular matrix leading to tissue remodeling - and we next focus on the role of Bre on key regulatory proteins of fibrosis^[12]. As a key pathological feature in the progressive deterioration of diabetic nephropathy, renal interstitial fibrosis is mainly characterized by excessive accumulation of extracellular matrix proteins such as fibronectin (FN1) and type I collagen (Coll α 1), and this pathological deposition not only undermines the structural integrity of the renal tubules, but also creates a pro-fibrotic positive feedback loop^[13]. In order to analyze the anti-fibrotic molecular mechanism of Bre, we detected the changes in the expression profiles of matrix remodeling-related proteins by Western blot, and found that Bre significantly inhibited the synthesis of FN1 proteins in HK2 cells and reversed the aberrant deposition of Coll α 1 by modulating the balance of the related signaling pathways, which revealed the potential role of Bre in improving the renal microenvironmental homeostasis from the perspective of multiple targets. These findings reveal the potential of Bre to improve the microenvironmental homeostasis from a multi-target perspective.

In this study, the comprehensive protective effect of Bre on diabetic nephropathy was revealed through a multidimensional systematic evaluation: at the pathomorphological level, microscopic observation showed that Bre intervention significantly reversed the high glucose-induced morphological changes in renal tubular epithelial cells, and restored the cellular L/D ratio to normal; at the cellular function level, based on the CCK-8 assay, it was confirmed that Bre increased the survival rate of high glucose-injured cells from the normal level to the high glucose-injured cells. At the level of molecular mechanism, by constructing the TGF- β 1/Smad3-ECM metabolic regulation axis model, it was found that Bre could simultaneously down-

regulate the expression of pro-fibrotic factors, such as FN1 and Coll α 1. These findings illustrate the new mechanism of Bre's renal protection through interfering with the "morphology-function-substrate metabolism" cascade, from the three levels of tissue structure repair, cell function maintenance to molecular network regulation.

Funding

no

Conflict of Interests

The authors declare that there is no conflict of interest regarding the publication of this paper.

References

- [1] SAMSU N. Diabetic Nephropathy: Challenges in Pathogenesis, Diagnosis, and Treatment [J]. BioMed Research International, 2021, 2021: 1497449.
- [2] MARTÍNEZ-CASTELAO A, NAVARRO-GONZÁLEZ J F, GÓRRIZ J L, et al. The Concept and the Epidemiology of Diabetic Nephropathy Have Changed in Recent Years [J]. J Clin Med, 2015, 4(6): 1207-16.
- [3] CHEN H Y, ZHONG X, HUANG X R, et al. MicroRNA-29b inhibits diabetic nephropathy in db/db mice [J]. Mol Ther, 2014, 22(4): 842-53.
- [4] KANASAKI K, TADURI G, KOYA D. Diabetic nephropathy: the role of inflammation in fibroblast activation and kidney fibrosis [J]. Front Endocrinol (Lausanne), 2013, 4: 7.
- [5] YARIBEYGI H, SIMENTAL-MENDÍA L E, BUTLER A E, et al. Protective effects of plant-derived natural products on renal complications [J]. Journal of cellular physiology, 2019, 234(8): 12161-72.
- [6] WEN L, HE T, YU A, et al. Breviscapine: A Review on its Phytochemistry, Pharmacokinetics and Therapeutic Effects [J]. The American journal of Chinese medicine, 2021, 49(6): 1369-97.
- [7] GAO J, CHEN G, HE H, et al. Therapeutic Effects of Breviscapine in Cardiovascular Diseases: A Review [J]. Frontiers in pharmacology, 2017, 8: 289.
- [8] BAYLISS G, WEINRAUCH L A, D'ELIA J A. Pathophysiology of obesity-related renal dysfunction contributes to diabetic nephropathy [J]. Current diabetes reports, 2012, 12(4): 440-6.
- [9] NOWAK K L, JOVANOVIĆ A, FARMER-BAILEY H, et al. Vascular Dysfunction, Oxidative Stress, and Inflammation in Chronic Kidney Disease [J]. Kidney360, 2020, 1(6): 501-9.
- [10] TONOLO G, CHERCHI S. Tubulointerstitial disease in diabetic nephropathy [J]. International journal of nephrology and renovascular disease, 2014, 7: 107-15.
- [11] XIAO L, XU X, ZHANG F, et al. The mitochondria-targeted antioxidant MitoQ ameliorated tubular injury mediated by mitophagy in diabetic kidney disease via Nrf2/PINK1 [J]. Redox biology, 2017, 11: 297-311.
- [12] LI X, LU L, HOU W, et al. Epigenetics in the pathogenesis of diabetic nephropathy [J]. Acta biochimica et biophysica Sinica, 2022, 54(2): 163-72.
- [13] KARIHALOO A. Anti-fibrosis therapy and diabetic nephropathy [J]. Current diabetes reports, 2012, 12(4): 414-22.

Comparative Analysis of Golden Gate and Classical Cloning Techniques in *E. coli*: A Study in Molecular Cloning Efficiency

Ziyao Liu*

School of biochemistry, University of Edinburgh, Edinburgh, EH8 9YL, UK

*Corresponding author: Ziyao Liu, ziyao010220@outlook.com

Copyright: 2025 Author(s). This is an open-access article distributed under the terms of the Creative Commons Attribution License (CC BY-NC 4.0), permitting distribution and reproduction in any medium, provided the original author and source are credited, and explicitly prohibiting its use for commercial purposes.

Abstract: Molecular cloning remains a cornerstone technique in genetic engineering and synthetic biology. In this study, we conducted a systematic comparative analysis between the classical cloning method and the Golden Gate assembly technique, utilizing *Escherichia coli* as the model organism. Through polymerase chain reaction (PCR) amplification, restriction enzyme digestion, ligation, transformation, and Sanger sequencing, we assessed the operational efficiency and cloning fidelity of both strategies. Our results demonstrated that Golden Gate assembly, leveraging type IIS restriction enzymes and simultaneous ligation, significantly enhanced cloning efficiency and precision, particularly for seamless multi-fragment assembly. In contrast, the classical cloning approach maintained certain advantages in simplicity and robustness for specific experimental conditions. Challenges encountered during transformation and sequencing highlighted the critical impact of technical accuracy on experimental outcomes. This study underscores the importance of selecting appropriate cloning methodologies tailored to experimental objectives and laboratory capabilities, providing a foundation for optimized molecular cloning workflows in future synthetic biology and biotechnology applications.

Keywords: Golden Gate Assembly; Classical Cloning; *Escherichia Coli*; Molecular Cloning; DNA Assembly; Recombinant DNA Technology; Transformation Efficiency; Synthetic Biology

Published: May 25, 2025

DOI: <https://doi.org/10.62177/apjcmr.v1i2.412>

1. Introduction

DNA recombination and cloning techniques are among the most fundamental techniques in molecular biology and are achieved by artificial means. It is widely used in various fields related to genetic manipulation and is central to synthetic biology experiments^[1]. This experimental study compares the methodologies of the Golden Gate technique and the classical technique for DNA assembly, revealing the characteristics of the two methods. Compared to Classic technology, Golden Gate technology is very effective in accurately assembling multiple DNA fragments, especially when precise and seamless DNA assembly is required, such as in protein engineering; however, the method's dependence on specific types of restriction enzymes may limit its flexibility^[2]. This will help to provide a basis for the selection of the most appropriate method based on the needs of the specific project and the expertise of the laboratory.

In addition, *E. coli* was used as the growth environment in this experiment. As an important tool in scientific research, *E. coli* has simple cultivation and genetic manipulation, its fast growth rate, its low cost, and its importance for the study of many basic biological processes^[3]. *E. coli* strains commonly used in laboratories are usually harmless and fall into a low biosafety

risk category, facilitating safe laboratory practices. The goal of this experiment was to utilize recombinant DNA methods to insert two gene segments into a plasmid vector—employing classic cloning and Golden Gate technology respectively. The modified vectors were then introduced into *Escherichia coli*, with the ultimate step involving the examination of the DNA sequences obtained.

2. Methods and Material

2.1 Amplification of DNA fragments

PCR reactions were set, reactants were made by adding the following reagents: 1× Q5 reaction buffer (New England Biolabs), 0.2 mM dNTP mix, 0.5 μM Forward primer, 0.5 μM Reverse primer; 0.01 ng/μL Template DNA (provided by University of Edinburgh); 20 units/mL Q5 DNA polymerase (New England Biolabs). Other unlabeled chemicals used were of the high grade available commercially.

2.2 Digestion of pGEX-6p-1 vector with restriction-enzyme

For restriction enzyme digest reaction: 5 tubes were set up following the given protocol, 3 remained incubating at 37°C overnight, then heat-inactivated at 65°C for 15 minutes; 2 tubes were heat-inactivated after 37°C water bath for 30 minutes. Tube 1 was set up with 3.7 μL sterile H₂O, 3 μL 10× CutSmart Buffer (New England Biolabs) and 3 μL 10× HcoRI-HF. Tube 2 was set up with 3.7 μL sterile H₂O, 3 μL 10× CutSmart Buffer (New England Biolabs) and 3 μL 10× XhoI. Tube 3 was set up with 10 μL each from both Tube 1 and Tube 2, and centrifuged briefly. These three tubes were incubated in a waterbath at 37 °C for 30 minutes. After 30 minutes, Tube 4 was set up with 10 μL Tube 1 and Tube 5 was set up with 10 μL Tube 2, then these two were heat inactivated at 65 °C for 15 minutes. The three remaining tubes remained incubating at 37 °C overnight and was heat-inactivated at 65 °C for 15 minutes the other day.

2.3 Preparation of agarose gel

0.8% w/v gels were assigned and made, the ratio was 0.8 mg agarose and 10 mL distilled water. When making gels, the given protocol was followed to ensure all agarose was fully dissolved, cooled for at least 10 minutes (cooled but still in a form of liquid) before adding gel stain. The given gel stain was diluted from 20000× to 1×, therefore, 5 μL of gel stain was added into the system.

2.4 Visualization of PCR product and vector after digestion

When visualizing and analyzing PCR product and vector digested by restriction enzymes by agarose gel electrophoresis, 0.8% w/v gels were assigned and made, the ratio was 0.8 mg agarose and 10 mL distilled water. When making gels, the given protocol was followed to ensure all agarose was fully dissolved, cooled for 10 minutes (cooled but still in a form of liquid). During the visualization of PCR product, 30 μL of PCR product, 10 μL of ladder and 10 μL of positive control group were added respectively. During the visualization of digested vectors, 5 μL of dye was added in each tube; therefore, the overall amount of solution injected was more than expected. The detailed amount that was added in the cube injected was 25 μL and 15 μL respectively.

2.5 Gel extraction of PCR products and digested vector; restriction-enzyme digest of PCR product for classical cloning; ligation of insert into pGEX-6P-1 vector

With the help of QIAquick Gel Extraction Kit from QIAGEN^[4, 5], DNA was extracted and purified from the gel slices from your PCR products and from the vector that was digested overnight with both restriction enzymes. Noted that ethanol was already been added to Buffer PE; collection tube was used instead of vacuum manifold; lid of a sterile Eppendorf tube should be carefully snapped off by scissors and kept safe and clean; volume of Buffer EB was changed to 35 μL and left for at least 2 minutes; do not discard the sample from the last step; keep the purified PCR products on ice.

6 μL H₂O (sterile, molecular biology grade), 15 μL purified PCR product, 3 μL 10× CutSmart Buffer (New England Biolabs), 3 μL 10× EcoRI-HF (New England Biolabs) and 3 μL 10× XhoI (New England Biolabs) were used during the restriction-enzyme digest of PCR product. After setting up the reaction, it was incubated overnight at 37 °C, then heated inactivated at 65 °C for 15 minutes.

After that, the PCR product was purified for classical cloning using a QIAquick PCR Purification Kit from QIAGEN. Noted that ethanol had already been added to Buffer PE; pH indicator had already been added to Buffer PB; collection tube was

used instead of vacuum manifold; use scissors to carefully snip off the lid of a sterile 1.5 ml Eppendorf tube; lid of a sterile Eppendorf tube should be carefully snipped off by scissors and kept safe and clean for ligation and placed on ice to pre-chill; the volume of Buffer EB was changed 35 μ L during the last step and left for at least 2 minutes; flow-through was kept.

2.6 Golden Gate Assembly

Four reactions (one reaction and three controls) were set, each with a final volume of 20 μ L, using the table below: one reaction and three controls. One reaction was set up with everything needed, including 1 μ L vector (provided by the University of Edinburgh), 1 μ L PCR product (provided by the University of Edinburgh), 14 μ L sterile H₂O, 2 μ L 10 \times DNA ligase buffer (New England Biolabs), 1 μ L BsaI and 1 μ L T4 DNA Ligase. For the other three control groups, one was set up with everything needed except for PCR product, one was set up with everything needed except for BsaI enzyme, one was set up with everything needed except for T4 DNA Ligase. Each reaction was mixed gently by pipetting up and down slowly (the pipette was set at no more than 10 μ L), then centrifuged briefly. PCR thermal cycler program was carried out for 90 minutes.

2.7 Transformation of both ligated vectors into E.coli

For each ligation reaction: 10 μ L of ligation reaction was transferred to new pre-chilled Eppendorf and returned to ice; 100 μ L of competent cells were transferred carefully and returned to ice.

For classical cloning only, two control groups were prepared similarly: For negative control, only 50 μ L cells was added; for positive control: 50 μ L competent cells was transferred to tube containing 1 μ L uncut vector.

Then, each ligation reaction was incubated on ice for 15 minutes. The cells were heat shocked at 42 °C for 1 minute and returned to ice for 1 minute.

After that, 250 μ L SOC was added and the sample was mixed intermittently by gently inverting the tube.

During the procedure of pouring LB agar, 0.25 mL volume of each antibiotic (kanamycin for pETGG and carbenicillin for pGEX-6P-1) was added to LB agar and mixed by swirling or rolling the bottle gently, avoiding introduction of air-bubbles, after that, each plate was poured and contained about 10 mL LB (provided by University of Edinburgh). Then, waited for about 15 minutes for the agar to chill, and 50 μ L of competent cells was pipetted carefully into the center of a plate and spread the solution carefully with the sterile blue spreaders. The remaining cells were concentrated and spined for 1 minute at 6000 rpm to pellet; cells were resuspended and spread onto a fresh plate. Finally, plates were transferred to a 37 °C incubator and colonies were picked to set up overnight 5 mL LB/antibiotic in a 50 ml Falcon tube for further sequencing step.

2.8 Extraction of DNA and Preparation for Sanger Sequencing

From the 5 mL cultures using a QIAprep Spin Miniprep Kit from QIAGEN, DNA was extracted and purified. Noted that there were some differences made in the handbook: LyseBlue reagent was used; RNase A has already been added to Buffer P1; Ethanol has already been added to Buffer PE; in step 1, the centrifugation conditions were changed to 4000 rpm for 10 minutes; discard the supernatant when it was clear without disturbing the cell pellet; then the pellet was centrifuged again at 4000 rpm for 10 minutes; the remaining supernatant was removed carefully with a pipette; in step 2, the cell pellet was resuspended by gently pipetting the liquid up and down; after step 9, the column was left to dry in air for approximately 15 minutes; the lid off a sterile Eppendorf tube was snipped and the QIAquick column was placed in the tube; the lid was stored somewhere clean; in step 10 Buffer EB was changed to 35 μ L and left for at least 2 minutes, before eluting DNA by centrifuging; flow-through was kept this time. Before sanger sequencing, samples were prepared by setting two tubes per pair. The concentration of purified DNA using the Nanodrop was 83.381 μ g/mL for Classic technology and 159.26 μ g/mL for Golden Gate method. Therefore, 15 μ L and 7.8 μ L of sterile water were added respectively.

For the sequencing reaction, each plasmid requires two primers, one forward (For) and one reverse (Rev): pGEX 6P-1 (For) and pGEX 6P-1(Rev) for the pGEX 6P-1 vector; T7 promoter (For) and T7 terminator (Rev) for the pET28GG vector. Labelled samples and these primers were sent for sequencing at DNA sequencing and Services at the Medical Sciences Institute in Dundee.

3. Results

3.1 Overall molecular cloning using Classic technology

3.1.1 Restriction-enzyme digest of pGEX-6P-1 vector by both EcoRI-HF and XhoI enzymes as well as its

visualization by agarose gel electrophoresis

Compare the visualization results of PCR products with predicted length: The control group of Classic method (C150) ran faster than that from Golden Gate method (GG150). Moreover, in Lane 1, the band was almost invisible, only a very faint band was visible at slightly above 100 bp. There were no bright band in Lane 3, Lane 4. For Lane 5 and Lane 6, Lane 5 was close to the control group of GG150 at 100 bp, while the band in Lane 6 was much wider than that in Lane 5. As for the ladder, the bands were diffuse and smeared, which was not ideal. (Figure 3).

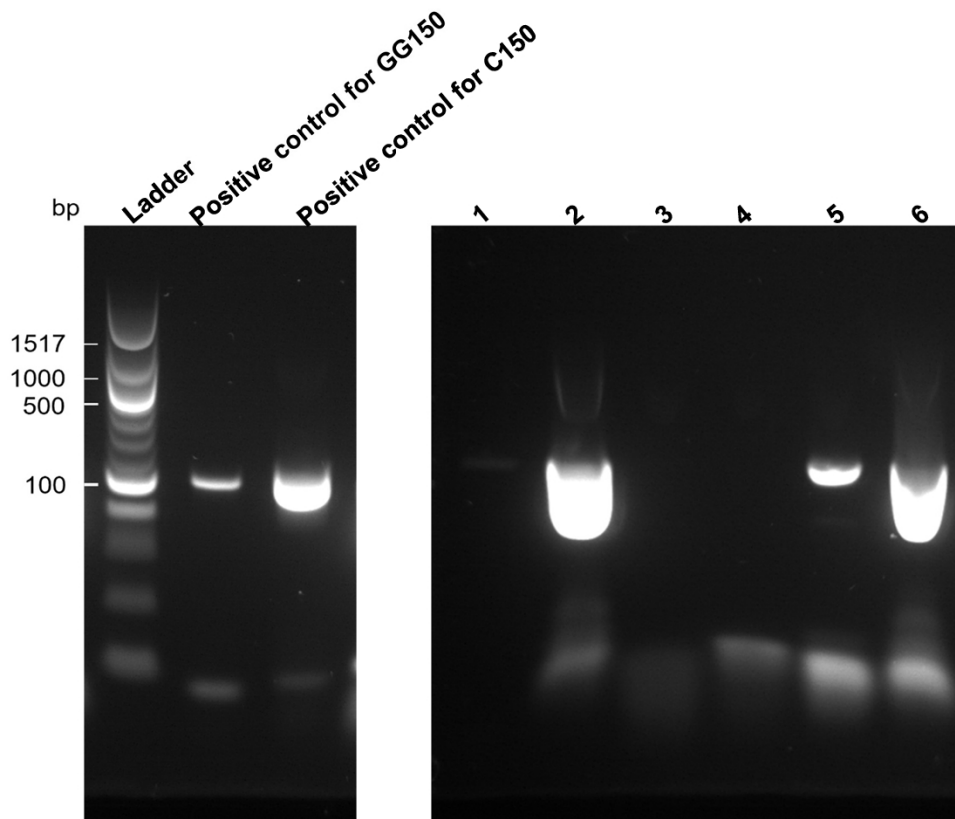


Figure 3. 1.2 % agarose for PCR products Lane 1, Lane 2 stood for PCR products gained from Classic technology; Lane 3, Lane 4 stood for PCR products gained from Golden Gate technology; while Lane 1 and Lane were added with excess dNTPs. With the given length of pGEX-6P-1 vector of 4984 bp, the digested pGEX-6P-1 vector by both EcoRI-HF and XhoI enzymes was expected to be 4969 bp (4984 bp minus 15 bp in Figure 4).

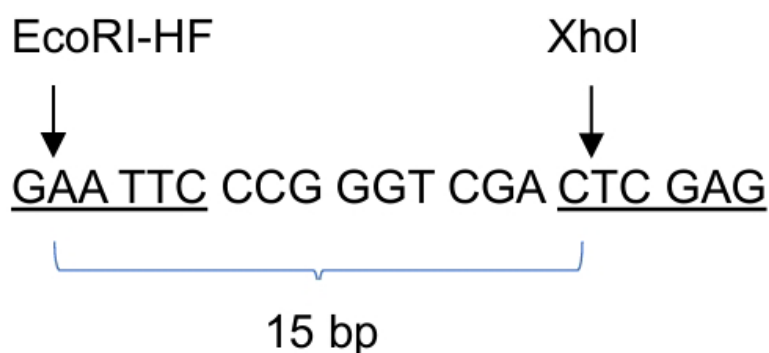
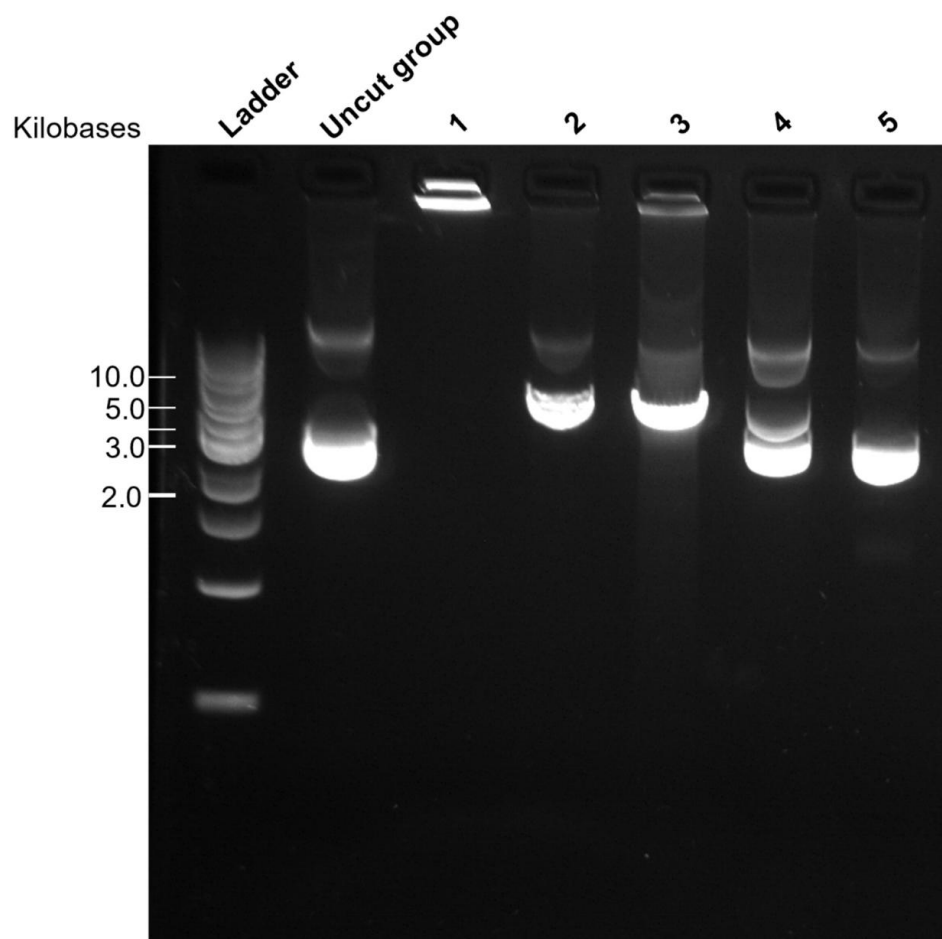


Figure 4. Agarose gel electrophoresis for vector analysis typically included five sample lanes alongside a ladder and an uncut pGEX-6p-1 (4984 bp) vector control. Lanes 1 to 5 represented: EcoRI digested overnight, XhoI digested overnight, EcoRI and XhoI co- digested overnight, EcoRI digested for 30 minutes, and XhoI digested for 30 minutes, respectively. Expected outcomes were: the fastest migration for the uncut control, followed by the 30-minute single enzyme digests (Lanes 4 and 5), then the overnight co-digest (Lane 3), and lastly, the overnight single enzyme digests.

The uncut group in Lane 2 showed a band below 3000 bp; Lanes 4 and 5 displayed bands parallel to the uncut control; in

Lane 1 and 2, with overnight incubation, Lane 1's sample was immobile, and Lane 2 migrated slower due to linearization. Lane 3 contained a mix of linear and smaller base-paired structures, with an approximate size of 4.5 kilobases, migrating similarly to the 30-minute incubation groups (Figure 5). The trailing phenomenon could be seen in every lane.

Figure 5. 0.8 % agarose for vectors, Lane 1 represented EcoRI digested overnight, Lane 2 represented XhoI digested overnight, Lane 3 represented EcoRI and XhoI co-digested overnight, Lane 4 represented EcoRI digested for 30 minutes, and Lane 5 represented XhoI digested for 30 minutes.



3.1.2 Extraction and ligation of digested PCR product into digested pGEX-6P-1 vector

Follow the instruction of QIAquick Gel Extraction Kit, PCR product and vector were extracted from the gel; two control groups were set to ensure the success and accuracy of transformation.

3.1.3 Transformation of pGEX-6P-1 ligated vectors into TOP strain of E.coli

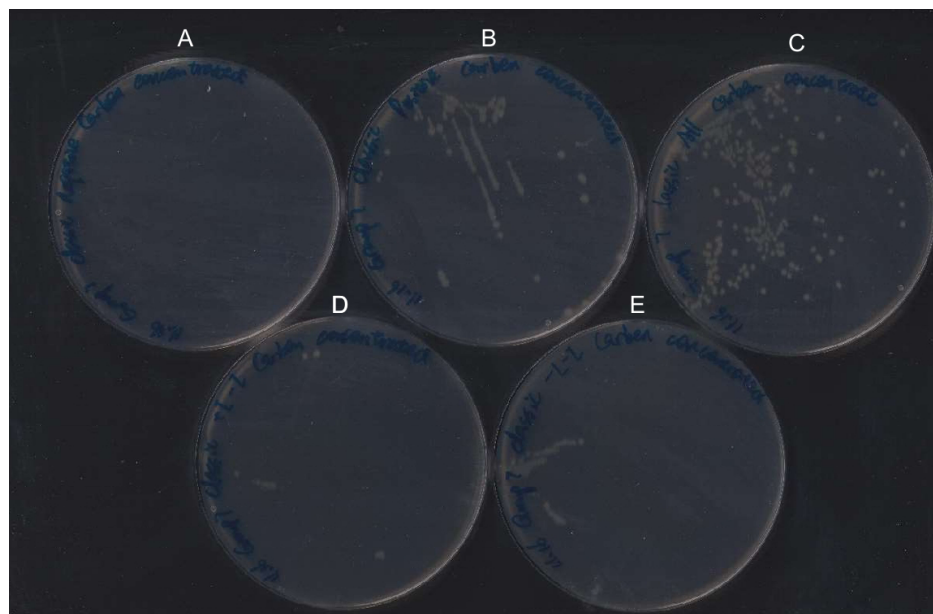
pGEX-6P-1 ligated vectors into TOP strain of E.coli. Five groups were set, and during the procedure, the negative group showed no bacterial growth; the positive group exhibited a small amount of colony growth and was unevenly distributed, with a linear dense presence in the middle portion, and only a few individual colonies were visible on the right side, the shape those separated bacteria was in regular rounded circles, white in color.

The plate grown with everything needed (both PCR product and T4 DNA ligase) showed higher densities of colonies and was segregated better, but it was still less homogeneous, mainly concentrated in the upper left corner, and the separated ones were in regular rounded circles, white in color.

For the plate grown with T4 DNA ligand but without PCR product, only a few scattered bacteria were seen on the plate, and were not very well grown; the shape was in regular rounded circles, white in color.

For the plate grown without both T4 DNA ligand and PCR product, few scattered bacteria were seen on the plate, unevenly shaped and poorly separated (Figure 6).

Figure 6. Plate demonstrating the transformation of pGEX-6P-1 ligated vectors into TOP strain of *E. coli*. A. Negative group with only half the amount of the cell B. Positive group half the amount of cells and 1 μ L uncut vector C. ALL grown with everything needed (both PCR product and T4 DNA ligase) D. +L-I with T4 DNA ligand but without PCR product E. -L-I grown without both T4 DNA ligand and PCR product.



3.2 Overall molecular cloning using Golden Gate technology

3.2.1 Restriction-enzyme digest of pETGG vector by BsaI enzyme as well as visualization by agarose gel electrophoresis

In the Golden Gate cloning method, cleavage by the BsaI enzyme and ligation of DNA fragments into pETGG vector was performed simultaneously in a single reaction. As this method only one enzyme to cleave, the length of vector remained unchanged; the length of PCR product was calculated as 469 bp (the length of PCR product for Golden Gate method was 493 bp shown in Appendix 1, and the number of base pairs cleaved was 24 bp, therefore it could be calculated that PCR products after digestion was 493 minus 24 bp).

3.2.2 Extraction and ligation of digested PCR product into pETGG vector.

Follow the instruction of QIAquick Gel Extraction Kit, PCR product was extracted from the gel; two control groups were set to ensure the success and accuracy of transformation.

3.2.3 Transformation of pETGG ligated vectors into TOP strain of *E. coli*

With three control group, a total of four groups were set during this procedure.

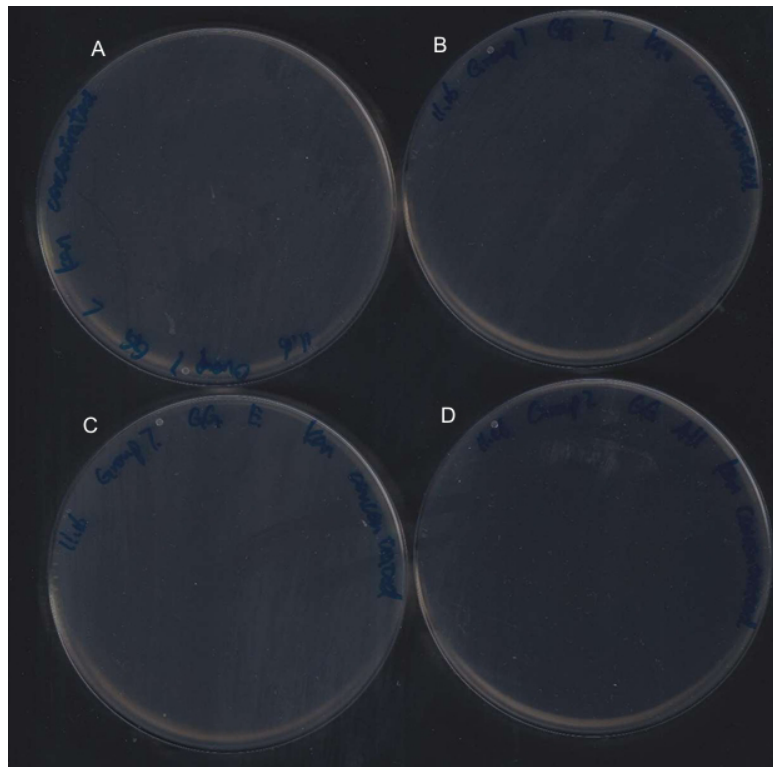
For the plate grown with everything needed, no bacteria growth can be seen; for the plate grown with everything needed except for PCR product for Golden Gate, no bacteria growth can be seen; for the plate grown with everything needed except for BsaI enzyme, no bacteria growth can be seen; for the plate grown with everything needed except for T4 DNA ligase, no bacteria growth can be seen.

A. Grown with everything needed but T4 DNA Ligase B. Grown with everything needed but PCR product C. Grown with everything needed but BsaI enzyme. D. Grown with everything needed/

3.3 Extraction of DNA and Sanger Sequencing

The concentration of purified DNA was determined (83.381 μ g/mL for Classic technology and 159.26 μ g/mL for Golden Gate method and samples were formulated accordingly. A total of four sequences were measured by sanger sequencing, including PCR product from Golden Gate technology using forward primer and reverse primer; PCR product from Classic technology using forward primer and reverse primer (Appendix 2). By comparing the clarity and definiteness of chromatography, PCR product from Classic technology using reverse primer and PCR product from Golden Gate technology using forward primer, compared to the expected sequences, no similarity was found for both methods.

Figure 7. Plate demonstrating the transformation of pETGG ligated vectors into TOP strain of *E.coli*.



4. Discussion

4.1 Analysis through Agarose Gel Electrophoresis

Gel electrophoresis sorts DNA fragments by size: smaller fragments migrate faster and further. A control comprising 517 bp and 493 bp fragments was used, alongside a ladder for size benchmarking. In this experiment, samples in various lanes contained PCR products from previous steps. Lane 1 had a Classic method PCR product with excess dNTPs; Lane 2 and Lane 3 had Classic method PCR products; Lane 4 had a Golden Gate method PCR product with excess dNTPs; Lanes 5 and 6 had Golden Gate method PCR products.

The separation of PCR protein using Agarose Gel Electrophoresis depends on size. The agarose gel matrix acts like a sieve through which smaller molecules can move more easily and therefore travel faster, while larger molecules move more slowly. Therefore, for the separation of PCR products (from Classic and Golden Gate method, 517 bp and 493 bp respectively), the PCR product from Golden Gate was expected to run faster than that from Classic method. And the base pairs expected in PCR products after they have been digested with restriction enzymes as 501 bp (the length of PCR product for Classic method was 517 bp shown in Figure 1, and the number of base pairs cleaved was 16 bp, therefore it could be calculated that PCR products after digestion was 517 minus 16 bp)

However, the actual result turned out to be the opposite of what was expected. In Lane

1, the band was almost invisible, this might be caused by operation error. During the injection of Lane 1 the injecting speed was too fast, causing the formation of bubbles, which took away many samples and resulting in the inadequate amount of sample in Lane 1. For Lane 5 and Lane 6, despite that they were duplicates of the same method amplifying products, great difference could be detected. Lane 5 was close to the control group for Golden Gate method at 100 bp, while Lane 6 might indicate error. As for the ladder, the ladder in agarose gel electrophoresis should appear as distinct bands of different sizes, each corresponding to DNA fragments of known lengths. While in this image, the ladder bands were diffuse and smeared, this could be caused by too much sample loaded; uneven gel; degraded or contaminated DNA ladder. It was also noted that there were no bright band in Lane 3, Lane 4. After recalling the experimental procedure and comparing it with the group that also used the instrument to rule out sample degradation, poor well formulation, electrophoresis issues, it was considered that the samples might not have been loaded into the wells properly due to an error in the sample loading process.

4.2 Analyzing Plasmid DNA Morphologies and Electrophoresis Outcomes in Enzyme Digest Experiments

Plasmid DNA is normally present in vivo in 3 forms: supercoiled, linear and relaxed circular or nicked. The superhelix morphology is the most compact and has the fastest migration rate in electrophoresis. Linear morphology followed. Therefore, the expectation was that overnight groups with linear structure ran slower than uncut group, which had superhelix structure; and groups that were incubated for 30 minutes (partially linear).

Expected outcomes were: the fastest migration for the uncut control, followed by the 30-minute single enzyme digests (Lanes 4 and 5), then the overnight co-digest (Lane 3), and lastly, the overnight single enzyme digests.

The uncut group in Lane 2 showed a band below 3000 bp, possibly due to structural conformation. Lanes 4 and 5 displayed bands parallel to the uncut control, suggesting that within 30 minutes, the DNA remained largely undigested with only minor successful cuts.

In Lane 1 and 2, with overnight incubation, Lane 1's sample was immobile, suggesting errors (this will be further analyzed in Discussion 5.3), and Lane 2 migrated slower due to linearization. Lane 3 contained a mix of linear and smaller base-paired structures, with an approximate size of 4.5 kilobases, migrating similarly to the 30-minute incubation groups (Figure 5). The sample of vector in Lane 2 (single enzyme EcoRI incubated for 30 minutes) was stuck in the well during electrophoresis analysis after PCR, possible reasons are as follows: the sample was too sticky; the amount of loading buffer added was insufficient; the sample might be loaded incorrectly; the agarose might be uneven, resulting in small bubbles in the pore or uneven structure, which affects the movement of the sample.

Moreover, the trailing phenomenon can be seen in every lane and may be caused by the introduction of impurities in the process.

4.3 Assessing pGEX-6P-1 Vector Integration and Control Group Efficacy

During the transformation of pGEX-6P-1 ligated vectors into TOP strain of E.coli, the result observed was not exactly as expected. For the positive group which exhibited a small amount of colony growth and was unevenly distributed, it was probably due to the fact that during the fact that when spreading the solution on the plate, it didn't spread very evenly; the fact that few individual bacteria could be seen indicating poor separation.

The plate grown with everything needed (both PCR product and T4 DNA ligase) showed higher densities of colonies and was segregated better, suggesting that a homogeneous inoculation might have been carried out, possibly through the coating method of liquid suspension media. The spacing between colonies showed that they were well separated, which helped in the subsequent selection of individual colonies for further analysis.

For the plate grown with T4 DNA ligand but without PCR product, few scattered bacteria could be seen and the shape was in regular rounded circles, white in color. In the absence of only PCR product but in the presence of T4 DNA ligase, the colonies should not have grown, but here a small number of colonies appeared, probably because of the presence of a small number of free base pairs spelled on the vector and the vector closed on itself with the help of the T4 DNA ligase, but this situation was more idealized.

For the plate grown without both T4 DNA ligand and PCR product, bacteria were seen on the plate, unevenly shaped and poorly separated. However, there should be no growth of colonies at all, but colonies appeared on this plate. Observe the shape of the bacteria, which is irregular, and consider that there may have been contamination during the operation that led to the growth of stray bacteria

Control groups were set for different reasons, for positive group, half of the cells and 1 μ L uncut vector was added, which was used for the conformation of plate efficient transformation. Negative group with only half the amount of the cell should not grow anything, it was set to verify the validity of the experiment to ensure that changes in the results are due to the experimental treatment and not to other variables in the experimental process. For the plate grown with T4 DNA ligand but without PCR product, the role and impact of PCR products in this experiment could be observed. For the plate grown without both T4 DNA ligand and PCR product, the chance or non- experimental factors on experimental results might be excluded to ensure the reliability of experimental results.

4.4 Assessing Anomalies in E. coli Transformation with pETGG Vectors

During the transformation of pETGG ligated vectors into TOP strain of E.coli, no bacteria growth could be seen, which was unreasonable. Comparing with other groups' results, it seemed that most of groups gained reasonable results with detectable bacteria growth. During the procedure, many steps could go wrong, improper storage of enzymes at too high a temperature; improper operation and so on. Here is the prediction of the reasonable results: The mCherry gene (mCherry is a red fluorescent protein commonly used as a marker protein) with flanking BsaI sites was cloned between the NcoI and XhoI sites to generate pETGG vector from the commercial vector pET28b, therefore, if the PCR product was ligated successfully, the bacteria should have grown in white color; on the other hand, if the PCR product was not ligated, then depending on the situation, the bacteria might have grown in pink color or did no grow at all. When it was grown with everything needed except for BsaI enzyme, it should have grown bacteria in pink color; when it was grown with everything needed except for T4 DNA ligase, it shouldn't have grown anything; when it was grown with everything needed except for PCR product, it shouldn't have grown anything, but there was a slight chance that the vector closed on itself with the help of T4 DNA ligase and free base pair.

4.5 Troubleshooting Primer Mix-Up in Sanger Sequencing Experiment

Sanger Sequencing was not a success with no similarity found in both methods. Then, there were indeed clear and well-defined sequences displayed in the mapping that just didn't match our target gene fragments. This happened in three groups of students, so the instructor assumed that it might have happened that the Golden Gate group was labeled backwards from the Classic method group during the final preparation for sanger sequencing, and the wrong primer was used, which led to the failure of the experiment, which was very likely to happen.

Specifically, the sequence was obtained from the Golden Gate ligated vector using the classic method primer, presumably because there happened to be a recognition site for the classic method primer in the vector.

In order to verify this, the Golden Gate sequence was compared with the complete pETGG ligated vectors sequence, but still no similarity found.

There are many possible causes of errors in sanger sequencing, which may be due to operational errors such as sample cross-contamination, volume errors, etc., and it is not possible to clearly determine the specific steps that went wrong

4.6 Efficiency and Specificity in Golden Gate Cloning

Compared with traditional methods, in the Golden Gate cloning method, cleavage by the BsaI enzyme and ligation of DNA fragments can be performed simultaneously in a single reaction. This is an advantage of the Golden Gate cloning technique, which allows multiple fragments to be constructed simultaneously with high efficiency and fidelity. Golden Gate cloning takes advantage of the properties of Type IIS restriction enzymes (such as BsaI), which cut on the outside of their recognition sequences, leaving excessively long fragments with sticky ends. These sticky ends can be designed to be complementary to each other, allowing multiple fragments to be ligated into the vector in the correct orientation in the same reaction. With the addition of a DNA ligase, cutting and ligation can be performed in the same tube and under the same conditions, simplifying the process and allowing for the orderly assembly of multiple fragments in one step. Comparing longer sticky ends (overhangs) formed by BsaI with shorter sticky ends; it offers several advantages: Longer overhangs can provide more specificity during the ligation step, reducing the chance of self-ligation or non-specific assembly; efficiency of this process is improved, as longer overhangs can increase the probability of correct fragment binding and assembly; ensure accuracy as unique overhangs created by the restriction enzymes ensure that DNA fragments can only join in one orientation and so on.

5. Conclusion

In conclusion, this report successfully highlights the importance of using Golden Gate and classical cloning techniques in scientific research. Using *Escherichia coli* as a model organism, the results of this study, obtained from accurate experiments, provide important insights into the efficacy and practical application of these DNA assembly methods. By comparing these techniques, this report not only fulfils its aims and objectives, but also enhances our understanding of the role of molecular cloning in the development of scientific knowledge. It highlights the importance of selecting appropriate cloning strategies according to specific experimental requirements and the potential of *E. coli* as a versatile tool for biotechnological research.

Funding

no

Conflict of Interests

The authors declare that there is no conflict of interest regarding the publication of this paper.

References

- [1] Jajesniak, P., & Wong, T. S. (2017). Rapid construction of recombinant plasmids by QuickStep-Cloning. In Springer New York (pp. 205–214). Springer New York.
- [2] Ausubel, F. M., Brent, R., Kingston, R. E., Moore, D. D., Seidman, J. G., Smith, J. A., & Struhl, K. (2001). Overview of post Cohen-Boyer methods for single segment cloning and for multisegment DNA assembly. *Current Protocols in Molecular Biology*, 3.26.1–3.26.20.
- [3] Blount, Z. D. (2015). The natural history of model organisms: The unexhausted potential of *Escherichia coli*. *eLife*, 4(e05826). <https://doi.org/10.7554/eLife.05826>

The Relationship between Loneliness and Mortality

Huiping Chu*

James cook university Singapore, 072750

*Corresponding author: Huiping Chu

Copyright: 2025 Author(s). This is an open-access article distributed under the terms of the Creative Commons Attribution License (CC BY-NC 4.0), permitting distribution and reproduction in any medium, provided the original author and source are credited, and explicitly prohibiting its use for commercial purposes.

Abstract: This literature review explores the complex relationship between loneliness and mortality, emphasizing its effects on physical and mental health across different age groups. Drawing on studies from both Western and Asian contexts, the review highlights that loneliness contributes to increased risks of depression, cardiovascular diseases, substance abuse, and ultimately premature death, particularly among the elderly. It investigates how social relationships, living arrangements, cultural traditions, and institutional frameworks shape the experience of loneliness and its health outcomes. While some findings suggest a direct correlation between loneliness and mortality, others point to mediating factors such as health behavior and access to social or religious support. The paper also examines intervention strategies and proposes that targeted community-based programs and educational engagement may mitigate loneliness-related health risks. The findings underscore the need for more cross-cultural, longitudinal studies and policy-level interventions.

Keywords: Loneliness; Mortality; Social Relationships; Elderly Health; Depression; Intervention Strategies; Cross-Cultural Comparison

Published: May 25, 2025

DOI: <https://doi.org/10.62177/apjcmr.v1i2.411>

1.Introduction

Whether loneliness affects mortality is a hot topic of discussion in society today. Past research has shown that loneliness may contribute to health problems such as smoking, suicide, depression, coronary artery disease, and the spread of HIV (Patterson & Veenstra, 2010)^[1]. A growing number of scholars believe that loneliness affects human health, leading to increased mortality. Loneliness is a significant contributor to health problems in known studies. Moreover, loneliness can and is easily treated by intervention. For this reason, studying the effects of loneliness and proposing solutions can be part of the healthcare system. The primary purpose of this literature review is to examine the factors that influence loneliness and mortality and find solutions. Here it is predicted that social relationships, age, social institutions, cultural traditions, and religion are all factors that can influence loneliness and mortality.

2.Health problems caused by loneliness

While there is evidence that loneliness reaches its peak during adolescence, it is increasingly prevalent with age due to experimental evidence (Yang, K., & Victor, C., 2011).^[2]For adolescents, loneliness mostly leads to changes in behavioral habits. For example, smoking and alcohol abuse. Although it has also been shown that for young people, loneliness can contribute to suicide or HIV transmission (Patterson & Veenstra, 2010). However, loneliness causes more health problems in older age groups and is more significant concern to society. Depression due to loneliness, alcohol abuse, smoking, cardiovascular problems, sleep difficulties, altered immune systems and Alzheimer's disease are all factors that may

contribute to early death in older people (Rico-Uribe et al., 2018).^[3] Some studies have shown that loneliness causes increased mortality in older people with chronic illnesses compared to those with social support (Olaya et al., 2017).^[4] Loneliness also poses a risk of eating disorders, as social isolation can lead to feelings of loneliness, and loneliness can lead some people to overeat (Heinberg & Steffen, 2021).^[5] Obesity is a major threat to human health. Lonely people are also more likely to be at risk of coronary artery disease, and the persistence of loneliness symptoms over many years can lead to hypertension and cardiac dysfunction (Patterson & Veenstra, 2010). In summary, research on the topic of loneliness is necessary to reduce human mortality.

3.The impact of social relationships on feelings of loneliness

According to Luo & Waite (2014)^[6], the notion that social relationships influence loneliness has been confirmed. Traditional Chinese culture emphasizes the importance of family and community. Due to the long-term rapid decline in fertility rates, the number of older adults left behind with children and those living alone is skyrocketing. In 2014, 25% of China's elderly households were living alone, and this figure is expected to rise to 90% in 10 years' time. Furthermore, as the number of older adults living alone skyrockets, so makes sense of loneliness among China's elderly. In a national survey it was found that in 1992 approximately 16% of older people felt lonely, however by 2000 nearly 30% felt lonely (Yang & Victor, 2008)^[7]. According to Luo & Waite (2014), the study used cross-lagged models combined with survival analysis to assess the relationship between loneliness and mortality and social relationships. The results of this study suggest that an older person's mortality rate may increase by 12% over three years if they feel lonely. Older adults living in nursing homes or alone are more likely to feel lonely and have the highest mortality rates.

The conclusions reached in this literature are similar to those reached in the West regarding the loneliness of older people in the West. According to Abell & Steptoe (2021)^[8], this paper examined the relationship between living alone and mortality over a period of 8.5 years using Cox proportional risk analysis and concluded that older people who live alone are more likely to feel lonely and have an increased risk of death. This would suggest that there is an effect of social relationships on loneliness and mortality, and that geography does not affect this view. However, the direct effect of loneliness on mortality was found to be diminished by the inclusion of behavioral and health variables in several papers. So the behavioral and health variables need to be examined in detail in order to confirm whether loneliness has a significant effect on mortality. However for social relationships to be linked to depression is well established. According to Holwerda et al. (2016)^[9], this literature used the De Jong Gierveld Scale and the Centre for Epidemiological Studies Depression Scale to test the relationship between loneliness and depression and found that isolation of social relationships is a cause as well as a consequence of depression. The relationship between loneliness and depression is reciprocal. The co-occurrence of loneliness and depression has an amplifying effect, and the combination of the two results in higher mortality rates. Studies have shown a link between suicide and early death in older people with depression and social relationships and interpersonal interactions.

4.Social ties do not affect loneliness and mortality

Some scholars disagree with the notion that social relationships influence loneliness and mortality. According to Chan et al. (2015), three loneliness scales based on the University of California, Los Angeles (UCLA) were used to assess loneliness in older participants. This longitudinal study considered variables including self-reported, limited ability to perform life activities, smoking, and depression. Previous studies have considered socio-demographic covariates such as age, gender, race, marital status, housing type, educational attainment and socio-economic status. In contrast to Western countries, there is not a large literature on issues related to loneliness among older people in Asia. The study on loneliness among older people in Singapore included almost all residential patterns of older people, which is representative for some Asian countries. This means that preliminary results have been obtained on the question of whether social relationships influence loneliness. The study found no significant differences in loneliness and mortality between older people who lived with their children and were not socially isolated and those who were. Even when living with family, older people still experience loneliness. Older people need more than family companionship and the availability of social connections may not be the key reason for feelings of loneliness. Further research is needed into the causes of loneliness in older people. As the results of this study differ from

those of studies on Chinese older people, it is speculated that this may be due to differences in social systems and cultural traditions. However, as Singapore has a large Chinese diaspora, this idea needs to be further investigated.

5. Interventions for loneliness

Loneliness can be treated by intervention. A large body of literature is devoted to finding available treatment options to improve human mortality, especially in the elderly. The first is a programme for depression. Loneliness and depression have been shown to be among the identifiable and measurable risk factors for early death (Holwerda et al., 2016). Some scholars believe that loneliness and depression are causally related to each other and that they co-exist, so intervening in loneliness is treating depression (Rico-Uribe et al., 2018). Because loneliness and depression show highly similar symptoms, interventions for depression are also effective for loneliness. The two can be improved together. Training primary care teams to deliver brief interventions in the community to people with depression or who feel lonely has been shown to significantly improve depression outcomes (Rost et al., 2001).^[10] Community health teams can use counselling, activities and community befriending parties as ways to improve loneliness. The establishment of counselling units in schools and nursing homes and regular counselling for students and the elderly are predicted to be effective interventions for loneliness. However, no literature has been found on this subject due to the need for long follow-up surveys and widespread availability to find results. After reviewing the extensive literature, it is clear that interventions for loneliness are not well established and widespread. Future research and government could focus on the popularization and development of interventions for loneliness.

6. Other moderating factors

In addition to medical moderation, there are other factors that can moderate the relationship between loneliness and mortality. For example, religion, education and social institutions. For religion, religious affiliation affects mortality rates. Suicide rates in areas of Muslim, Christian or Jewish faith are lower than in non-religious areas (Gearing & Lizardi, 2008)^[11]. The reason for this is that such religions are opposed to suicide in the sense that they believe it is wrong and that those who commit suicide are not truly liberated but are punished after death. However, because of the contradictory nature of the texts of some religions, it is believed that some religions also support suicide. For example, Hinduism teaches that death leads to rebirth and forgives suicide, especially as a ritual act of suicide is practiced in some areas of Hinduism (Gearing & Lizardi, 2008). In general, however, the teachings of most religions do not support suicide. It is clear from the above that loneliness leads to an increased chance of suicide, but that belief in religion discourages the act. Religious factors can therefore moderate the relationship between loneliness and mortality. According to Chan et al. (2015)^[12], university reduces loneliness in older people, whether living alone or with family. As loneliness in older people is not only caused by living alone or social isolation. It may also be due to the fact that there is nothing to do after retirement. Older people's universities are a place where they can learn and make friends so that education can affect loneliness. For more information on how the social system affects loneliness and mortality, see above on the differences in the causes of loneliness among older adults in China and Singapore. As the Chinese social system is collective and family-centered, older adults living alone are more likely to feel lonely in China. The impact of social relationships on loneliness is huge in China, but Singapore has a different system to China. There is no great difference in the odds of loneliness between older adults who live with their families and those who live alone. So the social system also moderates the relationship between loneliness and mortality.

7. Conclusion

In conclusion, the question of whether loneliness has a serious impact on mortality cannot be accurately measured as most of the current experiments have been studied using participants' self-reports. In particular, there are also health and behavioral factors. However, current research suggests that loneliness does have certain health effects on older people, such as depression and coronary artery disease. The effects of loneliness on human health can increase the risk of death. Widespread implementation of interventions for loneliness can be beneficial. The government could consider implementing measures to intervene in the community to reduce loneliness for the dual purpose of ensuring the physical and psychological well-being of humans. For future research, since most of the current research is about the effects of loneliness on older people, little consideration has been given to the effects of loneliness on young people. This is particularly the case with regard to smoking

and alcohol abuse. Therefore, future research could focus on how loneliness is related to smoking and alcohol abuse among adolescents.

Funding

no

Conflict of Interests

The authors declare that there is no conflict of interest regarding the publication of this paper.

Reference

- [1] Patterson, A., & Veenstra, G. (2010). Loneliness and risk of mortality: A longitudinal investigation in Alameda County, California. *Social Science & Medicine*, 71(1), 181–186. <https://doi.org/10.1016/j.socscimed.2010.03.024>
- [2] Yang, K., & Victor, C. (2011). Age and loneliness in 25 European nations. *Ageing & Society*, 31(8), 1368–1388. <https://doi.org/10.1017/S0144686X1000139X>
- [3] Rico-Uribe, L., Caballero, F., Martín-María, N., Cabello, M., Ayuso-Mateos, J., & Miret, M. (2018). Association of loneliness with all-cause mortality: A meta-analysis. *PLOS ONE*, 13(1), e0190033. <https://doi.org/10.1371/journal.pone.0190033>
- [4] Olaya, B., Domènech-Abella, J., Moneta, M., Lara, E., Caballero, F., Rico-Uribe, L., & Haro, J. (2017). All-cause mortality and multimorbidity in older adults: The role of social support and loneliness. *Experimental Gerontology*, 99, 120–126. <https://doi.org/10.1016/j.exger.2017.10.001>
- [5] Heinberg, L., & Steffen, K. (2021). Social isolation and loneliness during the COVID-19 pandemic: Impact on weight. *Current Obesity Reports*. <https://doi.org/10.1007/s13679-021-00447-9>
- [6] Luo, Y., & Waite, L. (2014). Loneliness and mortality among older adults in China. *The Journals of Gerontology Series B: Psychological Sciences and Social Sciences*, 69(4), 633–645. <https://doi.org/10.1093/geronb/gbu007>
- [7] Yang, K., & Victor, C. (2008). The prevalence of and risk factors for loneliness among older people in China. *Ageing & Society*, 28, 305–327. <https://doi.org/10.1017/S0144686X07006848>
- [8] Abell, J., & Steptoe, A. (2021). Why is living alone in older age related to increased mortality risk? A longitudinal cohort study. *Age and Ageing*. <https://doi.org/10.1093/ageing/afab155>
- [9] Holwerda, T., van Tilburg, T., Deeg, D., Schutter, N., van R., & Dekker, J., et al. (2016). Impact of loneliness and depression on mortality: Results from the Longitudinal Ageing Study Amsterdam. *British Journal of Psychiatry*, 209(2), 127–134. <https://doi.org/10.1192/bjp.bp.115.168005>
- [10] Rost, K., Nutting, P., Smith, J., Werner, J., & Duan, N. (2001). Improving depression outcomes in community primary care practice. *Journal of General Internal Medicine*, 16(3), 143–149. <https://doi.org/10.1111/j.1525-1497.2001.00537.x>
- [11] Gearing, R., & Lizardi, D. (2008). Religion and suicide. *Journal of Religion and Health*, 48(3), 332–341. <https://doi.org/10.1007/s10943-008-9181-2>
- [12] Chan, A., Raman, P., Ma, S., & Malhotra, R. (2015). Loneliness and all-cause mortality in community-dwelling elderly Singaporeans. *Demographic Research*, 32, 1361–1382. <https://doi.org/10.4054/demres.2015.32.49>

Preparation and Efficacy Evaluation of a Tibetan Gentiana Face Mask Suitable for Sensitive Skin

Luo Dan*

Tibet Autumn Girl Cosmetics Co., Ltd., Lasa, Xizang, 850000, China

*Corresponding author: Luo Dan, luodanxizang123456@163.com

Copyright: 2025 Author(s). This is an open-access article distributed under the terms of the Creative Commons Attribution License (CC BY-NC 4.0), permitting distribution and reproduction in any medium, provided the original author and source are credited, and explicitly prohibiting its use for commercial purposes.

Abstract: This study aims to investigate the antioxidant activity of Tibetan gentian (*Gentiana* spp.) extract and its essence when compounded with a facial mask matrix. It also evaluates the efficacy of facial masks containing gentian extract on sensitive facial skin and analyzes the comprehensive performance of the mask. A total of 90 patients with facial sensitive skin, enrolled between October 2022 and December 2024, were randomly assigned to either a control group or an observation group, with 45 patients in each. The control group used standard facial masks, while the observation group used masks containing gentian extract. Both groups underwent a 4-week intervention. The efficacy, lactic acid stinging test indicators, and skin physiological function parameters were compared between the two groups. Results showed that the overall effectiveness rate in the observation group reached 93.26%, significantly higher than 71.20% in the control group ($P < 0.05$). After the intervention, both groups showed notable improvements compared to baseline in lactic acid stinging test scores and physiological skin indicators. Specifically, the observation group had significantly lower stinging scores and a longer latency before the onset of stinging compared to the control group. Moreover, the skin pH values were lower, while sebum levels and stratum corneum hydration were higher than those in the control group ($P < 0.05$). No serious adverse events occurred in either group. These findings suggest that facial masks containing gentian extract effectively alleviate symptoms of sensitive facial skin, enhance skin barrier function and tolerance, and are safe for use.

Keywords: Tibetan Gentian; Traditional Chinese Medicine Extract; Facial Mask Matrix Compounding; Antioxidant Activity; Sensitive Facial Skin

Published: May 28, 2025

DOI: <https://doi.org/10.62177/apjcmr.v1i2.409>

Introduction

In recent years, plant-derived bioactive substances have been widely applied in the fields of food, medicine, and personal care due to their remarkable biological activities. Skincare products based on traditional herbal medicine are gaining significant traction in the global market owing to their natural properties and efficacy advantages ^[1]. China, with its abundant plant resources and well-established extraction technologies, has developed cosmetic ingredients that combine high efficiency and safety, forming a unique competitive edge in localized R&D. For example, *Gentiana* species, a distinctive medicinal plant from the Tibetan region belonging to the Gentianaceae family, is mainly distributed along the eastern edge of the Qinghai-Tibet Plateau and in the high-altitude areas of Gansu. It is a key component in many traditional Tibetan medicine formulations ^[2]. Despite its long history of traditional use, systematic research on this plant remains limited, with existing

studies primarily focusing on the isolation and identification of its active constituents. Sensitive skin is characterized by a heightened reactive state, manifesting as burning, stinging, and often accompanied by objective symptoms such as erythema and desquamation. The core pathological mechanism is closely linked to impaired skin barrier function^[3].

This study centers on the extract of Tibetan Gentiana as a core ingredient, combined with moisturizing and reparative excipients to develop a facial mask product. It systematically evaluates its antioxidant activity and clinical efficacy. By conducting comparative trials, this research aims to explore the mask's role in improving skin barrier function and to provide scientific support for the development of herbal cosmetics with both anti-sensitivity and reparative functions.

1. Materials and Reagents

1.1 Instruments and Equipment

Full-wavelength microplate reader (Boteng Instruments), Amenny skin tester (Shenzhen Fuheng).

1.2 Facial Mask Preparation

Tibetan Gentiana was sourced from a Chinese herbal medicine trading company, with in-lab extraction of the herbal components. The extract was prepared with a material-to-liquid ratio of 1:1. Moisturizing agents included sodium hyaluronate, 1,3-butylene glycol, glycerin, betaine, panthenol, 1,2-hexanediol, dipotassium glycyrrhizinate, and purified water, as well as EDTA-2Na, herbal extracts, xanthan gum, and p-hydroxyacetophenone.

The formulation ratios are detailed in Table 1. First, xanthan gum was swollen in an appropriate amount of purified water for 1 hour. Then, 40% of the total water volume was heated to 40°C in a beaker, followed by the sequential addition of sodium hyaluronate, the polyol mixture, chelating agents, and moisturizing actives. The mixture was stirred until completely dissolved. Xanthan gum was gradually incorporated while stirring continuously to form a gel matrix. After cooling, a phenylethanol-based preservative, hexanediol stabilizer, and the herbal active ingredient were added. The final product was obtained through homogenization and thorough mixing^[4].

Table 1 Mask formula

Raw materials	Formula	Function
Xanthan gum	0.2	Thickener
Sodium hyaluronate	0.1	Moisturizer
1,3-butylene glycol	2.0	Moisturizer
Glycerin	2.0	Moisturizer
Sodium EDTA	0.1	Skin conditioner
Betaine	0.9	Moisturizer
Panthenol	1.0	Moisturizer
Parahydroxyacetophenone	0.8	Antioxidant
1,2-hexanediol	1.5	Moisturizer
Dipotassium glycyrrhizinate	0.1	Moisturizer
Traditional Chinese medicine extract	0.4	Skin conditioner
Purified water	Fill to 100.0	Moisturizer

A 10.00 mL sample of the Tibetan Gentiana facial essence was prepared, and a serial dilution method was used with deionized water to obtain solutions of 50%, 25%, 12.5%, 6.25%, and 3.125%. Superoxide anion scavenging activity was measured according to the standardized protocol of the assay kit. The absorbance of the original (100%) and diluted solutions (50%, 25%, 12.5%, 6.25%, and 3.125%) was recorded, with each concentration tested in triplicate to calculate the average values. The superoxide anion scavenging capacity and the half-maximal effective concentration (EC₅₀) were determined^[5]. The moisturizing performance of the Tibetan Gentiana facial mask was evaluated under different humidity conditions. As shown in Figure 1, the hydration retention rate decreased over time at varying speeds depending on the ambient humidity. In an environment with 82% relative humidity, the mask exhibited excellent water-retention capacity. Over a 24-hour monitoring

period, its moisture retention rate consistently remained above the 90% baseline, with the lowest observed value still reaching 95.38%. When the relative humidity was reduced to 42%, the mask maintained a stable retention rate above 80% for 24 hours, with a temporary dip to 86.72%. Overall, its moisture-retaining performance remained at an industry-leading level. Under constant temperature conditions, higher humidity slowed the decline in moisture retention, resulting in improved moisturizing efficacy^[6].

Figure 1 Moisture Retention Variation

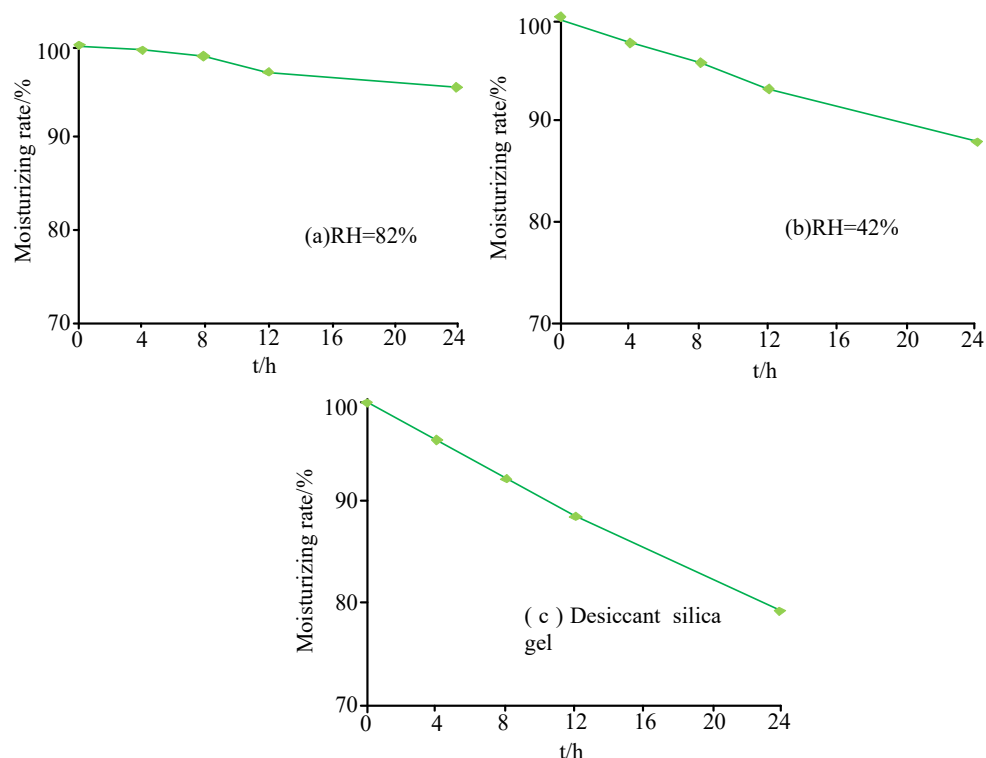


Figure 2. Free Radical Scavenging Activity of Tibetan Gentiana Facial Essence

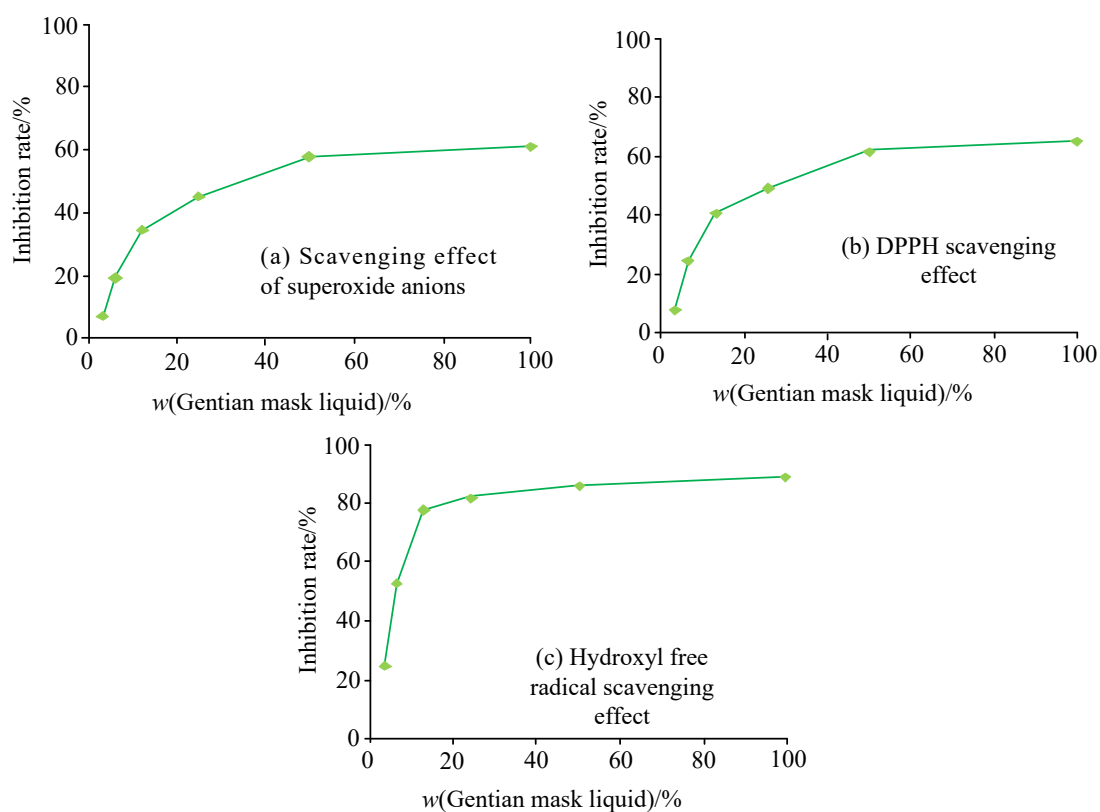


Figure 2 illustrates the free radical scavenging activity of the Tibetan Gentiana facial essence. The antioxidant efficacy of the Gentiana extract showed a significant dose-dependent relationship. At a concentration of 25%, the increase in hydroxyl radical scavenging rate began to plateau, with an incremental gain of less than 5%. When the concentration reached 50%, the scavenging curves for superoxide anion and DPPH radicals entered a plateau phase, with the slope decreasing to below 0.15. According to the in vitro antioxidant evaluation system, the half-maximal inhibitory concentrations (IC_{50}) of the facial essence for the three types of free radicals were determined to be 9.81% for superoxide anions, 3.42% for DPPH radicals, and 5.60% for hydroxyl radicals. These results suggest that the formulation possesses excellent free radical scavenging properties and demonstrates strong in vitro antioxidant activity [7].

2. Experimental Preparation

2.1 Study Subjects

This study enrolled 90 patients with clinically diagnosed facial sensitive skin who were admitted to the hospital between October 2022 and December 2024. Participants were randomly assigned into two groups using a random number table method. In the control group ($n = 45$), the gender distribution was 1:2 (15 males, 30 females), with an age range of 18–50 years (mean age: 35.60 ± 4.76 years). The disease duration ranged from 6 to 30 months, with a median of 17.48 months. The observation group ($n = 45$) had comparable baseline characteristics: gender ratio of 2:3 (18 males, 27 females), mean age of 36.94 ± 4.52 years, and mean disease duration of 16.33 ± 4.18 months. Statistical analysis confirmed that the two groups were well balanced with respect to gender, age, and disease duration.

The study protocol was conducted in strict accordance with the Declaration of Helsinki. Ethical approval was obtained from the Institutional Ethics Review Committee, and all participants provided written informed consent and completed GCP-compliant training.

Inclusion criteria:

Clinically diagnosed with sensitive facial skin

Skin lesions confined to the facial area

Good treatment compliance and ability to follow the intervention protocol

Exclusion criteria:

Coexisting facial infectious dermatoses or other skin disorders

Serious cardiovascular, cerebrovascular, hepatic, renal, or coagulation disorders

Underwent aesthetic procedures or used hormone therapy, immunosuppressants, anti-infectives, or antihistamines within 30 days prior to enrollment

History of hypersensitivity to the study product

Presence of psychiatric disorders or cognitive impairment

Pregnant or breastfeeding women

The observation group received facial masks containing Tibetan Gentiana extract, while the control group used commercially available standard masks. Both groups applied the mask once nightly before bed for four consecutive weeks.

2.2 Observatory Parameters

This study established a therapeutic efficacy evaluation system based on relevant clinical standards, with efficacy categorized as follows:

Complete remission: efficacy index $\geq 90\%$

Marked improvement: efficacy index between 60% and 89%

Partial improvement: efficacy index between 30% and 59%

Ineffective: efficacy index $< 30\%$

The efficacy index was calculated using the formula:

Efficacy Index (%) = $[(\text{Pre-treatment subjective and objective score} - \text{Post-treatment score}) / \text{Pre-treatment score}] \times 100\%$

The total effective rate was defined as the percentage of patients achieving either complete remission or marked improvement.

Assessment Methods:

Lactic Acid Stimulation Test:

A 5% lactic acid solution (prepared at a 50% concentration) was evenly applied to the nasolabial folds and both cheeks before and after treatment. The onset time of stinging was recorded, and the degree of stinging was evaluated using the Visual Analog Scale (VAS). A score ≥ 3 was considered a positive reaction.

Skin Physiological Function Testing:

After facial cleansing and a 10-minute rest period, a non-invasive skin analysis device was used to simultaneously measure transepidermal water loss (TEWL), sebum secretion, stratum corneum hydration, and skin pH levels.

Safety Evaluation:

Throughout the study, all adverse events—including itching, erythema, dryness, and desquamation—were recorded to assess the safety profile of the intervention.

2.3 Data processing and statistics

SPSS 22.0 statistical analysis platform was used to complete data processing. The measurement indicators were described in the form of mean standard deviation ($\bar{x} \pm s$). The paired t test was used to analyze the data within the group, and the independent sample t test was used for inter-group comparison. The categorical variable data were presented as frequency (constituent ratio), and the χ^2 test was used for inter-group comparison. All statistical inferences were based on ($P < 0.05$) as the significance threshold.

3.Result analysis

3.1 Comparison of the effects of the mask after use

The efficacy of the observation group and the control group is shown in Table 2. The effective rate of the observation group is as high as 93.26%, and the total effective rate of the observation group is significantly higher than that of the control group (71.20%).

Table 2 Efficacy of observation group and control group [cases (%)]

Group	Completely improved	Significant improvement	Improve	Invalid	Total effective
Observation group (n=45)	24(53.14)%	18(40.02)%	3(5.76)%	0(0.00)%	41(93.26)%
Control group (n=45)	9(22.21)%	20(49.01)%	9(19.98)%	4(8.99)%	32(71.20)%
χ^2 value	-	-	-	-	5.874
P value	-	-	-	-	<0.05

3.2 Lactic acid stimulation test

Table 3 compares the lactic acid stinging score and the onset time of lactic acid stinging. The research data show that there is no statistical difference between the two groups of subjects in the lactic acid stimulation score and the time of stimulation reaction ($P < 0.05$). After intervention treatment, the pain assessment values of both groups of patients decreased significantly compared with the baseline level, and the latency of pain reaction showed a trend of extension. The lactic acid stinging score of the observation group was relatively lower than that of the control group ($P < 0.05$), and the onset time of lactic acid stinging was longer than that of the control group ($P < 0.05$).

Table 3 Comparison of lactic acid stinging scores and lactic acid stinging onset time ($\bar{x} \pm s$)

Group	Lactic acid sting score/points		Lactic acid tingling sensation onset time/min	
	Before use	After use	Before use	After use
Observation group (n=45)	5.13 ± 0.82	$1.05 \pm 0.23^*$	3.45 ± 0.49	$6.96 \pm 0.83^*$
Control group (n=45)	5.11 ± 0.95	$2.86 \pm 0.39^*$	3.51 ± 0.54	$5.1+ \pm 0.62^*$
χ^2 value	0.472	4.528	0.634	4.791
P value	0.518	<0.001	0.381	<0.001

Note: *Compared with the same group before use, $P < 0.05$.

3.3 Comparison of skin function physiological parameters between groups

Before the intervention, there was no significant difference in the baseline data of core parameters such as transepidermal water loss (TEWL), sebum secretion, stratum corneum water holding capacity and skin surface pH value between the two groups of subjects ($P>0.05$). Compared with before use, the skin pH value and TEWL of the control group and the observation group were significantly reduced after use, and the sebum content and stratum corneum water content increased ($P<0.05$). The TEWL and skin pH value of the observation group were lower than those of the control group ($P<0.05$), and the sebum content and stratum corneum water content were significantly higher than those of the control group ($P<0.05$). Among them, * compared with the same group before use, $P<0.05$.

Table 4 Comparison of skin physiological function indicators between the two groups after use ($\bar{x} \pm s$)

Group	TEWL/[g/(m ² ·h)]		Sebum content $\mu\text{g/cm}$		Water content of stratum corneum %		Skin pH	
	Before use	After use	Before use	After use	Before use	After use	Before use	After use
Observation group (n=45)	24.36 \pm 4.66	12.59 \pm 1.32*	70.52 \pm 3.25	78.05 \pm 5.23*	52.17 \pm 2.36	61.93 \pm 4.35*	6.31 \pm 0.35	5.16 \pm 0.21*
Control group (n=45)	24.47 \pm 4.79	17.52 \pm 2.90*	70.48 \pm 3.35	74.31 \pm 3.59*	52.30 \pm 2.81	58.90 \pm 3.14*	6.27 \pm 0.41	5.80 \pm 0.30*
χ^2 value	0.679	6.381	0.826	5.191	0.542	4.250	0.825	3.805
Group	0.375	<0.001	0.290	<0.001	0.482	<0.001	0.171	<0.001

4. Discussion

The facial mask containing Gentiana extract from the Tibetan region exerts significant therapeutic effects on sensitive skin through a multi-target synergistic mechanism. It effectively reduces facial inflammatory responses, alleviates discomfort symptoms such as capillary dilation, burning sensation, and stinging, and inhibits histamine release, thereby providing anti-allergic and anti-itch benefits[8]. Simultaneously, it stabilizes the skin tissue structure, enhances stratum corneum hydration, reduces transepidermal water loss (TEWL), stimulates collagen synthesis, and accelerates tissue repair—thus promoting the restoration of the skin barrier function^[9]. Moreover, its antioxidant properties contribute to collagen regeneration, effective scavenging of free radicals, and the repair of damaged cells, leading to an overall improvement in skin physiological function^[10].

The experimental findings indicate that the Gentiana-based mask significantly enhances the care efficacy for sensitive skin by improving physiological skin parameters and skin tolerance, all while maintaining a favorable safety profile. Future research should expand the clinical sample size to provide more robust evidence supporting its application in the scientific management of sensitive skin.

5. Conclusion

This study investigated the reparative effects of a topical preparation containing active compounds from high-altitude Gentiana on facial sensitive skin. Results demonstrated that the use of the Gentiana-infused mask significantly reduced skin irritation scores and delayed the onset of irritation responses. It also decreased TEWL and skin pH while increasing sebum secretion and stratum corneum hydration levels. These outcomes suggest a synergistic effect when combining routine skincare with a facial mask containing Gentiana extract, leading to improved efficacy and excellent skin tolerance. As a targeted anti-sensitivity agent, the active compound from Gentiana exhibits several advantageous properties, including high selectivity, rapid onset of action, sustained efficacy, and broad-spectrum anti-inflammatory activity. These characteristics underscore its potential value in the management of sensitive skin.

Funding

no

Conflict of Interests

The authors declare that there is no conflict of interest regarding the publication of this paper.

Reference

- [1] Zeng, M., Guo, D., Fernández-Varo, G., Zhang, X., Fu, S., Ju, S., ... & Casals, E. (2022). The integration of nanomedicine with traditional Chinese medicine: drug delivery of natural products and other opportunities. *Molecular pharmaceutics*, 20(2), 886-904.
- [2] Chi, X., Zhang, F., Gao, Q., Xing, R., & Chen, S. (2021). A review on the ethnomedicinal usage, phytochemistry, and pharmacological properties of Gentianeae (Gentianaceae) in Tibetan medicine. *Plants*, 10(11), 2383.
- [3] Fluhr, J. W., Moore, D. J., Lane, M. E., Lachmann, N., & Rawlings, A. V. (2024). Epidermal barrier function in dry, flaky and sensitive skin: A narrative review. *Journal of the European Academy of Dermatology and Venereology*, 38(5), 812-820.
- [4] Nemati, M. M., Abedi, M., Ghasemi, Y., Ashrafi, H., & Haghdel, M. (2024). Formulation and evaluation of antioxidant and antibacterial activity of a peel-off facial masks moisturizer containing curcumin and Rosa Damascena extract. *Journal of Cosmetic Dermatology*, 23(6), 2156-2169.
- [5] Zhu, Y., Lao, F., Pan, X., & Wu, J. (2022). Food protein-derived antioxidant peptides: Molecular mechanism, stability and bioavailability. *Biomolecules*, 12(11), 1622.
- [6] Yoo, M. A., Kim, S. H., Han, H. S., Byun, J. W., & Park, K. H. (2022). The effects of wearing a face mask and of subsequent moisturizer use on the characteristics of sensitive skin. *Skin Research and Technology*, 28(5), 714-718.
- [7] Nursal, F. K., Amalia, A., Nining, N., Putri, D. A., & Larasati, K. D. (2024). Development of Coffee Fruit Skin (Coffea canephora) formula as Antioxidant peel-off Masks. *Jurnal Sains Farmasi & Klinis*, 11(2), 118-126.
- [8] Li, Y., Zhang, J., Fan, J. Y., Zhong, S. H., & Gu, R. (2023). Tibetan medicine Bang Jian: a comprehensive review on botanical characterization, traditional use, phytochemistry, and pharmacology. *Frontiers in Pharmacology*, 14, 1295789.
- [9] Liu, S., Tian, F., Qi, D., Qi, H., Wang, Y., Xu, S., & Zhao, K. (2023). Physiological, metabolomic, and transcriptomic reveal metabolic pathway alterations in *Gymnocypis przewalskii* due to cold exposure. *BMC genomics*, 24(1), 545.
- [10] Wang, N., & Zhu, H. (2024). Geo-authentic Tibetan medicine: a traditional pharmacological resource for promoting human health and wellness. *Frontiers in Pharmacology*, 15, 1432221.

Systematic Study on the Mechanism of Tanshinone IIA Based on Bioinformatics

Xing Gao¹, Xuehui Wang¹, Yihui Li¹, Hailing Ding¹, Keming Li^{1,2}, Shaoyang Hou³, Xinchao Wang³, Zhaobin Fan*

1.Qilu Institute of Technology, #3028 Jingshi East Road, Jinan City, Shandong Province, 250200, China

2.Shandong Xiehe University, #6277 Jiqing Road, Licheng District, Jinan City, Shandong Province, 250109, China

3.Heze University, #2269 Daxue Road, Mudan District, Heze City, Shandong Province, 274015, China

*Corresponding author: Zhaobin Fan

Copyright: 2025 Author(s). This is an open-access article distributed under the terms of the Creative Commons Attribution License (CC BY-NC 4.0), permitting distribution and reproduction in any medium, provided the original author and source are credited, and explicitly prohibiting its use for commercial purposes.

Abstract: Objective: Tanshinone IIA, one of the most abundant liposoluble components isolated from the traditional Chinese medicine *Salvia miltiorrhiza*, exhibits significant biological activities in anti-inflammatory, antibacterial, and antitumor effects. This study aims to systematically explore the mechanism of Tanshinone IIA through bioinformatics. **Methods:** We utilized the TCMSP database to retrieve the oral bioavailability (OB) and drug-likeness (DL) of Tanshinone IIA. The gene chip numbered GSE85871 was downloaded from the GEO database, and differential genes were analyzed using R language to identify potential targets of Tanshinone IIA. After obtaining these targets, GO analysis and KEGG pathway analysis were performed using the DAVID 6.8 database. Diseases related to Tanshinone IIA were explored through the CTD database. Finally, Cytoscape was employed to construct a visual network of multiple targets, pathways, and diseases associated with Tanshinone IIA. **Results:** Tanshinone IIA demonstrated good drug efficacy with an OB value of 49.89% and a DL value of 0.4. A total of 132 potential targets were identified, primarily exhibiting gene co-expression and physical interaction in the PPI network. These targets were enriched in biological processes and pathways such as ovarian steroidogenesis, cell cycle, and steroid hormone biosynthesis. Tanshinone IIA was found to be relevant in the treatment of diseases including breast tumors, hypertension, atherosclerosis, gliomas, vascular system injuries, left ventricular hypertrophy, leukemia, and hearing loss. **Conclusion:** Utilizing bioinformatics approaches, we systematically analyzed the possible molecular mechanisms of Tanshinone IIA, providing potential targets and insights into its pharmacological mechanisms and treatment strategies

Keywords: *Salvia Miltiorrhiza*; Tanshinone IIA; Bioinformatics; Mechanism of Action

Published: Jun 10, 2025

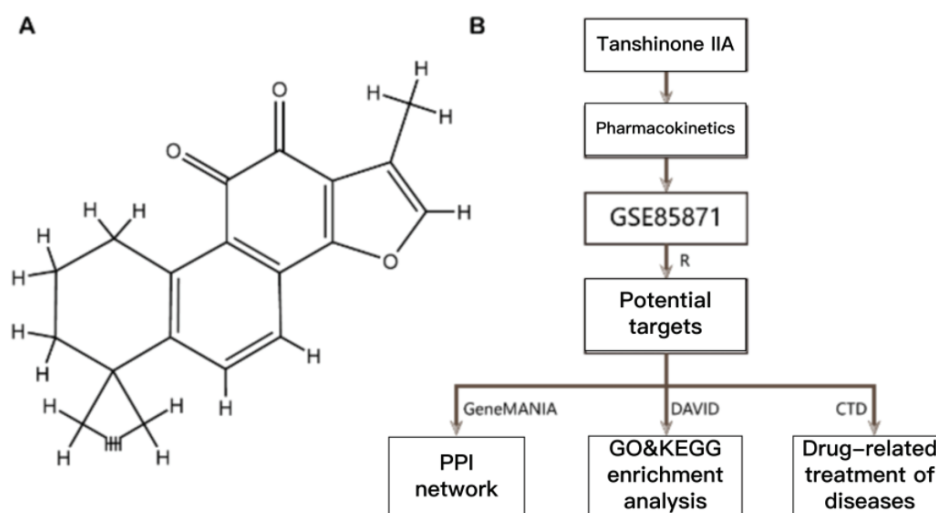
DOI: <https://doi.org/10.62177/apjcmr.v1i2.387>

Salviae Miltiorrhizae, first recorded in “Shennong’s Herbal Classic”, is bitter in taste and slightly cold in nature, pertaining to the heart and liver meridians. Its medicinal parts mainly consist of dried roots and tubers, which have been widely used in the treatment of vascular diseases^[1]. Tanshinone IIA, one of the significant bioactive components of *Salviae Miltiorrhizae*, belongs to the category of liposoluble phenanthrenequinone compounds. It exerts protective effects on the heart and nerves, possesses anticancer and antibacterial properties^[2-4]. However, there has been no systematic analysis of the complex mechanism of action of tanshinone IIA.

In this study, we innovatively employed the TCMSP database to comprehensively evaluate the pharmacological parameters

of tanshinone IIA. By screening potential targets of tanshinone IIA, we constructed and analyzed a protein-protein interaction (PPI) network. Additionally, we conducted enrichment analysis of Gene Ontology (GO) terms and Kyoto Encyclopedia of Genes and Genomes (KEGG) signaling pathways. We also searched for diseases and targets associated with tanshinone IIA and established a “component-target-pathway-disease” network. This approach provides valuable data support for further in-depth research or the development and utilization of *Salviae Miltiorrhizae* and tanshinone IIA.

Figure 1: Chemical structure of Tanshinone IIA and a roadmap of its predicted mechanism. (A) Chemical structure diagram of Tanshinone IIA (PubChem CID: 164676); (B) Flowchart illustrating the pharmacological mechanism of action of Tanshinone IIA.



1. Materials and Methods

1.1 Evaluation of Pharmacokinetic Parameters

The Traditional Chinese Medicine Systems Pharmacology Database and Analysis Platform (TCMSP) is a computational systems biology and medicine platform for evaluating the pharmacology of Chinese herbal medicines^[5]. This database encompasses not only chemical substances, target and drug-target networks, related drug-target networks, but also pharmacokinetic properties of natural compounds such as oral bioavailability, drug-likeness, Caco-2 permeability, half-life, and blood-brain barrier (BBB) penetration of some chemical components in Chinese medicine^[6]. OB, calculated using the internal model OBioAvail 1.1 in the TCMSP database, represents one of the most crucial pharmacokinetic properties of oral medications and plays a significant role in the efficiency of systemic drug administration. DL, which relies on molecular descriptors and the tavioto coefficient in the database, is a qualitative concept primarily used in drug design to evaluate the drug-likeness of compounds. In this study, “tanshinone IIA” was used as a search term to evaluate the pharmacokinetic parameters of tanshinone IIA at the molecular level.

1.2 Screening of Potential Targets

The raw data for the gene chip with the related number GSE85871 and the platform annotation file GPL571 for tanshinone IIA were downloaded from the Gene Expression Omnibus (GEO). The GSE85871 dataset contains gene expression profile information for MCF7 cells treated with 102 different Chinese medicinal molecules^[7], including two samples of tanshinone IIA and six blank control samples. Normalization and differentially expressed gene screening were performed using the Affy and limma packages in R. Quality control was conducted using fold change (FC) and P-value, with standards set at $P < 0.01$ and $|\log_2FC| \geq 1$. The gplots package was utilized to create a cluster diagram, and the plot package was used to generate a volcano plot.

1.3 Construction of PPI Network

GeneMANIA is primarily used to generate hypotheses about gene function, analyze gene lists, and prioritize genes for functional testing^[8]. The results of the differentially expressed genes mentioned above were organized, and GeneMANIA was

employed to construct a PPI network, analyzing the targets and their roles and relationships within the network.

1.4 Enrichment Analysis of GO and KEGG Signaling Pathways

The Database for Annotation, Visualization, and Integrated Discovery (DAVID) is a web-based software toolkit that effectively aids in understanding the interactive relationships in gene expression data and provides systematic information about genes of interest^[9]. DAVID database was used to perform GO and KEGG signaling pathway enrichment analysis on potential targets, and the ggplot2 package was used to create an enrichment analysis bubble chart.

1.5 Retrieval of Related Therapeutic Diseases

The Comparative Toxicogenomics Database (CTD) is a powerful, publicly available database that enhances understanding of the health effects of environmental exposures^[10]. CTD integrates various information about chemicals, including chemical structures, curated interacting genes and proteins, curated and inferred disease relationships, and rich pathway and functional annotations. In this study, “tanshinone IIA” was used as a search term to retrieve related therapeutic diseases.

2. Results

2.1 Pharmacokinetic Parameters

Through the TCMSP database, we conducted an in-depth study on the critical characteristics related to the pharmacokinetics of tanshinone IIA, including OB, DL, Caco-2, BBB, and the five rules of Lipinski’s rule of five (MW, AlogP, TPSA, Hdon, HACC). The results are presented in Table 1. It is worth noting that tanshinone IIA has an OB value of 49.89% and a DL value of 0.4, indicating good drug efficacy.

Table 1: Pharmacological and Molecular Characteristics of Tanshinone IIA

MW	AlogP	Hdon	Hacc	OB (%)	Caco-2	BBB	DL	FASA-	TPSA	RBN	HL
294.37	4.66	0	3	49.89	1.05	0.7	0.4	0.31	47.28	0	23.56

2.2 Potential Drug Targets

Based on screening criteria, this study analyzed the relevant raw data with the GEO accession number GSE85871 using R language. The analysis revealed that tanshinone IIA-treated MCF7 cells could induce 132 significantly differentially expressed genes, including 85 upregulated genes and 47 downregulated genes. The clustering plot and volcano plot are shown in Figures 2 and 3, respectively.

2.3 PPI Network

The intrinsic mechanism of drug regulation is often not determined by a single target or pathway but is commonly modulated by multiple targets and pathways. By organizing the aforementioned differentially expressed gene results and using GeneMANIA to construct a PPI network, it was revealed that among the 132 target proteins and their interacting proteins, 76.27% share similar co-expression characteristics, 14.91% exhibit physical interactions, and 3.83% possess co-localization relationships. Other results, including genetic interactions, pathways, predictions, and shared protein domains, are illustrated in Figure 4.

2.4 GO and KEGG Enrichment Analysis

To further categorize the biological functions of the potential targets of tanshinone IIA, GO and Pathway enrichment analyses were conducted using DAVID 6.8. The results indicated that the biological processes (BP) of the potential targets were significantly enriched in processes such as nuclear division, negative regulation of DNA-templated transcription, positive regulation of nuclear protein export from the nucleus, cellular response to hydrogen peroxide, and cell cycle arrest mediated by P53-class mediator resulting from DNA damage and signal transduction, as shown in Figure 5A. Changes in cellular components (CC) were primarily focused on the nucleus, nucleoplasm, cytosol, membrane, and CHOP-ATF3 complex, as illustrated in Figure 5B. Variations in molecular functions (MF) were predominantly manifested in protein binding, transcription factor activity, sequence-specific DNA binding, zinc ion binding, poly(A) RNA binding, and histone-lysine N-methyltransferase activity, as depicted in Figure 5C. KEGG pathway analysis revealed that the enrichment of potential targets was primarily observed in ovarian steroidogenesis, cell cycle, and steroid hormone biosynthesis, as shown in Figure 5.

Figure 2: Cluster diagram of differentially expressed genes in Tanshinone IIA-related datasets

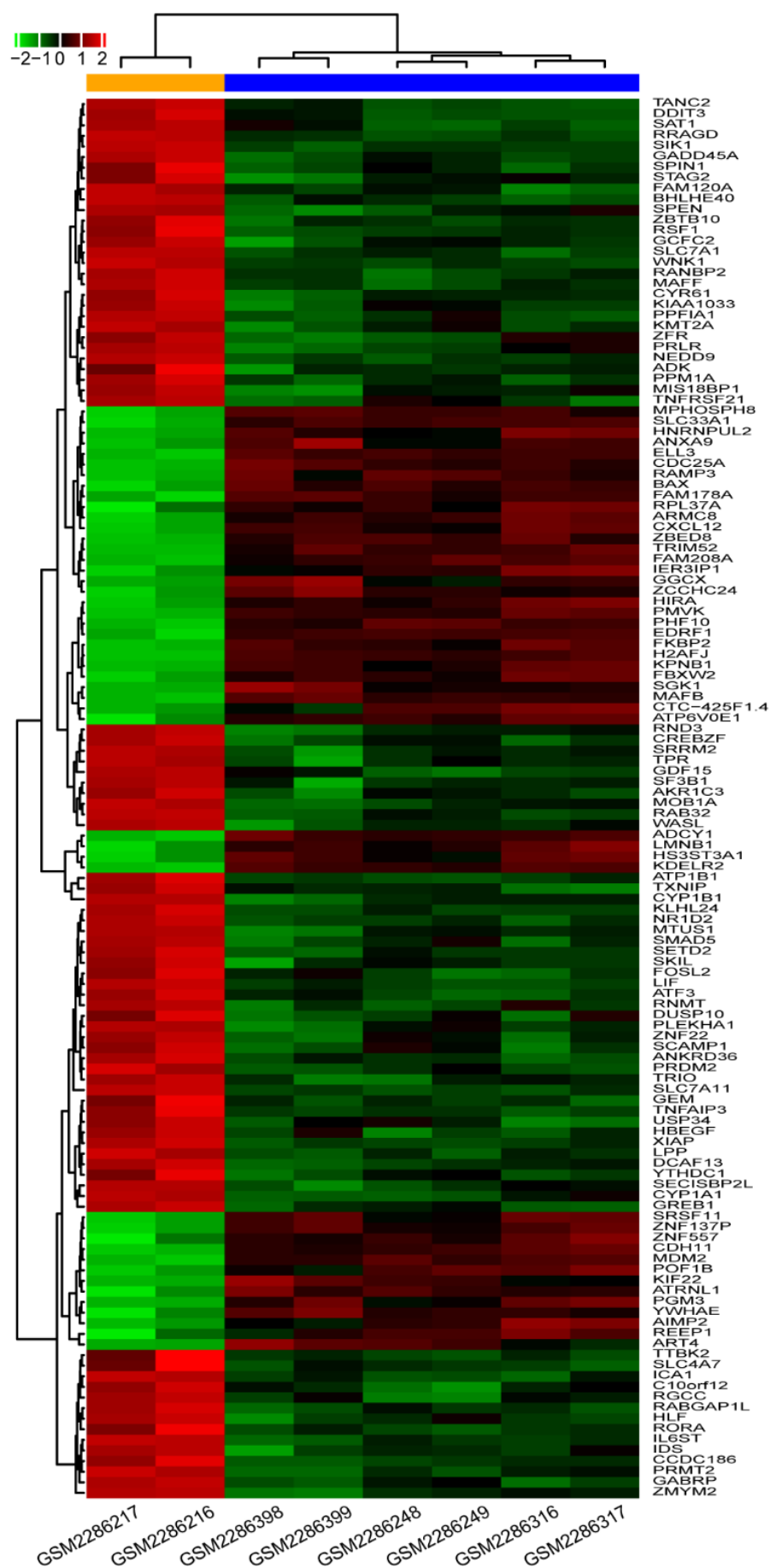


Figure 3: Volcano plot of differentially expressed genes in Tanshinone IIA-related datasets

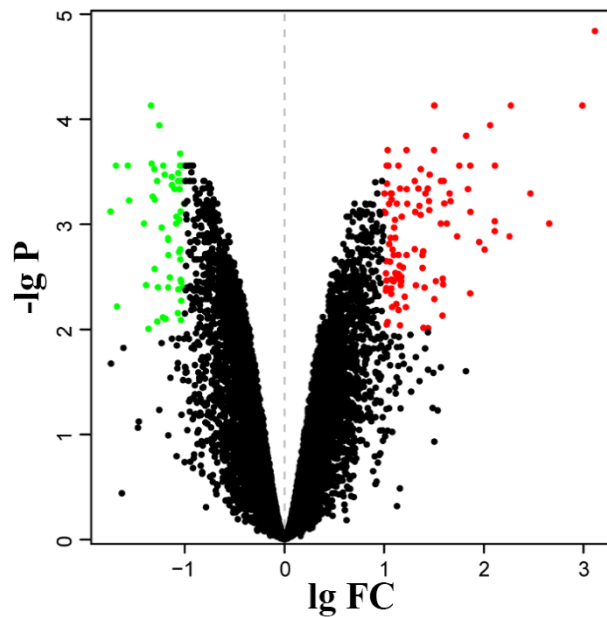


Figure 4: PPI network diagram of potential targets of Tanshinone IIA (Black nodes represent target proteins submitted as query terms in the search, gray circles represent genes associated with the query genes, and different connection colors represent different correlations)

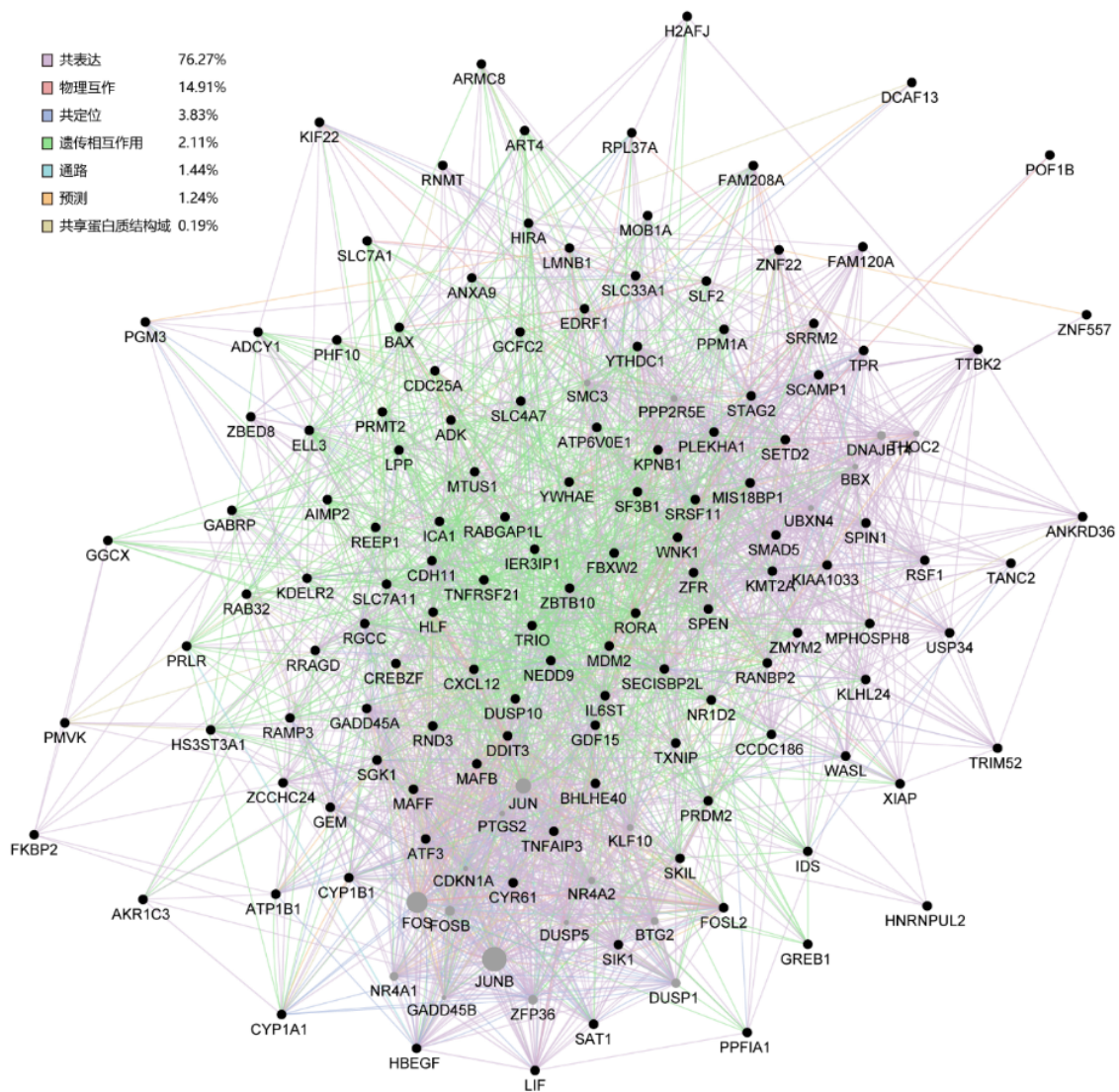
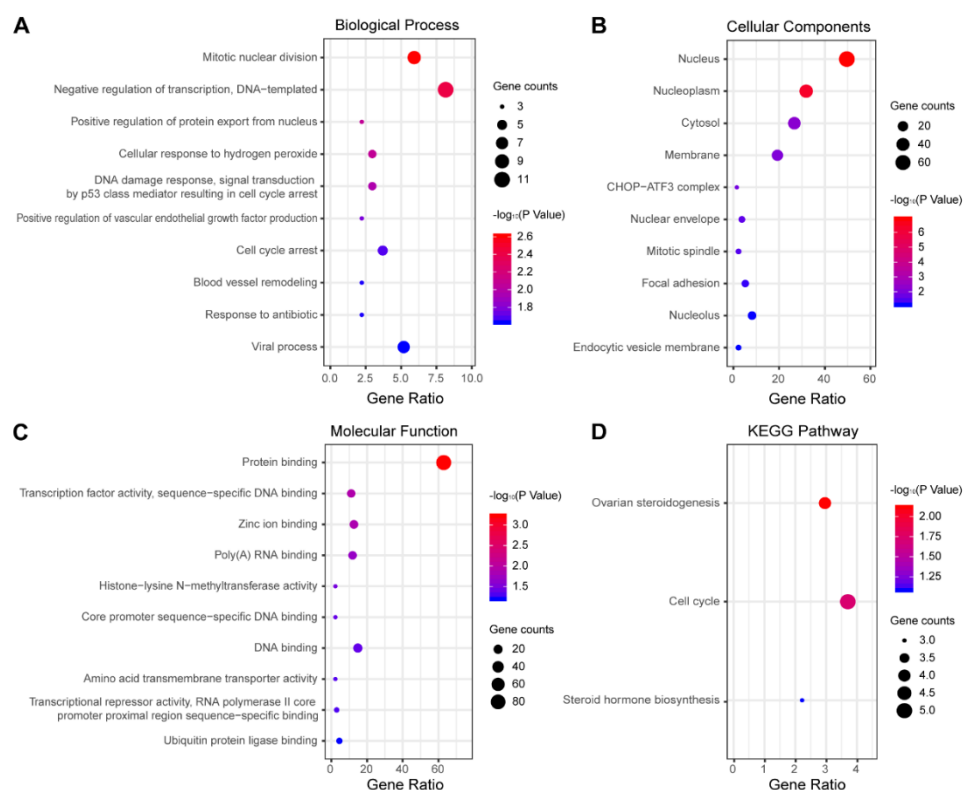


Figure 5: Bubble diagram of GO function and KEGG pathway analysis of potential targets of Tanshinone IIA



2.5 Diseases Related to Therapeutic Applications

The diseases with direct evidence of treatment by tanshinone IIA, retrieved from the CTD database, primarily include breast neoplasms, hypertension, atherosclerosis, gliomas, vascular system injuries, left ventricular hypertrophy, leukemia, and hearing loss. These are summarized in Table 2.

Table 2: Associated Therapeutic Diseases and Their Respective Targets and Scores

Diseases	Associated Targets	Scores
Breast tumor	AHR, BAX, BCL2, BIRC5, CASP8, CDKN1B, CST6, CTNNB1, CXCL8, CYP1A1, CYP3A4, DDIT3, EDNRB, ETS2, FOS, GRB7, GSTP1, HIST1H1C, HMOX1, IL1B, IL6, KRAS, MAP3K1, MMP1, MMP9, NFK-BIA, NOS2, NOS3, PARP1, PTGS2, RARB, RB1, RELA, SPP1, TNF, TNFSF10, TP53	81.64
Hypertension	AGT, AHR, BCL2, CD36, CYP1A1, DUSP5, EDN1, EDNRA, FOS, GSK3B, GSTP1, HMOX1, IL1B, IL6, INPPL1, MMP9, NOS2, NOS3, NR3C1, OLR1, PPARG, PTGS2, RELA, TLR4, TNF, TP53	46.65
Atherosclerosis	AGT, AHR, IL6, MMP1, NOS2, NOS3, PARP1, PPARG, PTGS2, TLR4, TNF, VEGFA	29.93
Glioma	GSTP1, PTGS2, SPP1, TNF, TNFSF10, TP53	14.22
Vascular system injury	HMOX1, SPP1, TNF	10.74
Left ventricular hypertrophy	AGT, AHR, EDN1, MYC	9.38
Leukemia	VEGFA	3.12
Hearing loss	TLR4	3.11

3. Discussion

One of the significant reasons for the high cost of late-stage drug development failures is unfavorable pharmacokinetics and toxicity profiles. The adoption of methods such as predicting and simulating pharmacokinetics, metabolism, and toxicity endpoints can simplify and accelerate the drug discovery process to some extent. Currently, this approach is gaining increasing favor and attention from relevant researchers^[11].

OB represents the percentage of an orally administered drug that reaches systemic circulation without alteration, indicating the convergence of pharmacokinetic processes. High oral bioavailability is often a critical indicator in determining the drug-like properties of bioactive molecules as therapeutic agents. DL, established based on the analysis of physicochemical properties or/and structural features of existing small molecule drugs and/or drug candidates, is a qualitative concept used in drug design to estimate how “drug-like” a compound is expected to be. This estimation aids in optimizing pharmacokinetic and drug properties, such as solubility and chemical stability. The TCMSP database suggests reference standards as OB: $\geq 30\%$; DL ≥ 0.18 . As evident from Table 1, the properties of tanshinone IIA meet these requirements, indicating that it is a promising candidate for drug discovery.

In this study, the dataset with the accession number GSE85871 from the GEO database was selected. This dataset encompasses the gene expression profiles established after treating MCF7 cells with tanshinone IIA. Through R language analysis, 132 significantly differentially expressed genes were identified, including 85 upregulated genes and 47 downregulated genes. These differential genes can be considered, to some extent, as potential targets of tanshinone IIA, and the pharmacological effects of some of these potential targets have been established in the literature. According to the research results of XU et al.^[12], tanshinone IIA can effectively increase the expression of hypoxia-inducible factors, thereby upregulating VEGF expression, improving cardiac function, protecting myocardium, and exerting anti-myocardial hypertrophy effects. Zhou et al.^[13] demonstrated that tanshinone IIA could reduce neuronal damage and protect against cerebral ischemia-reperfusion injury by decreasing the expression levels of NF- κ B and I κ B genes and proteins in a rat model of ischemia-reperfusion. Wang et al.^[14] found that tanshinone IIA downregulates the expression of VEGF and β -catenin genes and proteins, inhibits the growth of subcutaneous xenografts of human colorectal cancer in nude mice, and suppresses microvessel formation, thereby exhibiting antitumor effects.

To better understand the functions of the potential targets of tanshinone IIA, GO and KEGG signaling pathway analyses were performed using DAVID 6.8. The potential targets were mainly enriched in biological processes such as nuclear division, negative regulation of DNA-templated transcription, positive regulation of nuclear protein export, and KEGG signaling pathways including ovarian steroidogenesis, cell cycle, and steroid hormone biosynthesis. In this study, by searching the CTD, eight diseases with direct therapeutic evidence for tanshinone IIA were identified, including breast tumors, hypertension, atherosclerosis, gliomas, vascular system injuries, left ventricular hypertrophy, leukemia, and hearing loss. As shown in Table 2, there is a significant overlap between the targets supported by the literature for these diseases and the differential genes screened in this study, further corroborating the feasibility of the research approach.

The enrichment of KEGG pathways, particularly the cell cycle and steroid hormone biosynthesis, underscores the multifaceted mechanisms by which Tanshinone IIA (Tan IIA) exerts its therapeutic effects against diseases such as breast cancer. The cell cycle pathway, a critical hub for cancer progression, is tightly regulated by genes like TP53, BCL2, and CDKN1B, which were identified as key targets in this study. Tan IIA likely inhibits breast tumor growth by modulating these targets to induce cell cycle arrest. For instance, TP53, a tumor suppressor gene frequently dysregulated in cancers, promotes cell cycle arrest or apoptosis in response to DNA damage. Our data revealed upregulation of TP53 and downregulation of anti-apoptotic BCL2, suggesting that Tan IIA triggers pro-apoptotic signaling and halts uncontrolled proliferation in breast cancer cells. Furthermore, the downregulation of CDKN1B (p27), a cyclin-dependent kinase inhibitor, may disrupt cyclin-CDK complexes, thereby blocking G1/S phase transition and impeding tumor cell division.

Additionally, the steroid hormone biosynthesis pathway, enriched in this study, provides insights into Tan IIA's potential efficacy against hormone-dependent breast cancers. Estrogen receptor (ER)-positive breast cancers rely on steroid hormones for growth, and Tan IIA may interfere with this dependency by targeting enzymes like CYP19A1 (aromatase), which

catalyzes estrogen synthesis. Although not explicitly listed in our target results, the overlap between steroidogenic pathways and genes such as CYP3A4 (involved in hormone metabolism) implies indirect regulation of estrogen levels. By suppressing steroid hormone production or signaling, Tan IIA could attenuate ER-driven tumor proliferation.

In summary, this study evaluated the pharmacokinetic parameters of tanshinone IIA using the TCMSP database, identified its potential targets through high-throughput microarray data, and conducted further biological functional studies. The results suggest that tanshinone IIA may possess multiple functions, including nuclear division, ovarian steroidogenesis, cell cycle, and steroid hormone biosynthesis, which are closely related to its antitumor, anti-atherosclerotic, ischemia-reperfusion protective, and anti-inflammatory effects. Tanshinone IIA emerges as a highly potential drug candidate; however, further research is needed to determine its precise pharmacological effects and mechanisms of action.

Funding

no

Conflict of Interests

The authors declare that there is no conflict of interest regarding the publication of this paper.

Reference

- [1] Kang, Y., & Gao, M. (2019). Current status and progress in mechanistic studies of *Salvia miltiorrhiza* in the treatment of coronary heart disease. *Liaoning Medical Journal*, 33(2), 85–88.
- [2] Su, M., Qin, Y., Lou, Y., et al. (2019). Study on the angiogenic effect of sodium tanshinone IIA sulfonate in vitro and in vivo. *Drugs & Clinic*, 34(4), 934–940.
- [3] Ning, J., He, C., & Huang, J. (2019). Study on the anti-inflammatory effect of tanshinone IIA in vitro and in vivo. *Drugs & Clinic*, 34(2), 292–298.
- [4] Tian, Q. (2018). Meta-analysis of tanshinone IIA as adjunctive therapy for chronic heart failure [Master's thesis, Nanchang University].
- [5] Ru, J., Peng, L., Wang, J., et al. (2014). TCMSP: A database of systems pharmacology for drug discovery from herbal medicines. *Journal of Cheminformatics*, 6(1), 13.
- [6] Xu, X., Zhang, W., Huang, C., et al. (2012). A novel chemometric method for the prediction of human oral bioavailability. *International Journal of Molecular Sciences*, 13(6), 6964–6982.
- [7] Mostafavi, S., Ray, D., Wardefarley, D., et al. (2008). GeneMANIA: A real-time multiple association network integration algorithm for predicting gene function. *Genome Biology*, 9(Suppl 1), 1–15.
- [8] Huang, D. W., Sherman, B. T., & Lempicki, R. A. (2009). Systematic and integrative analysis of large gene lists using DAVID bioinformatics resources. *Nature Protocols*.
- [9] Davis, A. P., King, B. L., Mockus, S., et al. (2013). The Comparative Toxicogenomics Database: Update 2011. *Nucleic Acids Research*, 41(Database issue), D1104–D1114.
- [10] Lipinski, C. A., Lombardo, F., Dominy, B. W., et al. (2012). Experimental and computational approaches to estimate solubility and permeability in drug discovery and development settings. *Advanced Drug Delivery Reviews*, 64(1–3), 4–17.
- [11] Van De Waterbeemd, H., & Gifford, E. (2003). ADMET in silico modelling: Towards prediction paradise? *Nature Reviews Drug Discovery*, 2(3), 192–204.
- [12] Xu, W., Yang, J., & Wu, L.-M. (2009). Cardioprotective effects of tanshinone IIA on myocardial ischemia injury in rats. *Die Pharmazie*, 64(5), 332.
- [13] Zhou, L., Liu, Y., Wang, F., et al. (2013). Effects of tanshinone IIA on the activity of NF- κ B and I κ B in the brain tissue of I/R rats. *Chinese Medicinal Materials*, 36(7), 1136–1139.
- [14] Wang, Y., Liu, X., Zhou, L., et al. (2013). Inhibitory effect of tanshinone IIA on angiogenesis in nude mice with human intestinal cancer. *Chinese Journal of Experimental Traditional Medical Formulae*, 19(3), 167–171.

Dear Researchers and Scholars :

Greetings from Asia Pacific Science Press, a beacon of academic and scientific publishing, located in the vibrant city of Hong Kong.

We extend our heartfelt gratitude for your relentless pursuit of knowledge, and your significant contributions to the advancement of science and society. It is researchers and scholars like you who propel humanity forward, and we at the Asia Pacific Science Press are devoted to ensuring that your groundbreaking works receive the global recognition they rightfully deserve.

In light of our commitment to disseminating pioneering research across various disciplines, such as medicine, architecture, education, and electronics, we are reaching out with two pivotal opportunities to augment our collaboration with the global academic community:

Call for Paper Submissions:

We cordially invite you to submit your original research articles to our fast-growing, peer-reviewed, and open-access journals. Our platform guarantees an extensive, global reach, enabling your work to garner maximum visibility and citation in the academic sphere. Rest assured, your work will be meticulously assessed by experts in the field, ensuring it receives the acknowledgment and exposure it merits.

Join Our Esteemed Team:

We are fervently searching for passionate researchers and scholars interested in joining our burgeoning team at Asia Pacific Science Press. We offer numerous roles, such as peer reviewers, editors, and advisory board members, where your expertise will significantly shape the content and quality of our publications. In return, you will gain invaluable experience, network with preeminent scholars, and play a pivotal role in molding the future of global academic publishing.

Why Choose Asia Pacific Science Press?

Global Reach: Your work will be accessible to a worldwide audience, free from any access barriers.

Collaboration with Renowned Universities: We have established extensive publishing systems in cooperation with world-renowned universities, such as Wuhan University, Hong Kong University, and the University of Malaya.

Diverse Disciplines: Your research will be housed among numerous journals across a multitude of academic projects and disciplines.

As we stride forward in the academic landscape, we envision a future where our collective efforts shape a more enlightened, innovative, and interconnected global society. We sincerely hope that you consider this invitation to join us on this auspicious journey towards knowledge, discovery, and global impact.

Should you wish to submit your work or express interest in joining our team, please do not hesitate to contact us. You can submit your manuscript or personal profile to info@apspublisher.com or visit our website at www.apspublisher.com for more information.

Thank you for considering this opportunity, and we eagerly anticipate the possibility of welcoming you to the Asia Pacific Science Press family. Together, let's forge a future of unparalleled scientific advancement and discovery.

Warm regards
Asia Pacific Science Press

OUR JOURNALS

Asia Pacific Economic and Management Review is an international, peer-reviewed and open access journal which focuses on theoretical and applied studies of corporate and financial behavior. Aiming to promote the research in fields of business economics and management, it covers mainly but not limits to the following areas: accounting and financial management, economics, human resource management and organizational behavior, information management, international business, strategy and innovation, management science and operations management, marketing and retailing, finance.



Critical Humanistic Social Theory is an journal that publishes papers specifically using quantitative or qualitative research methods for social science research. The journal encourages scholars to conduct social science theory research from the perspective of social critical theory and emphasizes research concerned with issues or methods that cut across traditional disciplinary lines.



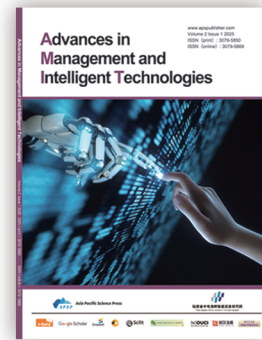
Journal of Educational Theory and Practice is an international, peer-reviewed and open access journal which is to promote the evaluative, integrative, theoretical and methodological research on contemporary education; shape a novel, broader view of issues in contemporary education; enhance the caliber of humanities research through active use of best domestic and foreign practices; and integrate the achievements of various sciences and knowledge areas with unconventional approaches.



Journal of Advances in Engineering and Technology is an international, peer-reviewed and open access journal which publishes original articles, reviews, short communications, case studies and letters in the field of electronic research and application.



Advances in Management and Intelligent Technologies is an international, peer-reviewed, open-access academic journal, hosted by the Fujian Strait Institute of Intelligent Equipment and managed and published by Asia-Pacific Science Press. It focuses on the latest research in the fields of management and intelligent technologies, and aims to advance both theoretical and applied research in management, technological innovation, and intelligent development.



Asia Pacific Journal of Clinical Medical Research is an international, peer-reviewed, open access journal dedicated to advancing clinical medical research across multiple disciplines. The journal serves as a platform for publishing high-quality original research, reviews, and clinical studies that enhance the understanding of medical practices, treatment innovations, and healthcare outcomes, thereby supporting patient care and medical advancements in the Asia Pacific region and beyond.



Asia Pacific Journal of Educational Research is an international, peer-reviewed, open-access academic journal focusing on educational theory and practice. It publishes high-quality research on educational reform, teaching methods, educational equity, and policy studies. The journal addresses practical needs and institutional changes in the education systems of the Asia-Pacific region, advocating a balance between theoretical inquiry and practical experience. It encourages original studies from multicultural, comparative, and interdisciplinary perspectives, aiming to support educational innovation and policy development across the region.



Asia Pacific Economic and Social Development is an international, peer-reviewed, open-access academic journal openly distributed to the global academic community. The journal is committed to publishing original research with theoretical depth and practical value in the fields of economic and social development. It focuses on issues such as economic behavior, social structure transformation, policy innovation, and regional coordinated development in the Asia-Pacific region. The journal encourages interdisciplinary perspectives and promotes the integration of economics, sociology, management, and related disciplines.

